Title

Effects of microclimate, dispersal, species interactions, and environmental stochasticity on demography

Author

Ray, Courtenay A

Publication Date

2023

Peer reviewed|Thesis/dissertation

Effects of microclimate, dispersal, species interactions, and environmental stochasticity on demography

by

Courtenay A Ray

A dissertation submitted in partial satisfaction of the

requirements for the degree of

Doctor of Philosophy

in

Environmental Science Policy and Management

in the

Graduate Division

of the

University of California, Berkeley

Committee in charge:

Assistant Professor Benjamin Wong Blonder, Chair
Professor David Ackerly
Associate Professor Roberto Salguero-Gómez
Assistant Professor Onja Razafindratsima

Fall 2023

Effects of microclimate, dispersal, species interactions, and environmental stochasticity on demography

Abstract

Effects of microclimate, dispersal, species interactions, and environmental stochasticity on demography

by

Courtenay A Ray

Doctor of Philosophy in Environmental Science Policy and Management

University of California, Berkeley

Assistant Professor Benjamin Wong Blonder, Chair

The spatial distribution and species composition of plant communities depend on a multitude of potentially interacting drivers. These drivers include abiotic factors, such as climate conditions, and biotic factors, such as species interactions. Long-term data on vital rates (i.e., survival, growth, reproduction) for individuals in a community can reveal the influence of factors such as climate and neighboring individuals on performance. In this dissertation, I use a demography dataset that tracks the location and vital rates of over 3,300 individuals of 18 species across nine years in an alpine plant community. Here, I test whether vital rates respond to microenvironment modification of ground temperatures and soil moisture by neighboring plants. In the next chapter, I assess how abiotic dispersal may promote the co-location of seeds and host plants and, thus, influence species interactions. Finally, I explore how species respond to increased vital rate variance from environmental stochasticity by estimating the extent that population stochastic growth rates are buffered to perturbations. Collectively, this dissertation demonstrates the sensitivity of demographic processes to macroclimate, seed dispersal, and environmental stochasticity within and across co-occurring species using a highly resolved model system.

This dissertation is dedicated to Matthew Grindy

Contents

Acknowledgments

This dissertation would not have been possible without the support of my advisor, Benjamin Blonder. I also thank my committee, Rob Salguero-Gómez, David Ackerly, and Onja Razafindratsima. My field research was funded by the Rocky Mountain Biological Laboratory (RMBL) Graduate Fellowship, Snyder Endowment, RMBL Graduate Fellowship, Langenheim Endowment, RMBL Graduate Fellowship, Colorado Mountain Club Kurt Gerstle Fellowship, Colorado Native Plant Society: John Marr Grant, Arizona State University Research and Training Initiatives Graduate Student Support, the Peder Sather Center: Peder Sather Grant, and the Berkeley Chapter of Sigma Xi's Grants-in-Aid of Research Award. Writing and research funding at UC Berkeley was provided by the UC Berkeley Environmental Science Policy and Management (ESPM): William and Mary Liu Fellowship, Bryan Wilson Fellowship, William Carroll Smith Fellowship, and through Rausser College, Dr. E. Ralph de Ong Student Support. Research permits were granted through the United States Forest Service. Extra special thanks to my graduate representatives, Ryann Madden and Zarah Ersoff.

Chapter 1

Introduction

Assembly mechanisms shape patterns of community structure. For a species to establish in a community from the regional pool, it must disperse into that community and tolerate the environmental and biotic conditions [44]. Disentangling the contributions of individual community assembly mechanisms to observed community patterns is challenged by the high number of processes that contribute to community assemblages, feedbacks between processes, and their context dependencies.

Place-based studies that collect long-term demography data in tandem with spatial and environmental data are invaluable in linking processes to patterns in communities because they provide snapshots of processes across multiple timesteps and, thus, under multiple environmental contexts. Here, in three chapters, this dissertation seeks to understand the contributions of three mechanisms of community assembly relative to observed demographic and spatial patterns at a long-term research site: microclimate modification, dispersal-mediated plant-plant interactions, and demographic buffering. Through consideration of these mechanisms, which are often overlooked in community assembly models, my research addresses key gaps in our understanding of community assembly.

Alpine communities are among the most threatened by climate change [30]. In response to warming, high-elevation plant communities are changing in composition and traits [34, 11]. However, species response to climate change is variable, with some species responding positively and others negatively [39]. Alpine communities are also often characterized by high light radiation, strong winds, and short snow-free windows during which to flower and grow [59]. Due to these environmental conditions, alpine communities are ideal settings to explore processes that structure communities because plants may utilize species interactions, dispersal to preferred microsites, and demographic buffering to persist under adverse conditions. Further, alpine systems often have tractable species richness (i.e., <50 species), increasing the feasibility of demographic observations at the individual level.

For my thesis research, I work in an alpine plant community in Colorado, 3540 m above sea level. I use a demography dataset that tracks the location and vital rates of over 3300 individuals of 18 alpine plant species across eight years of data (2014-2021). During this time, we observed large shifts in community structure. From 2016-2018, we documented

a 57% reduction in total plant abundance paralleling prolonged regional drought. In the chapters below, I explore the drivers of these declines, as well as potential feedbacks of these declines on community assembly mechanisms.

In my first research chapter, I measured the alteration of soil surface temperatures and soil moisture by neighboring plants (i.e., microenvironment modification). Although microenvironment modification may indirectly lead to changes in species interactions due to its effects on environmental context, the consequences of microenvironment modification for demography remain unclear. In this chapter, I examined the context-dependency of microenvironment modification effects on vital rates by using spatial co-occurrence as a proxy for modification strength.

My next chapter examined how seed dispersal may enable interactions between seeds and plants. Seed functional traits, such as seed mass and size, influence plant population dynamics through effects on dispersal distance, burial depth, and survival [91]. As the seed stage is the only mobile life stage for most plants, selection on seed traits is thought to optimize dispersal to microsites (i.e., locally preferable habitats within a wider area of suitable habitat) with low competition from neighboring plants. However, recent global reviews on seed functional traits have not included alpine ecosystems [1], where dispersal expectations may be reversed. In the alpine, dispersal to microsites with more neighbors may improve plant performance due to a higher prevalence of positive (rather than competitive) interactions [19]. In this chapter, I test whether plants can physically promote the retention of seeds (seed trapping) and prevent further dispersal (retention).

Finally, I compared the differential responses of species and developmental stages to environmental stochasticity. In response to environmental stochasticity, some organisms utilize demographic buffering, in which the stochastic population growth rate, λ_s, remains unvaried despite environmentally-driven perturbations to vital rates. Although differences in demographic buffering strength (buffering values) likely contribute to differential population response to environmental stochasticity, in plants, the extent to which buffering values differ between developmental stages and across co-occurring species is unclear.

Studying multiple assembly mechanisms in the same community can provide an integrated perspective of processes that contribute to community structure. Together, these chapters demonstrate the complexity of community assembly processes and give insight into community response to climate change.

Figure 1.1: A photograph of the field site in 2022 with monsoon rains in the distance.

Chapter 2

Linking microenvironment modification to species interactions and demography in an alpine plant community

This chapter was previously published as "Ray, C.A., Kapas, R.E., Opedal, Ø.H., and Blonder, B.W. (2023)"[97]. It is included in this dissertation with permission from all co-authors.

Chapter 2 explores a key challenge in community ecology—the contextuality and proximate causes of species interactions. In particular, we examined microclimate modification as a species interaction by 1) comparing microclimate (surface temperature and soil moisture) across taxa and in paired non-vegetated areas, and 2) determining vital rate response to proxies for modification (e.g., plant identity, size, and degree of spatial overlap) and climate. Further, as this chapter uses both aboveground biomass measurements and estimated belowground extents to calculate spatial overlap, we can address how each of these ecological realms affects plant demography. The novelty of this study is in its utilization of long-term demography datasets in combination with spatial, microclimate, and macroclimate data to analyze species interactions. This chapter sets the stage for Chapter 3 by providing insight into the demographic consequences of co-location that dispersal may facilitate. Further, this chapter motivates future research built off of the findings in Chapter 4, namely, whether demographic buffering values also depend on species interactions.

2.1 Background

Species interactions affect vital rates (i.e., survival, growth, fecundity) and may scale up to impact species distributions, co-occurrence patterns, and abundances [28, 18, 124, 118]. The strength and direction of species interactions and their effects on vital rates are increasingly

well understood, yet generalization has been challenged by the dependence of these interactions on the abiotic and biotic context [111, 74]. For example, the outcome of species interactions may vary across macroclimatic conditions (i.e., regional climate) [126] or shift in the presence of other species [103]. Context dependency creates challenges in scaling up from pairwise to multispecies interactions due to species-specific responses to environmental context [111]. An improved understanding of species interactions at the community scale and their sensitivity to context is needed to better understand community assembly, and would contribute toward more accurate forecasts of community response to environmental change [32, 87].

Modification of abiotic conditions (i.e., microenvironment modification) is a widespread mechanism of species interactions [9]. However, few generalities exist concerning which factors may influence modification strength and when microenvironment modification may be important for species interactions. One reason why microenvironment modification is difficult to generalize is that alterations of the abiotic environment influence individual plant performance as well as the environmental context of interactions between other plants. In plant communities, for example, a plant can shift resource availability for another plant [14], change the diversity and availability of suitable niches [112], and through both processes generate performance feedbacks on the modifying species [94]. The importance of microenvironment modification as a species interaction may also increase under harsher macroclimatic conditions such as those associated with decreased precipitation [126]. Such variable effects of microenvironment modification represent a challenge for predicting when and how microenvironment modification as a species interaction shapes community assembly.

Scaling microenvironment modification effects from individuals to multispecies assemblages remains a challenge. Previous work addressing how microclimate modification affects vital rates often has used presence/absence comparisons, such as inside versus outside plants (e.g., [81, 72, 82]). Such studies have shown that the effect of microenvironment modification on plant success often depends on the identity and proximity of the modifying species [69, 98]. However, net interaction effects in multi-individual and multispecies assemblages are more complex and may depend on neighborhood biomass [126] and diversity [125], with many possible feedbacks. As spatial overlap among plants is common across ecosystems, an increased understanding of how plants interact when aggregated would provide insight into the drivers of plant distributions and occurrence patterns.

Above- and belowground microenvironment modification may influence species interactions. Aboveground, for example, plants may alter wind exposure, increase relative humidity, or alter ambient and surface temperatures [14]. In tundra environments, plants (particularly shrubs) may impact snow accumulation patterns [114]. Belowground, plant interactions via microenvironment modification may reflect alterations to resource availability, such as water e.g., [128], as well as effects of soil biota associations [101]. The strength and direction of species interactions may also differ above- and belowground. For example, plants may compete for nutrients belowground, while ameliorating microclimates aboveground [57]. While canopy size may predict the spatial area that a plant modifies aboveground, lateral root extent may predict modification belowground because it influences the distance over which

a plant can acquire and redistribute resources. Due to differences in the relative size of above- versus belowground biomass, modification extent and the number and diversity of interacting partners may vary between these dimensions [88]. It is unclear the extent that above- or belowground overlap affect vital rates, as well as whether these effects are context dependent.

Alpine environments are an ideal setting to test how microenvironment modification affects plant performance as species interactions are known to be important for demography in this biome. For example, microenvironment modification is considered a common community assembly mechanism in the alpine as it may ameliorate abiotic conditions and increase the range of available niches [45, 23, 19, 29]. Other benefits of the alpine include low local species richness and extreme abiotic conditions where modification could have important demographic consequences [59]. By comparing vital rates in communities with high microenvironment modification and under different biotic contexts (i.e., varying species assemblages), we can gain insight into how microsite variation influences community assembly through effects on demography.

Here, we use microenvironment and spatial distribution data from a long-term alpine plant community demography study. We determine how vital rates (survival, growth, fecundity) vary in response to vegetative overlap with other plants as a proxy for microenvironment modification, as well as how vital rates vary in response to environmental context, individual state, and utilization of above- or belowground spatial data. Vegetative overlap is a metric of co-occurrence and thus may be a good proxy of microenvironment modification through physical and physiological processes. We asked (Q1) whether and how much microenvironment modification occurs for several focal species in this community. We then asked (Q2) how vital rates respond to microenvironment modification, using vegetative overlap as a proxy of microenvironment modification, and whether the response depends on context (macroclimate) and an individual state parameter (focal plant size).

2.2 Methods

Data collection

Demographic census

We analyzed a demography dataset from an alpine community located in southwestern Colorado (38.978725°N, 107.042104°W, ∼3540 m above sea level). From 2014 to 2019, we tracked all individuals (> 2,300) of 18 species occurring on fifty 2 × 2 m permanent plots organized in a 5 × 10 array. The site is on a southeast-oriented ridgeline with a ∼20° slope. Soil development at this site is very limited, with only 5-10 cm of fine scree over bedrock. The growing season is short, as snow cover typically occurs from October to June. Vegetation is patchy with low cover (∼14.5% in 2014) (Figure 2.1). Eighteen perennial species are found at the site, including (in order of greatest abundance during the 2014 census) *Lupinus argenteus* (33.6%, Fabaceae), *Ivesia gordonii* (17.1%, Rosaceae), *Eriogonum umbellatum* (14.2%,

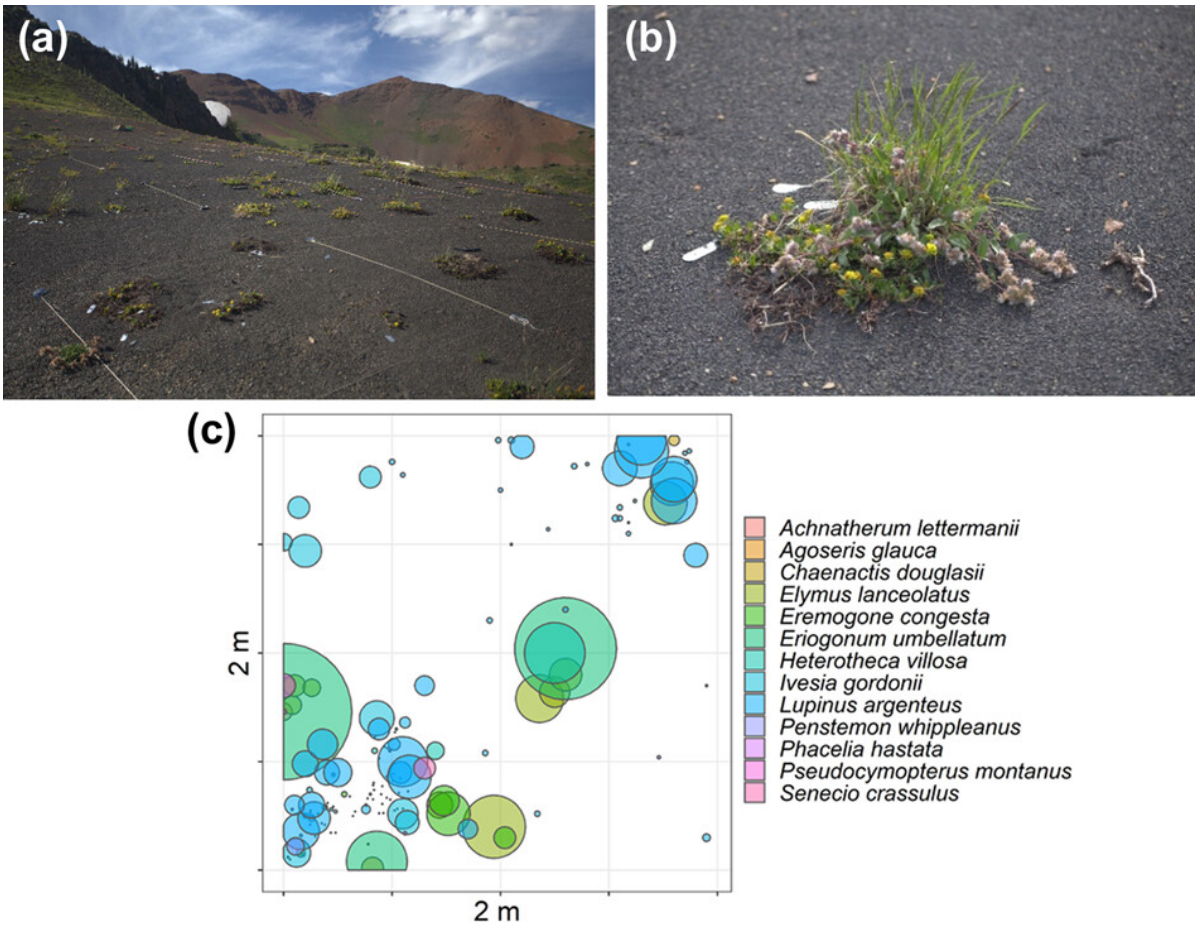

Figure 2.1: (a) A photograph of the study site during the growing season showing an open landscape with clustered vegetation. Plots are visible via white string boundaries. (b) An example vegetative cluster with high overlap featuring *E. umbellatum* (yellow flowers), *E. lanceolatus* (grass), and *P. hastata* (pink flowers). (c) Circular polygons generated from census data from plot 20 in 2015. Polygons are scaled to the size of the plant with a distinct color for each taxon.

Polygonaceae), *Elymus lanceolatus* (13.7%, Poaceae), *Heterotheca villosa* (7.7%, Asteraceae), and *Carex siccata* (3.4%, Cyperaceae). The site and species list are described in detail in [12].

Microenvironment descriptors

To address Q1, we determined the existence and strength of microenvironment modification of surface temperature and soil moisture across several species. In 2016 and 2018, we measured surface temperatures (°C) across this site using iButton data loggers (Thermochron DS1921G, Maxim, San Jose, CA, USA). Data loggers were placed at soil level after being sealed in Parafilm (Bemis Company, Inc, Neenah, WI, USA) and grey duct tape

for waterproofing and to roughly match the reflectance of the soil substrate, following the method of [112]. Temperatures measured by data loggers are not exactly equal to substrate temperature due to radiative loading, among other factors, especially in high light environments such as the alpine [70]. Deviations from true temperatures are expected to be greatest for maximum temperatures (typically during the afternoon), rather than minimum temperatures (typically during low light conditions). However, temperatures should be comparable across species. All temperature data were collected at 20-minute intervals. We summarized these data as maximum and minimum temperatures during deployment for each logger and each year.

We measured microenvironment within the canopy of a subset of species that were abundant in the plots and represented a range of growth forms, including erect dicotyledons (*Agoseris glauca* (Asteraceae), *L. argenteus*, *Senecio crassulus* (Asteraceae)), rosette dicotyledons (*Eremogone congesta* (Caryophyllaceae), *I. gordonii*, *Phacelia hastata* (Boraginaceae)), erect monocotyledons (*E. lanceolatus*, *Stipa lettermanii* (Poaceae)), and deciduous dicotyledonous shrubs (*E. umbellatum*, *H. villosa*) (sensu [121, 17]). We avoided measuring microenvironment within focal plants growing in clusters of multiple individuals. For plant-level measurements, data loggers were placed under the vegetative edge of each individual.

For 26 days during the growing season in 2016, we collected surface temperatures beneath 86 randomly selected focal plants of 9 common species (*A. glauca* (n=6), *E. lanceolatus* (n=13), *E. umbellatum* (n=11), *H. villosa* (n=10), *I. gordonii* (n=13), *L. argenteus* (n=10), *P. hastata* (n=8), *S. crassulus* (n=7), *S. lettermanii* (n=8)). Focal plants were selected randomly among censused individuals with vegetative diameters > 1 cm. Concurrently, we also collected temperature data at 91 plot corners, with data loggers at the upper left and bottom right corners of each plot. These plot corners were non-vegetated and selected to allow comparison with the plant-level measurements.

Using similar methods, in 2018, we augmented the data by measuring surface temperatures for 26 days under the canopy edge of 81 randomly selected individuals of 7 species: *E. lanceolatus* (n=12), *E. congesta* (n=10), *E. umbellatum* (n=14), *H. villosa* (n=10), *I. gordonii* (n=12), *L. argenteus* (n=13), *S. crassulus* (n=10). Six of these taxa were also sampled in 2016. However, in contrast to 2016, as a non-vegetated comparison, the iButtons were placed in a non-vegetated location 10 cm from the plant edge in a randomly selected direction. We used this paired vegetated versus non-vegetated sampling design in 2018 to reduce any effects of spatial distance on microsite microclimate.

We measured soil volumetric water content (%) at 3.8 cm depth on 9 August 2016 with a FieldScout TDR 100 probe (Spectrum Technologies, Aurora, IL, USA). We selected this depth because the substrate becomes very rocky at deeper depths. Upon inserting the probe vertically into the substrate, we allowed the instrument to equilibrate for a few seconds prior to measurement. We used the same calibration for all measurements. Measurements were taken at the edge of 134 individuals of 11 species: *A. glauca* (n=9), *Chaenactis douglasii* (Asteraceae, n=7), *E. lanceolatus* (n=17), *E. congesta* (n=6), *E. umbellatum* (n=16), *H. villosa* (n=14), *I. gordonii* (n=19), *L. argenteus* (n=21), *P. hastata* (n=9), *S. crassulus* (n=8), and *S. lettermanii* (n=8). For comparison, a paired measurement was also taken in

a non-vegetated area at least 10 cm from each focal individual, and as far as 50 cm to avoid other plants. Soil moisture was measured after rains on 6 August 2016. This timing allowed soil conditions to equilibrate across the site and for microsite variation in soil moisture to develop over least two full days of zero precipitation.

Vital rates

To address Q2, we mapped plant locations and determined survival, growth, and fecundity using the following methods for each individual and census year. Survival: we considered plants to be alive if they produced aboveground biomass. Because vegetative dormancy is common in this community, especially in response to stress, we did not consider plants to be dead unless they failed to produce any aboveground biomass for two consecutive years. Growth: we calculated growth as the change in the maximum length of the individual (cm) from year t to year t+1. Fecundity: we counted the number of inflorescences per individual during the peak growing season.

Macroclimate

To capture interannual differences in macroclimate (i.e., regional climate) as a predictor in the vital rate models (Q2), we calculated the total precipitation during the growing season of each year (defined as the period between the first snow-free day in early summer and the last day before the first severe freeze in fall (below 25°F/-3.89°C), following [51]. We included growing season precipitation in the vital rate models to capture interannual macroclimatic variation because we observed strong variation in precipitation throughout the study period including decreases in the mean and standard deviation between 2016-2019. We also anticipated that growing season precipitation would be an important driver of plant population dynamics because the substrate at our site is very shallow (∼5-10 cm) and porous. All climate data were downloaded from the 'Schofield Pass' SNOTEL (737) station (USDA-NRCS, downloaded 24 Oct 2019), ∼4.3 km from and ∼300 m lower than the field site.

Belowground spatial extent

In 2015 and 2016, we measured belowground maximum rooting diameters in an area adjacent to our field site by excavating 3-5 individuals for each of 16 species and measuring the maximum horizontal rooting extent [12]. Of the 18 species in our census plots, we were unable to measure belowground maximum diameters for two species: *Poa stenantha* (Poaceae) and one species recorded as a single unknown seedling in 2014. To estimate the belowground spatial extent for all individuals, we calculated a taxon-specific allometric scaling factor between aboveground maximum diameter and belowground maximum diameter. For each taxon, we fitted linear regression models between aboveground and belowground maximum extent. For all regressions, the y-intercept was set to 0 to match the expectation of zero belowground root extent for individuals with aboveground diameters of 0 cm, recognizing that this may vary for individuals experiencing aboveground dieback. We used the product of the above-to-belowground scaling factor (i.e., the corresponding taxon-specific regression slope) and the maximum aboveground length to estimate the belowground size

of all individuals. In subsequent analyses, the above-to-belowground scaling factor of *P. stenantha* was assumed to be equivalent to *E. lanceolatus* as they are both in the same subfamily (Pooideae). The calculated R^2 values ranged from 56% (*L. argenteus*) to 99.6% (*Penstemon whippleanus* (Plantaginaceae)) with a mean of 88% (sd = 13%, $n = 16$).

Intraspecific and interspecific percent overlap

We measured how vegetative overlap affects vital rates using interspecific and intraspecific percent overlap as proxies for microenvironment modification. This proxy was chosen because results from the above measurements demonstrate that overlap influences microenvironment modification. However, we used overlap instead of the direct microenvironment modification values measured above, as modification may not scale additively in multi-individual and multi-species-level contexts. We defined percent overlap as the percent cumulative overlap, summed for each instance of overlap. To determine which individuals have overlapping distributions and the extent of overlap, we mapped each individual at our site using x-y coordinates measured in the field. We then assumed that each plant was a circular polygon with a diameter equal to its maximum length as measured in the field. Although *E. congesta*, *E. umbellatum*, and *H. villosa* have a greater tendency to deviate from a circular growth form than other species, especially due to dieback, this growth pattern is uncommon, and a circular polygon is appropriate in the vast majority of cases. From the mapped polygons, we determined the area of overlap for each occurrence and what percentage of each plant was overlapped by inter- and intraspecific individuals. Because plants may extend outside of the censused plot area where we do not have data on plant distributions, only the area of each plant within the plot was used in these calculations. To compare how microenvironment modification estimates vary above- and belowground, inter- and intraspecific percent overlap was similarly determined using polygons calculated based on observed aboveground extent and estimated belowground extent.

Statistical Analyses

Microenvironment modification by taxon (Q1)

Surface temperature

Because surface temperature measurements in non-vegetated areas in 2018 were paired with measurements made within individual plants, we first tested for species-level differences in minimum and maximum temperatures in 2018 using ANOVA ($\alpha = 0.05$) to determine whether they could be treated as comparable to the 2016 non-vegetated plot corner measurements. Minimum and maximum temperatures were the lowest and highest values recorded while deployed for each temperature data logger, respectively. We used Tukey's honest significance test for post hoc analysis following ANOVA ($\alpha = 0.05$). Temperatures measured in non-vegetated areas in 2016 (at plot corners) and 2018 (10 cm from focal plants) were used as references to assess temperature modification extent and were treated similarly in all subsequent analyses. For each year (2016 & 2018), we separately tested whether minimum and maximum surface temperatures differed between vegetated and non-vegetated

areas using generalized linear models (GLM) with Gaussian families and identity link functions. As the 2016 surface temperature data was unpaired to a specific individual or taxon, we used taxon as our predictor variable and treated non-vegetated areas as an additional 'species' in our model. For each species, we used Tukey contrasts, ($\alpha = 0.05$), to assess differences from non-vegetated areas. We also compared site-wide variation in minimum and maximum temperatures between vegetated and non-vegetated microenvironments for 2016 and 2018 data. For this, we used Mann-Whitney U tests for non-normally distributed data and Welch's t tests for normally distributed data with unequal variance, as appropriate.

Soil moisture

We compared soil volumetric water content (%) at the edge of plants (distance = 0 cm) and paired non-vegetated areas across 11 species using a generalized linear mixed model (GLMM) with taxon, distance, and their interaction as fixed effects (family=Gaussian, link=identity). Plot was a random effect to address across-site variation. To compare soil moisture in vegetated and non-vegetated areas within taxa we used least-squares means ($\alpha = 0.05$). We assessed site-level variation in soil moisture between plants and paired non-vegetated areas using a Welch's two-sample t test. Soil moisture data were log-transformed before analysis to achieve normality. For the site-level analysis, we also included data from 10 individuals from 5 taxa that had insufficient replication for inclusion in the taxonomic analysis: *Arnica latifolia* (n=4, Asteraceae), *C. siccata* (n=1), *P. stenantha* (n=2), *Cymopterus lemmonii* (n=2, Apiaceae), and *Viola praemorsa* (n=1, Violaceae).

Vital rates response (Q2)

For each vital rate, we fitted an aboveground model (AG) and a belowground model (BG), using above- and belowground spatial overlap estimates. Correlation among fixed effects was low in both above- and belowground models. We used GLMMs to model vital rate responses to microenvironment modification via our vegetative overlap proxies. For each vital rate (survival, growth, fecundity), we constructed a GLMM with the following structure (in lme4 syntax).

$$
\begin{aligned}
&\textit{Vital Rate} \sim \\
&\textit{Growing.season.precipitation} \times \textit{Size} \times \textit{Interspecific.percent.overlap} + \\
&\textit{Growing.season.precipitation} \times \textit{Size} \times \textit{Intraspecific.percent.overlap} + \\
&(1|\textit{Plot}) + \\
&(1|\textit{Taxon})
\end{aligned}
$$

In addition to growing season precipitation and inter- and intraspecific percent overlap, plant size was included as a fixed effect because it is a strong driver of variation in vital rates, including alpine systems [56, 85]. In all models, we used taxon-scaled size values (divided by the 90th percentile across all years) to reduce variation in size across species. All fixed effects were z-transformed (zero mean, unit variance) before model fitting to allow standardized comparison and interpretation of the estimated effects. For those vital rates

quantified as probabilities (survival and flowering probability), we used odds ratios to determine significance. Predictors with odds ratios < 1 have a negative association with the vital rate, predictors with odds ratios > 1 have a positive association, and predictors with an odds ratio of 1 have no association. We included taxon as a random effect to account for nesting of individuals within species and to estimate among-species variance in mean vital rates. Plot was included as a random effect to partially account for spatial autocorrelation. We conducted vital rate analyses for the six most abundant species (*C. siccata*, *E. lanceolatus*, *E. umbellatum*, *H. villosa*, *I. gordonii*, *L. argenteus*). In the growth models, the number of individuals per species ranged from 27 (*H. villosa* in 2018) to 372 (*L. argenteus* in 2016). The average number of individuals per taxon and year in the growth models was 124.6 (sd=82.7).

As required by the model structure and to address our questions, we formatted the vital rate data and constructed the GLMMs as follows.

Survival: we used macroclimate (growing season precipitation), size, and neighborhood data in year t to predict survival in year t+1. This model structure allowed us to include size as a predictor because by definition all plants with size=0 cm for two consecutive years are dead. We fitted a logistic regression model (binomial error distribution, logit link function). Data from the 2020 census were used to confirm the mortality of plants with size=0 cm in 2019.

Growth: We analyzed growth using a Gaussian model (identity link function). We used taxon-scaled growth values (divided by the 90th percentile across 2015-2019) and excluded dead plants from the model because any change in their size would reflect mortality. We also excluded first-year plants and plants from the initial census year (2014) as they did not have growth data.

Fecundity: we analyzed fecundity using two models. For the first model, we fitted a logistic regression model (binomial error distribution, logit link function) to model flowering probability. For the second model, we analyzed the number of inflorescences of flowering individuals using a Gaussian model (identity link function). Dead individuals and seedlings were excluded from both fecundity models, while non-flowering individuals were excluded from the model of the number of inflorescences. To account for taxonomic differences in inflorescence number, the number of inflorescences was scaled by dividing by the 90th fecundity percentile across all years for each taxon because the number of inflorescences is comparable within, but not between species. The scaled fecundity values were also log-transformed to limit overdispersion. Model residuals met assumptions in all models.

We conducted all analyses in R, version 4.1.2 [115]. We used lme4 [7] to calculate the GLMMs. Post-hoc tests for the microenvironment analyses were done using multcomp [46] and emmeans [64]. We used the packages sf [89], sp [90], and rgeos [10] to estimate spatial overlap. We used DHARMa [42] to check for over- and underdispersion of the residuals and PerformanceAnalytics [92] to assess correlations among model terms. GGally [106] was used to generate correlation plots and we used pdp [41] to generate partial dependence plots.

2.3 Results

Microenvironment modification by taxon

Surface temperature

In non-vegetated areas in 2018, maximum temperatures ranged from 51.5-64.0 ℃ across species. We detected no significant differences in maximum temperatures among species (ANOVA: F6, 73 = 1.75, P =0.12). In contrast, the range of minimum temperatures in non-vegetated areas in 2018 was much narrower (1.5-4.5 ℃) and differed depending on the focal plant species (ANOVA: F6, 73 = 2.23, P =0.05), likely reflecting species-specific variation in microenvironment preference. However, we did not detect differences in minimum temperatures in post hoc pairwise comparisons of species, though differences between *E. congesta* and *L. argenteus* were close to the ($\alpha = 0.05$) threshold (Tukey contrast: P=0.054).

Maximum temperatures were lower within versus outside vegetation in 2016 (Mann-Whitney: U = 1532, n1 = 91, n2 = 83, P < 0.001) and 2018 (Welch's two-sample t-test: t=-5.1572, =122.54, P < 0.001). Maximum surface temperatures were lower within the canopies of 7 out of 9 species in 2016 and 4 out of 7 species in 2018 compared to non-vegetated areas (Figure 2.2a). We observed cooling effects for all focal erect monocotyledons:*E. lanceolatus* (Mean cooling, ℃: 2016=-5.19; 2018=-4.40), *S. lettermanii* (2016=-6.80). Among erect dicotyledons (*A. glauca*, *L. argenteus*, *S crassulus*), we only observed cooling effects for *L. argenteus* (2016=-5.58, 2018=-8.02). For rosette dicotyledons, maximum temperatures were lower in *I. gordonii* (2016=-6.30, 2018=-4.15) and *P. hastata* (2016=-8.73), but not *E. congesta*. Finally, for deciduous dicotyledonous shrubs, maximum temperatures were cooler for *H. villosa* in both years (2016=-4.97, 2018=-6.23), but were only cooler for *E. umbellatum* in 2016 (-6.17).

Minimum temperatures were higher within versus outside vegetation in 2016 (Mann-Whitney: U = 6678, n1 = 91, n2 = 83, P < 0.001) and in 2018 (Mann-Whitney: U = 4940.5, n1 = 80, n2 = 80, P < 0.001). Minimum temperatures were higher within the canopies of 8 out of 9 species than in non-vegetated areas in 2016 and 3 out of 7 species in 2018 (Figure 2.2b). Minimum temperatures were warmer for erect monocotyledons in 2016 (mean warming, ℃: *E. lanceolatus* (2016=+1.43); *S. lettermanii* (2016=+1.51)), but not for *E. lanceolatus* in 2018. Warmer minimum temperatures were also observed for some, but not all, rosette dicotyledons and years: *L. argenteus* (2016=+1.73, 2018=+1.13); *S. crassulus* (2016=+1.51). Modification trends for warming for rosette dicotyledons and deciduous dicotyledonous shrubs were similar to those found for cooling. Warming was observed in 2016 and 2018 in *I. gordonii* (2016=+2.31, 2018=+1.26), *P. hastata* (2016=+2.43), and *H. villosa* (2016=+1.84, 2018=+0.90), but was only observed in 2016 for *E. umbellatum* (+2.23).

Soil moisture

At the site level, soils were wetter within plants compared to non-vegetated areas (Welch's two-sample t-test: t= 6.2668, =271.97, P < 0.001). The substrate below 5 out of 11 plant species had higher volumetric water content (%) than in adjacent non-vegetated areas

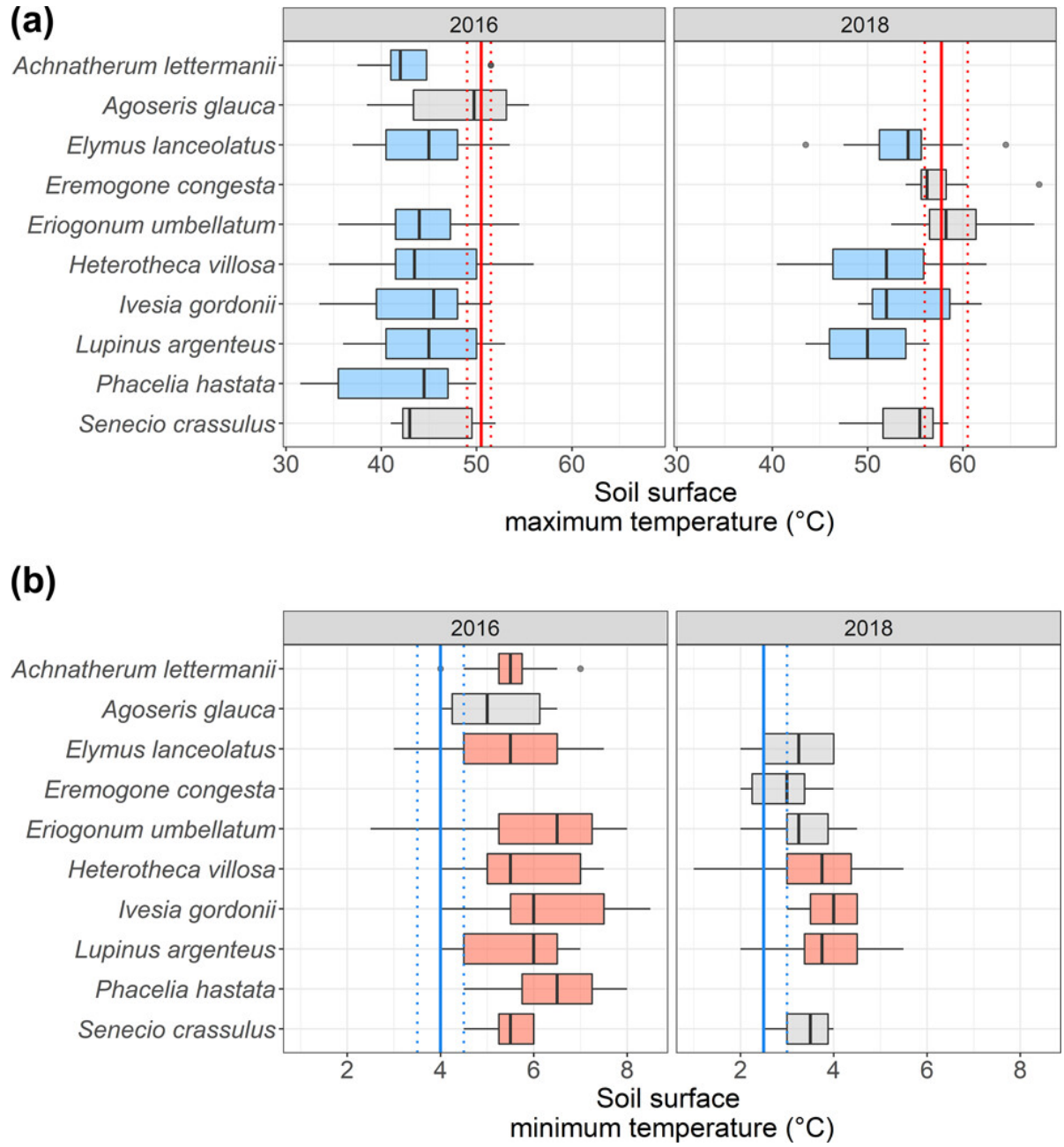

Figure 2.2: (a) Maximum and (b) minimum temperatures (°C) of data loggers within the canopies of selected alpine plant species (n = 9 in 2016 and 7 in 2018) and non-vegetated areas. The selected taxa were among the most abundant in the community and represented a range of growth forms. All focal plants had a vegetative diameter > 1 cm. Vertical bands indicate measured values in non-vegetated areas: leftmost line = 1st quartile, middle line = median, rightmost line = 3rd quartile, with red bands for maximum temperatures and blue bands for minimum temperatures. For minimum temperatures in 2018, the first quartile is equal to the median. Blue and red boxplots indicate statistically significant differences from non-vegetated areas.

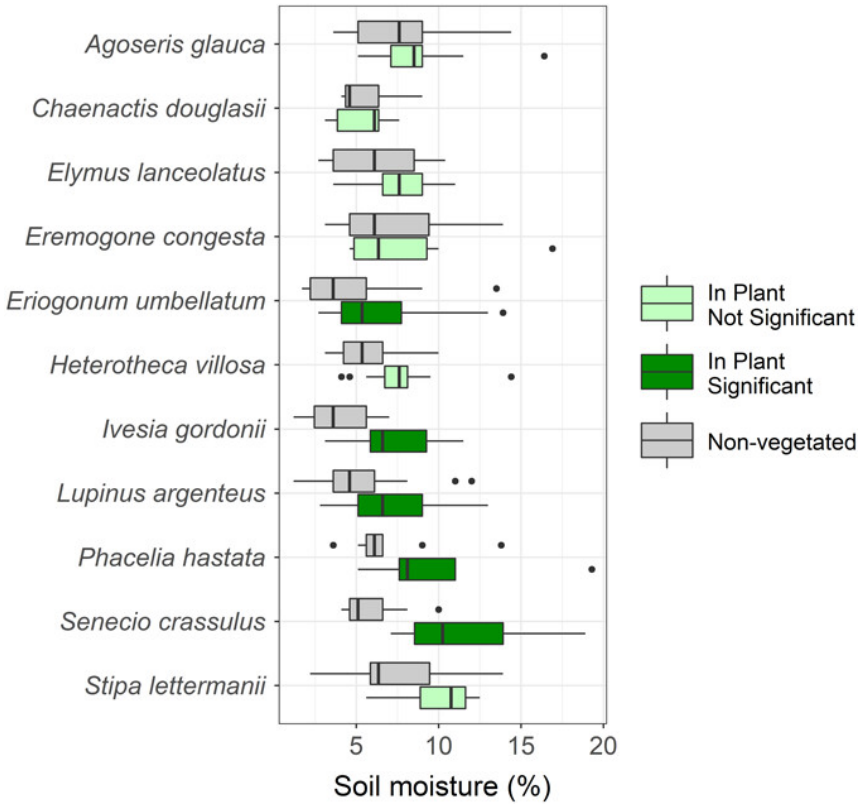

Figure 2.3: Soil moisture inside and outside of plants for 11 species in 2016. The selected taxa were among the most abundant in the community and represented a range of growth forms. All focal plants had a vegetative diameter > 1 cm. Dark green boxes indicate statistically significant differences compared to the non-vegetated comparison.

(mean difference below plants, %: *E. umbellatum* (+1.87), *I. gordonii* (+3.33), *L. argenteus* (+1.99), *P. hastata* (+2.48), and *S. crassulus* (+5.34)) (Figure 2.3). Two additional species (*H. villosa* and *S. lettermanii*) trended towards wetter soil at the plant level (median in plant values > 3rd quartile non-vegetated values), but with weak statistical support.

Vital rate responses

For our microclimate modification proxies, interspecific and intraspecific overlap, effects on vital rates varied. Interspecific percent overlap had negative effects on survival probability (Aboveground model (AG): confidence interval=0.83–1.00; Belowground model (BG): 0.65–0.81), flowering probability (AG: 0.75–0.94; BG: 0.68–0.89), and number of inflorescences (AG: -0.13 to -0.02), but a positive effect on growth (BG: 0.05–0.13). Intraspecific percent overlap, on the other hand, had a positive effect on flowering probability (BG:

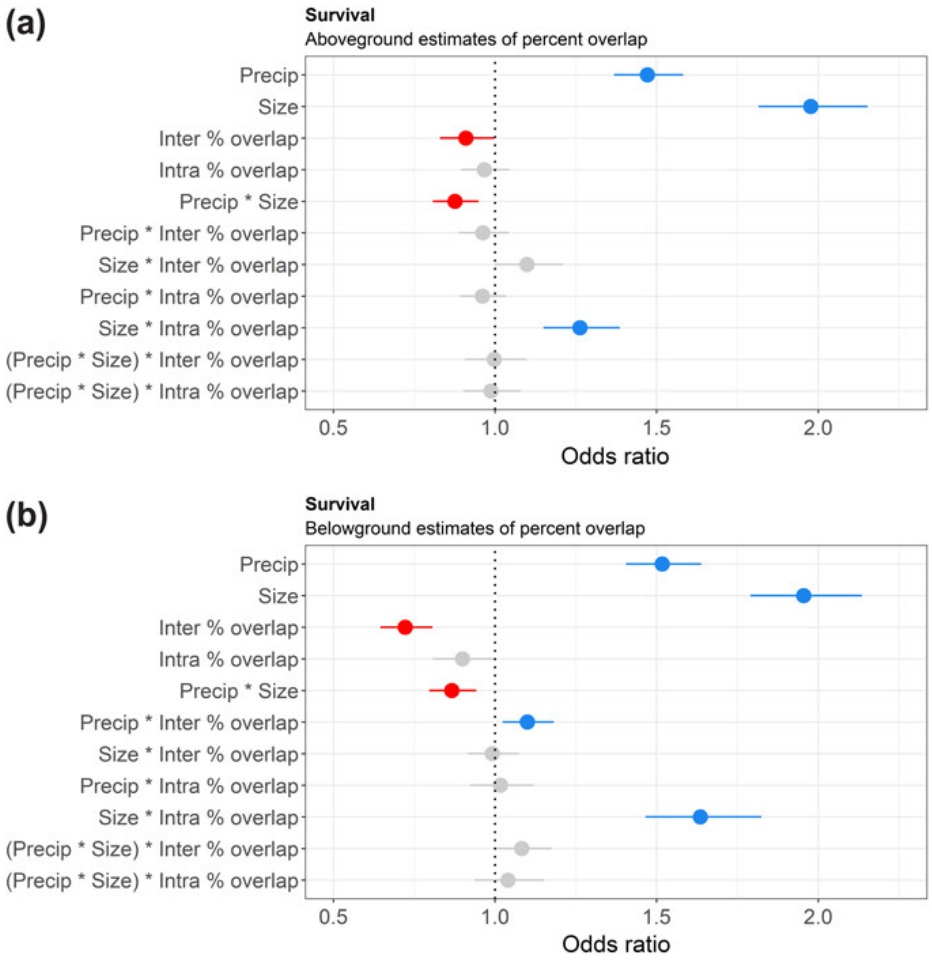

Figure 2.4: Odds ratios with 95% confidence intervals for standardized fixed effects in the models describing survival probability. Estimates of vegetative percent overlap were based on (a) aboveground and (b) belowground biomass.

1.03–1.35) and a negative effect on inflorescence production (BG: -0.17 to -0.04).

The effects of species interactions on vital rates were also context dependent. For larger plants, interspecific percent overlap had a weaker effect on growth (AG: -0.08 to -0.01), flowering probability (BG: 0.72–0.88), and inflorescence production (AG: -0.10–0.00; BG: -0.13 to -0.04). In contrast, for larger plants, there was an increased positive effect of intraspecific overlap on survival (AG: 1.15–1.39; BG: 1.47–1.82), growth (AG: 0.01–0.08), flowering probability (BG: 1.34–1.78), and inflorescence production (BG: 0.02–0.12).

The effects of species interactions on vital rates also depended on interactions with macroclimate. In wetter years, there was a positive effect of interspecific overlap on survival (BG: 1.02–1.18) and growth (AG: 0.04–0.10; BG: 0.01–0.07). Flower production was lower for plants with greater interspecific overlap in wetter years (AG: -0.11 to -0.01; BG: -0.11–0.00).

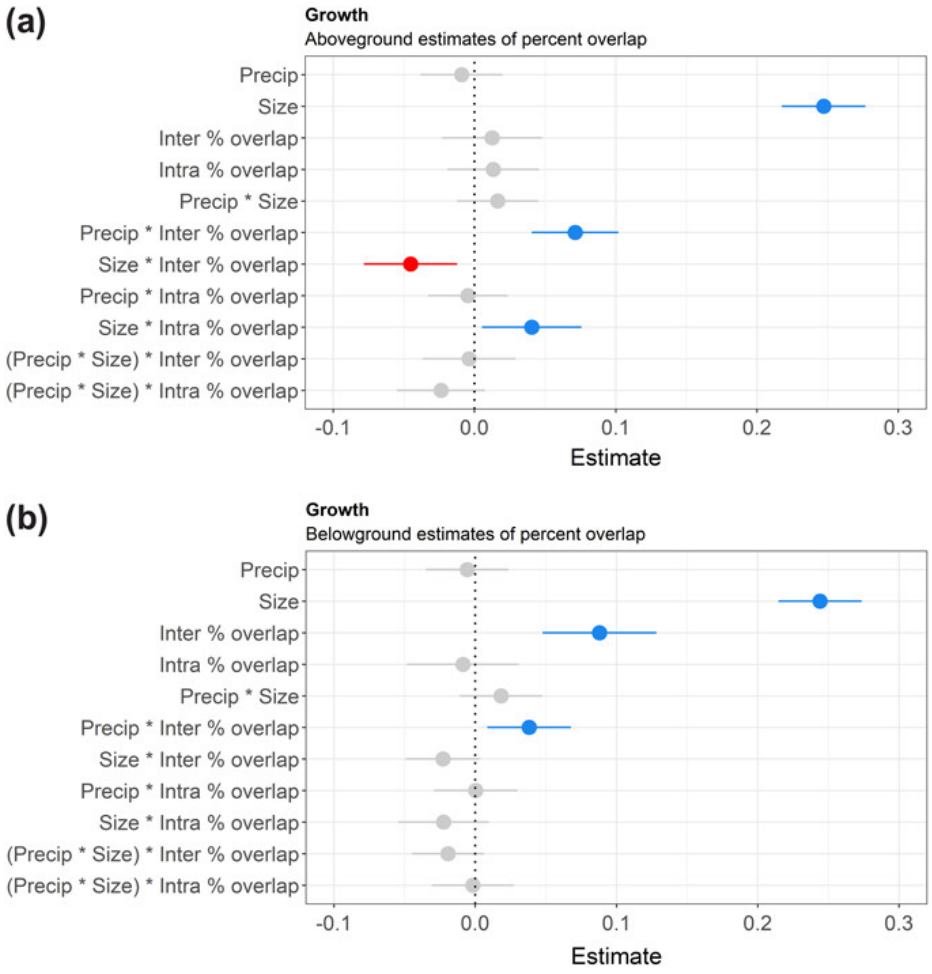

Figure 2.5: Parameter estimates with 95% confidence intervals for standardized fixed effects in the models describing growth. Estimates of vegetative percent overlap were based on (a) aboveground and (b) belowground biomass.

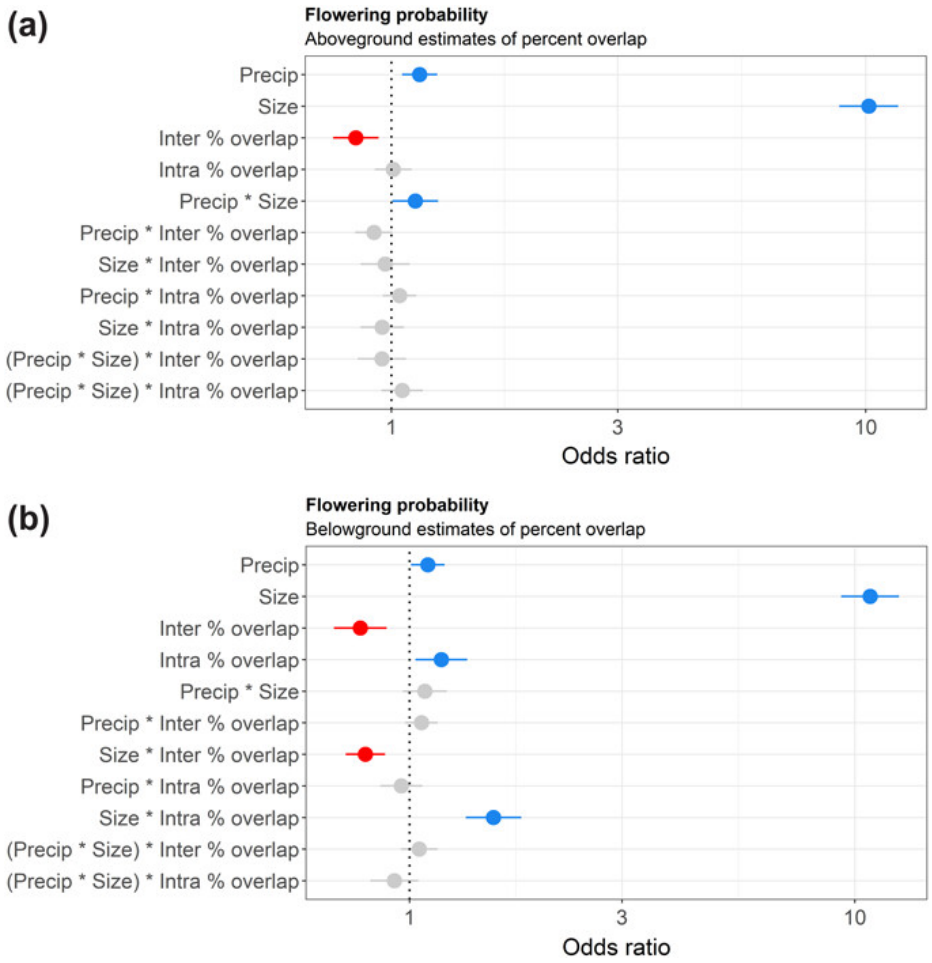

Figure 2.6: Odds ratios with 95% confidence intervals for standardized fixed effects in the models describing flowering probability. Estimates of vegetative percent overlap were based on (a) aboveground and (b) belowground biomass. The x-axes were log10 transformed to improve data visualization.

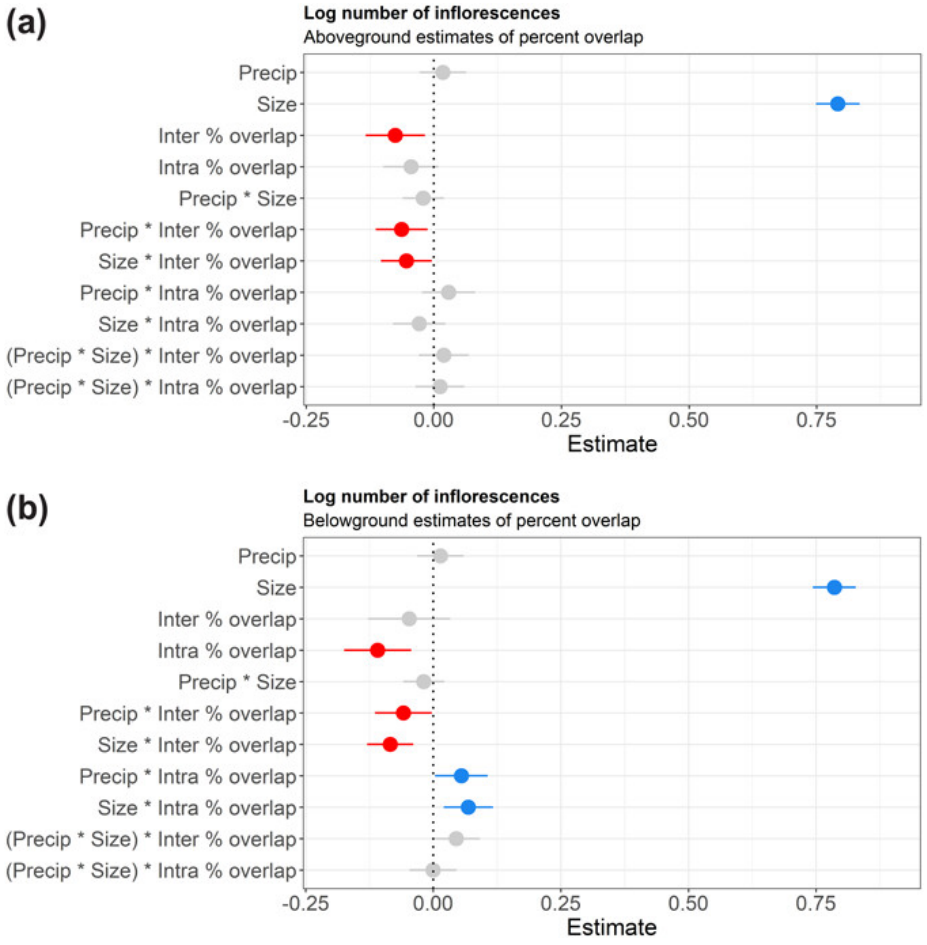

Figure 2.7: Parameter estimates with 95% confidence intervals for standardized fixed effects in the models describing the log number of inflorescences. Estimates of vegetative percent overlap were based on (a) aboveground and (b) belowground biomass.

However, intraspecific percent overlap had a positive effect on inflorescence production in wetter years (BG: 0.00–0.11).

Additionally, we observed positive effects of growing season precipitation and size on vital rates. Survival increased in years with higher precipitation (AG: 1.37–1.58; BG: 1.41–1.64). Flowering was also more likely in wetter years (AG: 1.05–1.25; BG: 1.01–1.20). Larger plants survived better (AG: 1.82–2.15; BG: 1.79–2.13) and grew more (AG: 0.22–0.28; BG: 0.21–0.27). Flowering was more likely for larger plants (AG: 8.79–11.71; BG: 9.32–12.57) and larger plants produced more inflorescences (AG: 0.75–0.83; BG: 0.74–0.83). Larger plants were more likely to flower in wetter years (AG: 1.01–1.26). However, the effect of size on survival was weaker in wetter years in the above- and belowground models (AG: 0.81–0.95; BG: 0.80–0.94). Above- and belowground model results for survival, growth,

flowering probability, and number of inflorescences are in Figures 2.4-2.7.

2.4 Discussion

In this alpine plant community, plants modified microenvironments by buffering temperature extremes (lower maximum and higher minimum surface temperatures) and by increasing soil moisture relative to open areas. Variation in multiple vital rates was attributable to variation in above- and belowground microenvironment modification proxies (inter- and intraspecific percent overlaps), which were frequently context dependent. These results illustrate the complex interplay between spatial overlap, microenvironment, and macroclimate on demography and community assembly.

Microenvironment

Surface temperatures and soil moisture differed between vegetated and non-vegetated microsites. Nearly all considered taxa buffered temperatures in this community and 5 out of 11 increased soil moisture. Temperature buffering operated separately from increasing soil moisture for some taxa. For example, *E. lanceolatus*, *H. villosa*, and *S. lettermanii* buffered maximum and minimum temperatures in 2016 but did not increase soil moisture. On the other hand, soil moisture near *S. crassulus* was higher than non-vegetated areas in 2016, but we did not detect buffered maximum temperatures in the same year.

As alpine areas are frequently characterized by high levels of microenvironment heterogeneity, with plant distributions reflective of this variation [95, 86, 84], these microclimate differences may reflect plant microenvironment preference. However, we consider this to be unlikely because nearly all non-vegetated microclimate data were collected at fine-scales—10 cm from the edge of the focal plants. Also, as we observed limited dependency of six environmental variables on plant size; thus, plants with greater capacity to modify microenvironments and potential to host neighbors, do not preferentially occupy more buffered microsites. Finally, our prior work examining other abiotic gradients [12] suggests it is unlikely that sub-meter scale variation or modification in soil texture or nutrient availability is occurring, though we lack data to directly assess such factors.

Our results indicate that the extent of microenvironment modification can vary across years. We observed fewer statistically detectable differences in surface temperature buffering in 2018 compared to 2016, although nearly all taxa trended towards temperature buffering for both years. Different methodology may have contributed to lower buffering values in 2018 compared to 2016 as focal plants varied between years and non-vegetated measurements were typically taken spatially closer to vegetation in 2018. Decreased plant health may have also led to weaker surface temperature buffering in 2018. Average growing season precipitation values were low in 2016-2018, and after multiple drought years, plants in 2018 appeared sparser compared to previous years. Buffering temperatures may have also been more difficult in 2018 as median soil surface temperature maximums were higher in 2018

than in 2016 and median soil surface temperature minimums were lower in 2018 than in 2016.

Context dependency of interactions

The effects of inter- and intraspecific percent overlap varied among vital rates and depended on whether above- or belowground spatial extents were considered in the models. As belowground extents were estimated from aboveground plant length, differences between model results using above- versus belowground percent cover could be greater if 'true' rather than estimated belowground extents could be included. However, even with estimated belowground extents, our results demonstrate the sensitivity of the vital rate analyses to the microenvironment modification proxy used and highlight the importance for future studies to consider how the spatial extents of modification may differ across ecological realms (e.g., above- and belowground).

Interspecific overlap had detectable effects on vital rates in six out of eight models, five of which were negative. In comparison, we found positive effects of intraspecific percent overlap on flowering probability (belowground, BG), but negative effects on the number of inflorescences produced (BG). Based on our microenvironment data and microenvironment modification results from previous studies in tundra systems (e.g., [83, 73]), we expect that plants with higher inter- or intraspecific percent overlap experience a more buffered microenvironment compared to plants with low to no overlap. Thus, the divergent responses in vital rates to inter- and intraspecific percent overlap might indicate greater competition among heterospecific neighbors compared to conspecific neighbors. Alternatively, this divergence may represent different demographic strategies under distinct microenvironment conditions. However, we are unable to disentangle the microenvironment effect from other possible effects of overlap, including increased structural support, and higher pollinator visitation rates. As many plants in this community grow in dense, heterogeneous clusters, individuals may simultaneously experience an array of competitive and facilitative neighbor effects that cannot be disentangled through net effect measurements like ours [4].

We found that growing season precipitation was a positive driver of survival (aboveground, AG & BG) and flowering probability (AG & BG). We observed weaker effects of precipitation on survival for larger plants (AG & BG), suggesting that larger individuals were less prone to drought-induced mortality. Larger plants were also more likely to flower with increased growing season precipitation (AG), further indicating that demographic strategies may differ for large versus small individuals.

Macroclimatic conditions varied substantially during this study and species interactions often varied in response to variation in growing season precipitation. Because water limitation may have led to widespread physiological stress in this community, facilitation among species may be limited during drought years [71] or masked by competitive effects. Under lower growing season precipitation, intraspecific overlap negatively affected the number of inflorescences (BG), and interspecific overlap negatively affected growth (AG & BG) and survival (BG). We also did observe some evidence for facilitation in dry years which may be due

to microclimate modification—a negative interaction between precipitation and interspecific overlap on number of inflorescences (AG & BG). As the integrated effects of environmental context on vital rates determine plant performance, the contrasting effects of these predictors may represent demographic tradeoffs [99, 113] with multiple potential drivers. For example, prioritizing growth and thus accessibility to resources could be advantageous when potential interspecific competitors are also benefiting from favorable environmental conditions. Additionally, there could also be facilitative effects between growing season precipitation and interspecific and intraspecific overlap if neighboring plants are better able to ameliorate the microclimate under good conditions, such as by increasing soil water retention or shading due to higher leaf output.

By directly testing for microenvironment modification and pairing that to data on vegetative overlap, we show that modification is associated with variation in vital rates. Previously at this site, [12] found that spatial distributions of plants were predictable by microenvironment (including soil moisture, soil nutrients, and surface temperatures), neighborhood density, and plant functional traits. This finding was based partially on neighborhood density indices, which are less precise proxies for microenvironment modification. Additional levels of complexity influencing vital rates, but not included in this study include species-level variation in vital rate response [53] and vital rate lability [54].

Implications for community assembly

First, our results indicate that microenvironment modification affects two community assembly processes, environmental filtering (whether a plant can survive and persist in a given habitat) and biotic interactions (ability to co-occur with other community members) [44]. Second, shifts in spatial patterning due to microenvironment modification likely can result in order-dependent assembly, as seedling establishment depends on habitats created by resident species.

How microenvironments are modified by plants has important implications for how communities will respond to climate change [3]. Future alpine communities may experience increased dependence on species interactions to buffer temperature extremes and decreases in water availability. However, macroclimate shifts may also lead to context-dependent effects on microclimate modification and thus on demography. For example, growing season precipitation was a positive predictor of plant survival and flowering probability in our models. In response to the predicted intensification of drought conditions in this region [25, 123], this study site is likely to experience shifts in species composition and abundance. Critically, these community shifts could drive feedbacks on species interactions, including microenvironment modification, propelling further community change. Also, climate change response may vary due to the high habitat heterogeneity and decoupling from atmospheric conditions that often occur in alpine communities [59, 105, 102].

Conclusions

In this alpine plant community, we demonstrated substantial microenvironment modification by multiple species, and that the strength of microenvironment modification can vary across years in response to variation in macroclimatic conditions. We observed positive, negative, and neutral effects of inter- and intraspecific vegetation overlap on vital rates, with frequent dependency on context (individual plant size and growing season precipitation). This study indicates that climate change may affect species' ability to modify microenvironments, as well as the effect of microenvironment modification on vital rates.

Chapter 3

Alpine plant species interact via wind-driven seed dispersal and seed retention

Chapter 3 addresses a central challenge in understanding plant community assembly mechanisms—identifying the factors influencing abiotic seed dispersal outcomes. In plant community assembly models, abiotic seed dispersal is frequently assumed to be stochastic or a function of plant height and seed terminal velocity due to the difficulty of tracking small seeds across space. In two experiments, we explore how interactions between seeds and vegetation shape dispersal outcomes. Thus, building off insights into the positive impacts of neighbors from Chapter 2, Chapter 3 explores the mechanical mechanisms that can promote spatial co-occurrence.

3.1 Background

Among sessile and mobility-limited organisms (e.g., plants, fungi, many aquatic invertebrates), species interactions and dispersal mechanisms are often inseparable. Dispersal at early-life stages (e.g., seeds, juveniles, and larvae) allows organisms to find space to establish, acquire resources, and avoid unfavorable conditions at their place of origin (balanced against the risks of ending up in a place less favorable) [52, 79]. For plants in harsh environments such as desert and alpine tundra, seeds frequently depend on dispersal to establish by facilitative neighboring plants (e.g., [110]). While seed dispersal frequently occurs through interactions with animals, including through hitchhiking (e.g., [5]) and gut passage (e.g., [116]), abiotic dispersal mechanisms may also promote plant-plant interactions through wind, rain, snow, and gravity. For example, a plant may affect seed dispersal of another individual or itself by limiting seed movement and through effects on the mechanical processes that underlie abiotic dispersal (e.g., locally slowing or intensifying wind speeds) [67]. Although plant-plant dispersal interactions can impact seed establishment and community assembly processes, in-

cluding density-dependent competition [2, 16], it is unclear for what contexts and species pairs these interactions are most expected [40].

Seed traits and plant morphology may help explain plant-plant dispersal interactions due to their potential to influence seed trapping and retention (Fig 3.1). Seed trapping is when another plant impedes seed movement, while seed retention is when a seed remains in a plant after trapping. Seed size can influence seed trapping [16], but less considered are the contributions of other traits linked to dispersal, including seed shape parameters (length, width, thickness), seed mass, and pappus traits (but see [67]). There is also evidence that seed bank diversity [40] and seed rain [16] differ near and far from plants and vary by functional group (e.g., grasses vs. shrubs) [2]. However, we do not know of any comprehensive comparison of plant ability to trap and retain seeds for multiple species within a community.

Plant-plant dispersal interactions could influence seed success in many contexts. If neighboring plants locally mitigate resource scarcity or buffer unfavorable climatic conditions through processes such as microclimate modification, then species co-location may be favored. These facilitative interactions are often stronger than competition among plants in stringent environments such as drylands and tundra [18, 19], particularly among seedlings and juvenile plants (e.g., [78]). Thus, dispersal mechanisms that promote seed-plant co-location may be under strong selection as an assembly mechanism in communities where facilitation is common.

To explore the potential of seed trapping and retention to mediate plant-plant interactions, we conducted two experiments in an alpine tundra plant community that is frequently windy and where microclimate modification is prevalent [96]. We asked (Q1) if seed functional diversity varies among six common taxa in the community. Then, in the first experiment, we asked (Q2) whether the probability of trapping depended on the host plant taxon, seed taxon, and plant size. In a second experiment focused on retention, we asked (Q3) whether the likelihood of a seed dispersing following entrapment depended on interacting seed and plant taxa, seed traits, and the time between monitoring checks. For Q2 and Q3, we hypothesized that trapping and retention differ among host plant taxa and predicted that plants with shrub form or dense vegetation would have the highest seed trapping and retention rates. We also predicted higher trapping rates in larger plants. Finally, we hypothesized that seed trapping rates and retention would vary by seed traits, and predicted higher trapping and retention rates for seeds that were large, heavy, or had a pappus. We anticipated that post-trapping secondary dispersal would increase with time between monitoring checks.

3.2 Methods

Site Description

We conducted seed trapping and retention experiments in an alpine tundra plant community, 3540 m above sea level, in southwestern Colorado (38.978725°N, 107.042104°W) (Fig 3.2). The site is on a southeast-facing ridgeline with limited soil development and strong winds. The vegetation is patchy, highly clustered, and dominated by perennial graminoids,

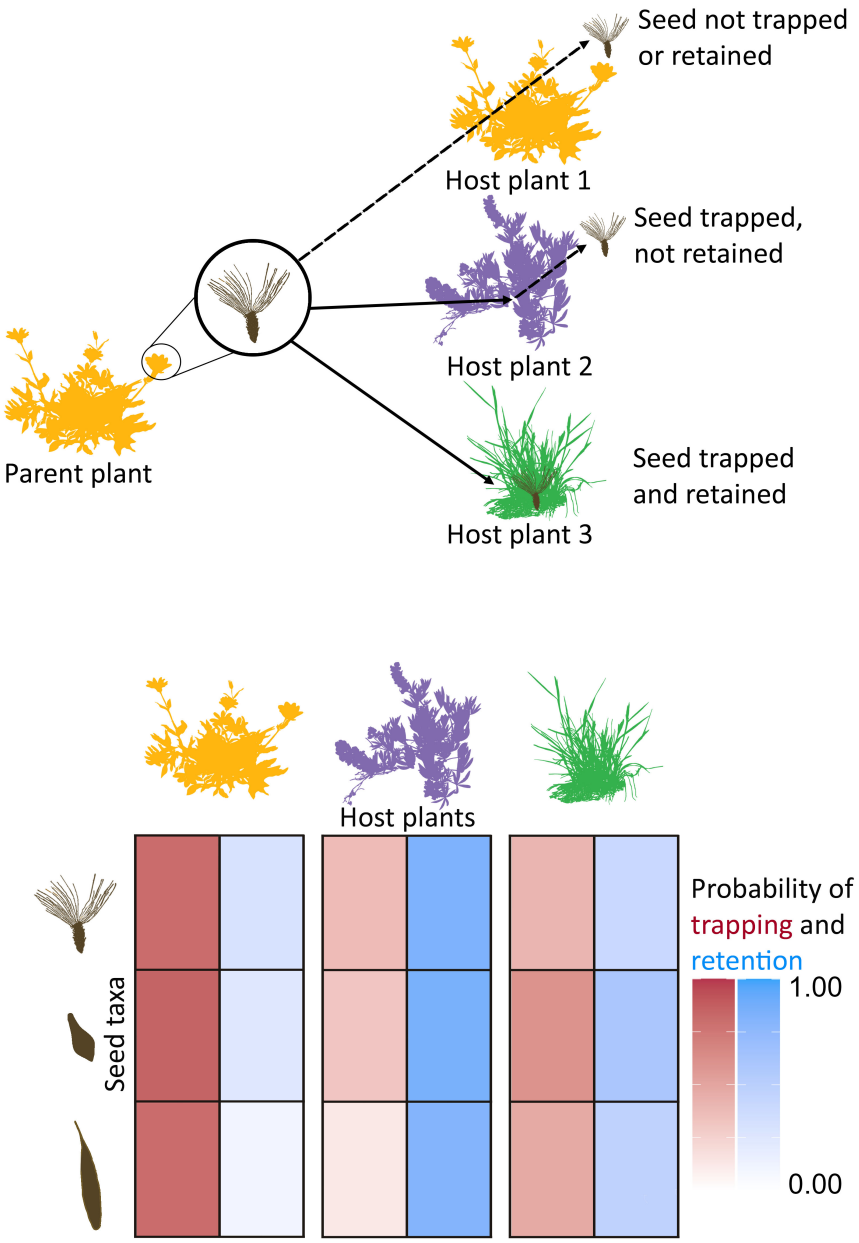

Figure 3.1: Top) Seeds dispersed from a parent plant to host plants may either be 1) not trapped or retained, trapped but not retained, or trapped and retained. Bottom) We hypothesize that due to physical attributes (i.e., size and growth form), plants could be good trappers, but not good retainers (Panel 1), vice versa (Panel 2), or have similar trapping and retention probabilities (Panel 3). Plants may also trap and retain seed comparably across seed taxa (Panel 1 and 2), or trapping may vary by seed taxa (Panel 3).

forbs, and woody shrubs. The growing season is typically from late May to early October. We conducted the seed trapping and retention experiments adjacent (< 150 m) to a long-term demography study (Fig 3.2, [12]. Nineteen taxa occur in the demography study, with higher species richness in the surrounding area. We conducted both experiments late in the growing season (trapping experiment: 1-8 August 2021; retention experiment: 29 August - 11 September 2019) when most species are past flowering and seed dispersal of resident plants is common.

Focal plant and seed description

We selected focal plant and seed taxa to optimize availability and functional differences. For the trapping experiment, we selected two common host taxa, *Heterotheca villosa* (Asteraceae), an erect dicotyledon with a bushy canopy, and *Lupinus argenteus* (Fabaceae), a deciduous dicotyledonous shrub with open canopy (sensu [121, 17]) (Fig 3.3). For the retention experiment, we selected plant taxa that had high abundance in 2018 in the adjacent demography plot and, thus, represented the majority of vegetation in the area that could interact with seeds–erect dicotyledons (*Lupinus argenteus*, *Senecio crassulus* (Asteraceae)), an erect monocotyledon (*Elymus lanceolatus* (Poaceae)), a rosette dicotyledon (*Ivesia gordonii* (Rosaceae)), and deciduous dicotyledonous shrubs (*Eriogonum umbellatum* (Polygonaceae), *Heterotheca villosa*) (Fig 3.3). We selected focal seed species with high abundance to minimize community impacts. We measured trapping and retention probabilities for *Agoseris glauca* (Asteraceae), *Elymus lanceolatus*, *Eriogonum umbellatum*, *Heterotheca villosa*, and *Senecio crassulus* (Fig 3.4). We measured trapping of *Eriogonum umbellatum* seeds in two conditions, in flower and out of flower, as seed dispersal and germination in this species occurs in both states. In the retention experiment, we also included *Eremogone congesta* (Caryophyllaceae), which was too small to locate reliably in the trapping experiment (Fig 3.4). Three seed species, *Agoseris glauca*, *Heterotheca villosa*, and *Senecio crassulus*, had a pappus, hair-like structures at the terminal end of a seed, that are important for wind dispersal. Fine hairs were also present on the seed surface of *Heterotheca villosa*.

Measurement of seed functional traits (Q1)

We measured five seed functional traits considered important to dispersal (length, width, thickness, pappus length, and dry mass) for six taxa (*Agoseris glauca*, *Elymus lanceolatus*, *Eremogone congesta*, *Eriogonum umbellatum*, *Heterotheca villosa*, *Senecio crassulus*). We measured all traits on ten seeds from ten plants for 100 seeds per taxon following the protocols detailed in [91]. For seeds with a pappus, we measured the average length of three arbitrarily chosen pappi per seed. We measured morphological traits in ImageJ from images captured under a dissecting microscope. Before measuring the dry mass, we removed pappi and dried seeds at 70°C - 80°C for at least three days. We individually weighed seeds to the nearest 0.001 mg immediately following removal from the oven.

Trapping experiment (Q2): overview

We compared the trapping ability of *Lupinus argenteus* and *Heterotheca villosa* by blow-

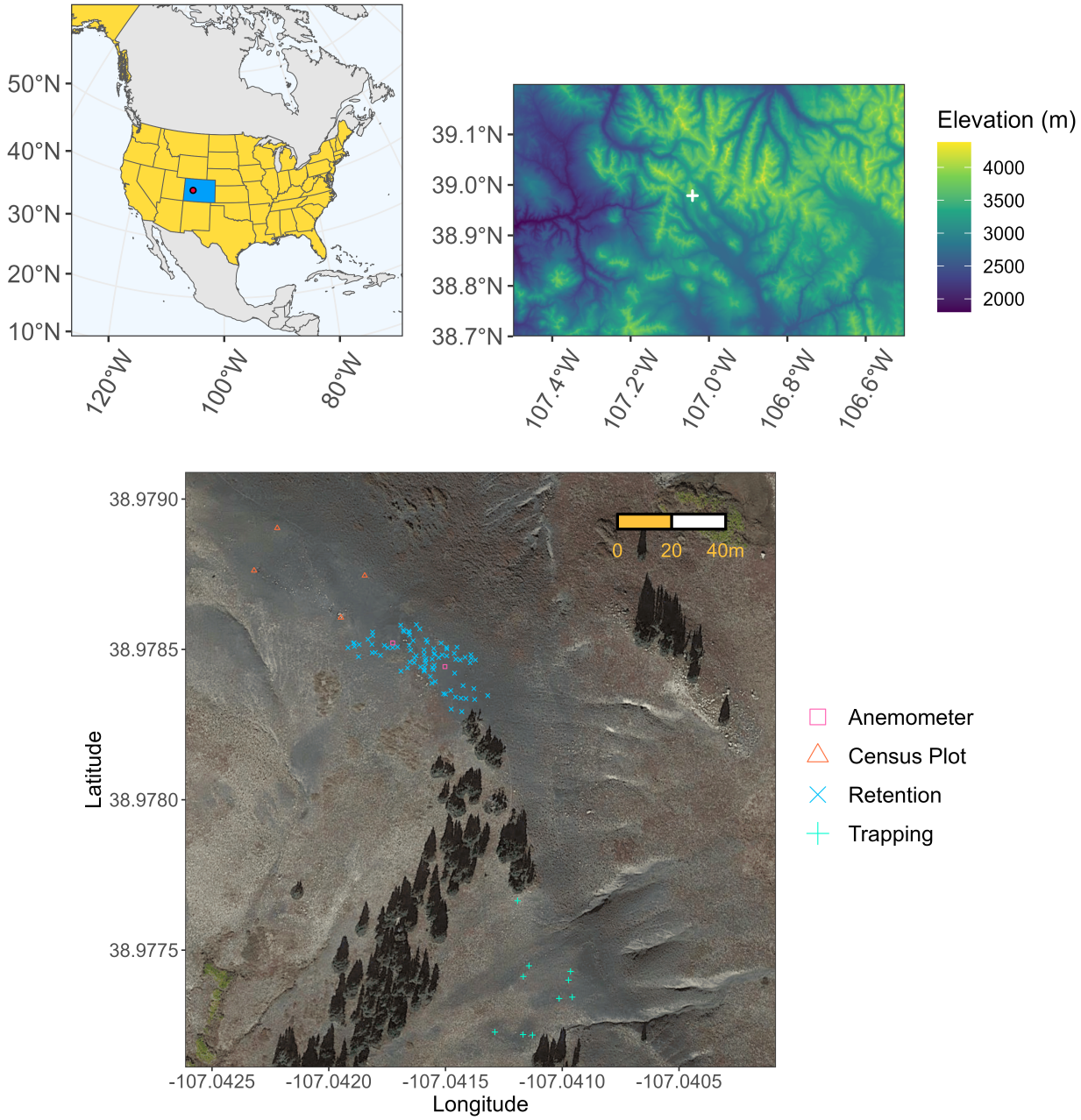

Figure 3.2: Top left) Location of field site (red circle) within Colorado (blue state). The United States is indicated in yellow. Top right) Topographic map of the area surrounding the field site (white cross) demonstrating the high topographic variation of the region. Bottom) Map of experiments at the field site. The bounding corners of the demography census plot are marked with orange triangles, while the focal plants in the trapping and retention experiments are marked with green crosses and blue x's, respectively. Pink squares indicate the location of the two cup anemometers used during the retention experiment.

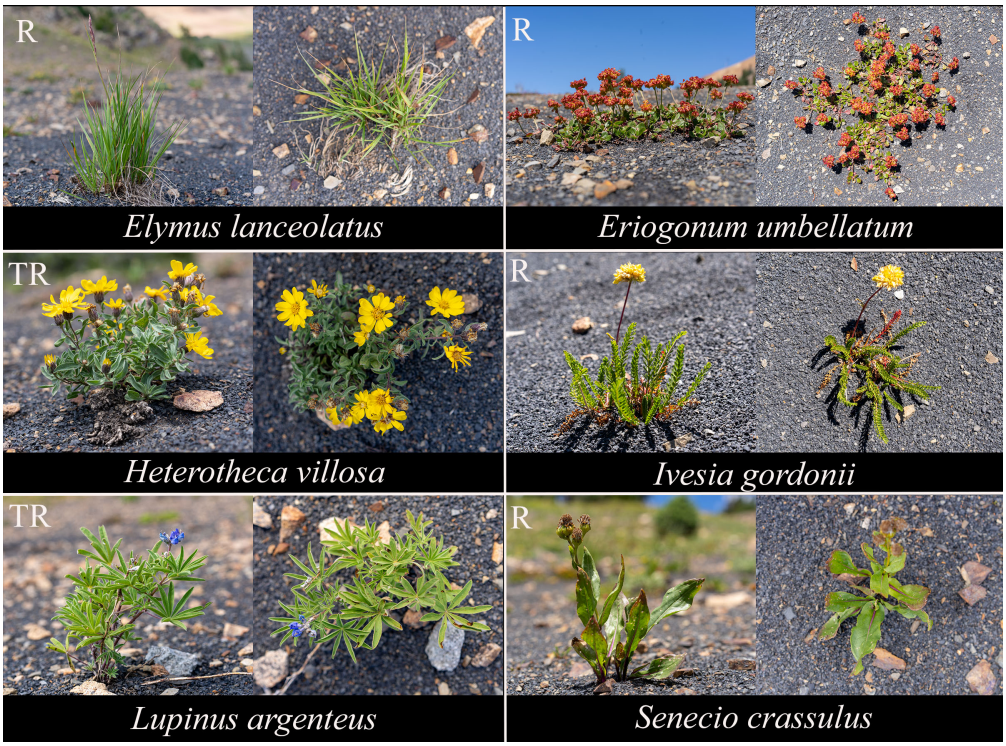

Figure 3.3: Profile and aerial images of host plants (*Elymus lanceolatus*, *Eriogonum umbellatum*, *Heterotheca villosa*, *Ivesia gordonii*, *Lupinus argenteus*, *Senecio crassulus*) used in the trapping (T) and retention (R) experiments. Plants in these images range from ∼10 to 30 cm in diameter.

ing seeds into focal plants using a custom-constructed wind tunnel (Fig 3.5). We measured trapping on five plants per taxon from a range of sizes by measuring the length of the longest axis of each plant: *Heterotheca villosa* (length = 7 - 54 cm, mean = 27.2 cm, sd = 20.5 cm) and *Lupinus argenteus* (length = 4 - 45 cm, mean = 20.2 cm, sd = 16.9). We collected seeds in August-September 2019 and stored them in open air following [91]. To increase seed visibility, we dusted all seeds with UV reactive powder (brand GloMania, Texas, USA), similar to [108]

Trapping experiment (Q2): data collection

We tested seed trapping on plants inside a portable wind tunnel. The wind tunnel consisted of the following components, from 'wind source' to output: a leaf blower (B250 27-cc 2-Cycle 205-MPH 450-CFM Handheld Gas Leaf Blower, Craftsman), an intake bell, an aluminum honeycomb flow straightener ($\frac{1}{8}$" cell), a testing chamber, and a rear mesh seed trap.

The trapping experiment setup was consistent for each seed-plant comparison (Fig 3.5). We blew seeds into the path of host plants. We considered seeds trapped if they were

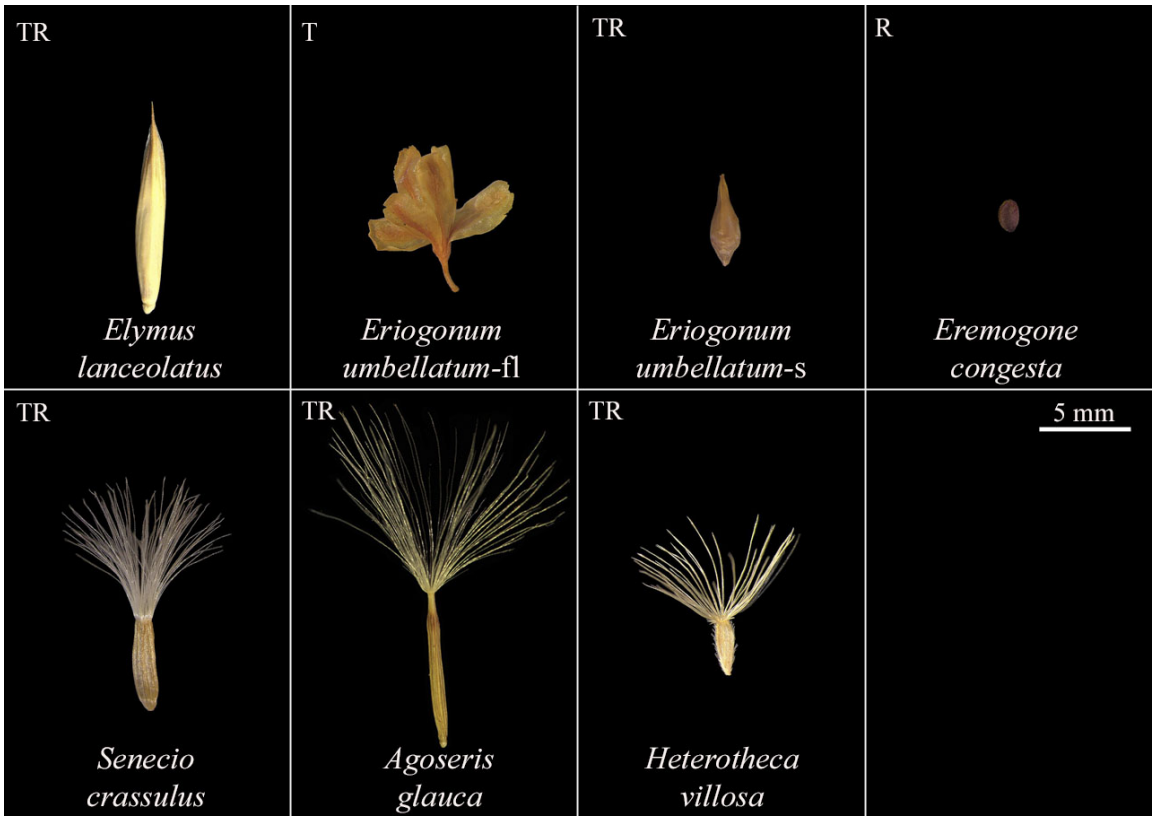

Figure 3.4: Scaled images of the seeds (*Elymus lanceolatus*, *Eriogonum umbellatum*, *Eremogone congesta*, *Senecio crassulus*, *Agoseris glauca*, and *Heterotheca villosa*) used in the trapping (T) and retention (R) experiments in ascending order of mean PC 1. We measured the trapping of *Eriogonum umbellatum* in two states, in flower (fl) and seed (s).

physically touching the focal plant or directly beneath the canopy for the entirety of the trial (e.g., after five successful launches of five individual seeds). A launch was successful if the seed contacted the plant without touching the ground. After five successful launches, we left the blower on for 30 seconds. We conducted 284 successful launches after discarding data from 15 launches for one *Heterotheca villosa* plant (seed taxa = *Eriogonum umbellatum*-fl, *Senecio crassulus*, *Heterotheca villosa*) due to a non-standard wind tunnel set-up). In one case, only four seeds were successfully launched for a seed-plant pair rather than five. Trapping trials were conducted only under dry conditions to maintain consistency. Inside the wind tunnel, we placed a wooden launch platform centered and adjacent to the flow straightener. Before every trapping trial, we confirmed that the launch platform was level and that the focal plant was 15 cm away and centered on the launch platform. To avoid backflow into the tunnel, we did not face the end of the tunnel toward ambient wind. Local slopes at focal plants ranged from 0-15°. For one *Lupinus argenteus* on a 15° slope, we faced the output of the tunnel downhill. We placed the leaf blower on a 4.6 cm platform to achieve

desired airspeeds.

To mirror wind conditions near the ground in alpine communities and maintain consistency across trapping trials, we calibrated the wind tunnel to have airspeeds at or near 5 m/s (11.2 mph) at the end of the launch platform. We chose to test seed trapping at 5 m/s because it was the minimum airspeed at which all seeds could launch off the platform. These airspeeds are also realistic for near ground level in this community as maximum wind velocities captured by the anemometers at 1.2 m aboveground during the retention studies were approximately twice as fast (uphill daily wind speed maximum: mean = 10.56, sd = 1.90; downhill: mean = 9.30, sd = 1.47) and wind speeds decrease nearer to the ground. Once airspeeds were within range of 5 m/s, we individually launched seeds by placing the seed with forceps at the center edge of the launch platform, with the seed's longest axis pointed at the plant and the pappus (when applicable) pointed towards the blower. Airspeeds at the launch site were 5-5.25 m/s, mean = 5.15 m/s, sd = 0.034 m/s.

Retention experiment (Q3): overview

In August 2018, we collected seeds within ∼500 m of the study site. Seeds were stored in open air until August 2019 and were dusted with colored fluorescent powder before deployment. In August 2019, we compared seed retention times in different microsites in a blocked experiment stratified by host and seed taxa and size under natural wind regimes. We selected host plants across the range of plant sizes for each taxon. To isolate the effects of host species on retention, we avoided individuals with neighbors within 30 cm distance as focal plants and multi-individual clusters.

We established a controlled comparison in a non-vegetated area adjacent to each focal plant (Fig 3.5). Each non-vegetated site was 30 cm away from the vegetated edge of the paired focal plant, marked with an orange nail, and did not have any other vegetation within 30 cm of it. The location of the non-vegetated site relative to the focal plant was determined by randomly selecting bearings until we identified a suitable area. Substrate characteristics, including scree size, were similar across all deployment sites, minimizing spatial edaphic effects on secondary dispersal [22]. We recorded the average wind speed (m/s) and direction of origin (°) at 1-minute intervals throughout the experiment using two-cup anemometers (Davis Cup Anemometer, Decagon Devices, Inc.). We installed an anemometer at the upslope and downslope ends of the study site (Fig 3.5). Each anemometer faced north and was 1.2 m above ground.

Retention experiment (Q3): data collection

We deployed seeds using forceps by individually placing them beneath the plant canopy on the scree surface, or at non-vegetated microsites, within 0-3 cm of the 30 cm marker (nail head). We deployed seeds from 1 taxon (5 seeds) into the smallest plants and the seeds of up to 6 taxa (30 seeds) in the largest plants to avoid seed overlap. We deployed the same quantity and identity of seed taxa at the paired non-vegetated sites but with contrasting colors. We avoided similar color combinations at neighboring sites to reduce the risk of misattributed seeds. In total, we deployed 2924 seeds from 167 individuals: *Agoseris glauca* (n

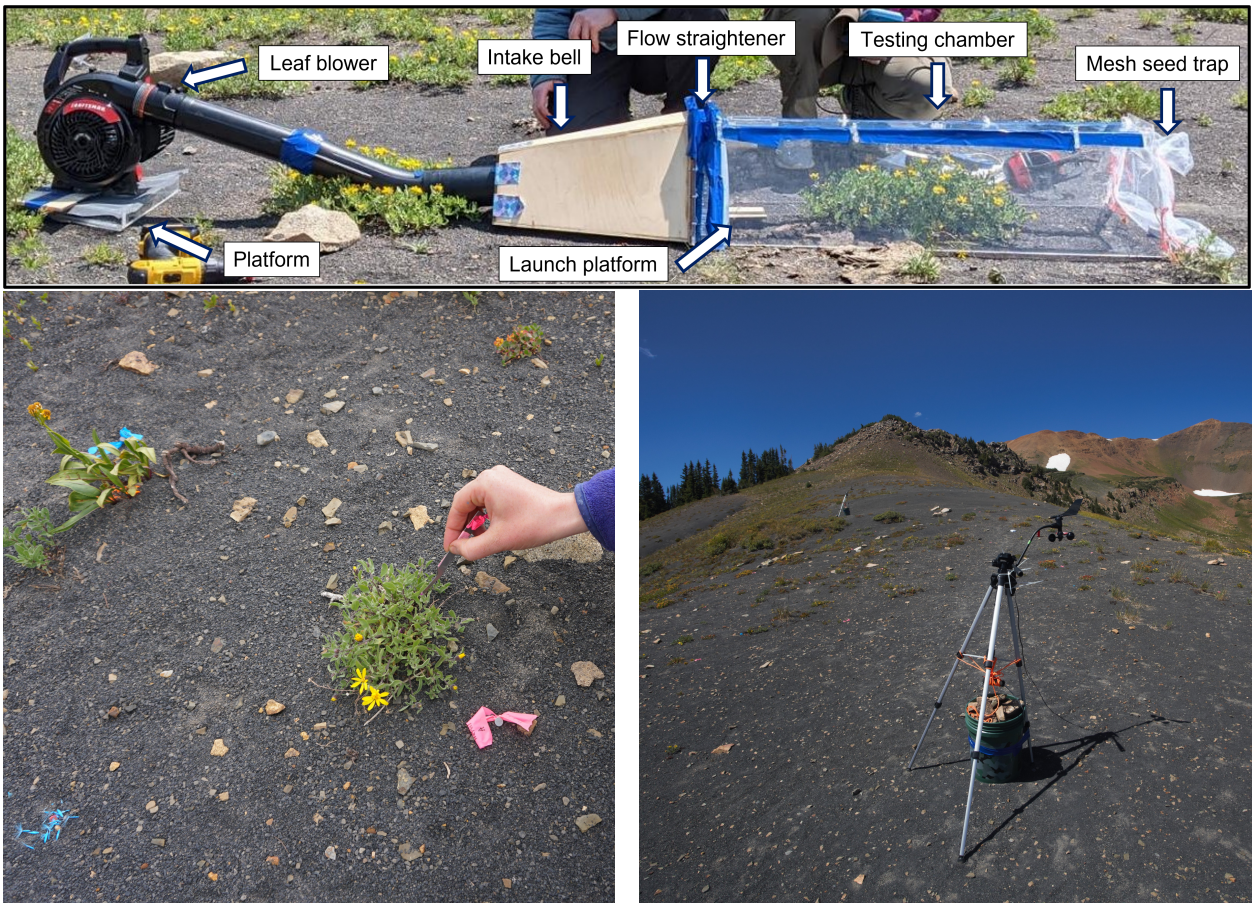

Figure 3.5: Top) The seed trapping setup with labeled components. Bottom left) The insertion of a seed into a *Heterotheca villosa* plant during the retention experiment. Blue-dyed seeds in the paired non-vegetated site are visible in the lower left-hand corner. A second focal plant (*Senecio crassulus*, marked with blue flagging) is visible in the background. Bottom right) A cup anemometer in the retention experiment. A second cup anemometer is visible in the background.

source plants = 25, n seeds = 579), *Elymus lanceolatus* (28, 450), *Eremogone congesta* (16, 161), *Eriogonum umbellatum* (54, 589), *Heterotheca villosa* (23, 581), and *Senecio crassulus* (21, 564). Eighty-three host plants and 80 non-vegetated sites received seeds: *Elymus lanceolatus* (n = 12), *Eriogonum umbellatum* (n = 14), *Heterotheca villosa* (n = 12), *Ivesia gordonii* (n = 14), *Lupinus argenteus* (n = 15), and *Senecio crassulus* (n = 16). In three cases, plants did not have a paired non-vegetated site due to insufficient seed availability. We deployed six seeds for one seed taxon rather than five in two cases. In seventeen cases, we deployed four seeds due to seeds dispersing before being correctly placed. We deployed seeds at 40 sites on the first day of the experiment (29 August 2019) and completed deployment the next day. Seeds were retained if they were under or within host plant vegetation or, at non-vegetated sites, were within 5 cm of the nail head. We selected 5 cm as a threshold to allow for small seed movements by the seeds during deployment. We censused how many seeds remained at each site in three checks after one, three, and eleven days. We checked plants in the same order each time to minimize variation in time between checks across plants. Variation in check times was greater in Check 3 as rainfall reduced the visibility of the fluorescent powder and caused smaller seeds to settle beneath the scree surface. Although we attempted to locate all seeds by brushing aside scree and using a black light, detectability may have decreased.

Analyses

Seed functional traits (Q1)

To assess seed functional diversity, reduce trait data dimensionality, and account for trait correlation, we calculated principal components for the seed traits using the individual plant-average trait values for each seed taxon. We set the average pappus length for seed taxa without a pappus to 0 cm and retained principal components with eigenvalues greater than 1 (n = 2).

Trapping experiment (Q2)

We estimated the effect of host plant taxon, seed taxon, and log plant size on the proportion of seeds trapped in each trial using a generalized linear mixed model (GLMM) and the R package, glmmTMB [15]. We used a binomial family and logit link function with the following model structure (glmmTMB/lme4 syntax):

$$
\begin{aligned}
&\textit{Proportion trapped} \sim \\
&\textit{Plant taxon} + \\
&\textit{Seed taxon} + \\
&\textit{Log plant size (cm)} + \\
&(1|\textit{Plot})
\end{aligned}
$$

Plant and seed taxon were factors with two and six levels, respectively. We log-transformed plant size to improve the appearance of Q-Q plot residuals. Plot was a factor and random

effect to account for variation between the ten focal plants. The trapping proportions were weighted by the five (in one case, four) successful launches for each focal plant and seed taxon. We used pairwise Tukey contrasts with α=0.05 in the emmeans package [64] to assess microsite and seed level variation in trapping. We back-transformed the estimated marginal means to the response scale prior to contrasting.

Retention experiment (Q3)

To address Q3, we assessed whether dispersal rates (i.e., the rate that retention did not occur) differed by seed taxa, microsite, the interaction of those predictors, and interval duration using a GLMM with a binomial family and a complementary log-log (cloglog) link function. Between Check 1 and 2, we observed 51 cases of increased seed counts by 1-2 seeds. Between Checks 2 and 3, we observed 21 cases. We assumed any seed increases were due to missed seeds in previous checks and accounted for these 'missed seeds' by adding them back to prior checks during data cleaning. Each seed could only disperse once. We analyzed the data with two model structures (glmmTMB syntax):

$$
\begin{aligned}
&\textit{Dispersal (0,1)} \sim \\
&\textit{Seed taxon} \times \textit{Microsite} + \\
&\textit{Interval duration} + \\
&(1|\textit{Check}) + \\
&(1|\textit{Plot})
\end{aligned}
$$

Then, to isolate the role of seed traits in retention:

$$
\begin{aligned}
&\textit{Dispersal (0,1)} \sim \\
&\textit{Microsite} \times \textit{Seed trait PC 1} + \\
&\textit{Microsite} \times \textit{Seed trait PC 2} + \\
&\textit{Interval duration} + \\
&(1|\textit{Check}) + \\
&(1|\textit{Plot})
\end{aligned}
$$

The cloglog link function provided a natural time decay to account for different interval durations between checks. Microsite was a factor with seven levels, one for each of the six host plant taxa and one for the non-vegetated microsite. We did not include plant size in this model due to the inclusion of non-vegetated microsites, which lack a plant size value. Interval duration accounted for time in days between checks. As weather and the number of seeds remaining varied between the three checks following deployment, we included Check as an ordered factor ($1 < 2 < 3$) and random effect in the model. The Plot term was a unique identifier for each plant and non-vegetated site and was a factor with 161 levels. We used pairwise Tukey contrasts with α=0.05 in the emmeans package to ask whether the dispersal from host plants and non-vegetated microsites differ by microsite and seed taxa (Q3). We back-transformed the estimated marginal means to the response scale prior to contrasting.

We assessed the significance of the main effects using joint tests (emmeans). We checked model fit and residuals for Q2 and Q3 using DHARMa [42]. Estimated marginal means plots were made using emmeans, ggh4x [13], and ggtext [122].

3.3 Results

Seed functional traits (Q1)

In the principal component analysis of seed functional traits, the first principal component explained 67.1% of the variance, and the second principal component explained 23.7% (Fig 3.6). Thicker, wider, and heavier seeds (*Elymus lanceolatus* and *Eriogonum umbellatum*) diverged from the pappused seeds (*Senecio crassulus*, *Agoseris glauca*, and *Heterotheca villosa*) and the non-pappused *Eremogone congesta* along PC 1. Longer seeds (*Elymus lanceolatus* and *Agoseris glauca*) diverged from shorter seeds along PC 2.

Trapping experiment (Q2)

In the trapping model, the fixed effects alone explained 51.4% of the variation (marginal R2, conditional R2=53.6%). Larger plants trapped more seeds (estimate (est) = 1.908, standard error (SE) = 0.413, $p < 0.0001$, with *Heterotheca villosa* as the plant taxon and *Elymus lanceolatus* as the seed taxon in the intercept). *Heterotheca villosa* trapped more seeds than *Lupinus argenteus* (est = 0.098, SE = 0.045, p = 0.035, Table 3.1), but we did not find a difference in trapping among seed taxa (all p values > 0.05, Table 3.2) (Fig 3.7). We did not assess interactions because we did not have sufficient sample sizes.

Retention experiment (Q3)

In the retention model with seed taxa as predictors, the fixed effects alone explained 35.5% of the variation (marginal R2, conditional R2 = 48.3%). Interval duration (df1 = 1, df2 = 6175, F = 7.499, p = 0.0062), seed taxa (df1 = 5, df2 = 6175, F = 24.004, $p < 0.0001$), microsite (df1=6, df2=6175, F=39.357, $p < 0.0001$), and the interaction between seed taxa and microsite (df1=30, df2=6175, F=4.050, $p < 0.0001$) influenced dispersal. Dispersal was higher in non-vegetated microsites compared to the host plants *Elymus lanceolatus* (est = 0.371, SE = 0.070, $p < 0.0001$), *Eriogonum umbellatum* (est = 0.356, SE = 0.067, $p < 0.0001$), *Heterotheca villosa* (est = 0.317, SE = 0.061, $p < 0.0001$), and *Ivesia gordonii* (est = 0.356, SE = 0.067, $p < 0.0001$) (Fig 3.8). Retention in non-vegetated areas did not differ from *Lupinus argenteus* or *Senecio crassulus*. Dispersal was lower in all plant taxa compared to *Lupinus argenteus*, except *Senecio crassulus* (Table 3.3). In pairwise contrasts of seeds (Table 3.4), seeds without a pappus generally dispersed less than *Senecio crassulus*, *Heterotheca villosa*, and *Agoseris glauca* seeds, which have pappi. All seed taxa dispersed less than *Senecio crassulus*, except *Eremogone congesta*. *Elymus lanceolatus* and *Eriogonum umbellatum* seeds dispersed less than *Heterotheca villosa* seeds. Finally, two larger non-pappused seeds, *Elymus lanceolatus* and *Eriogonum umbellatum*, dispersed less than *Agoseris glauca* and the smallest seed, *Eremogone congesta*.

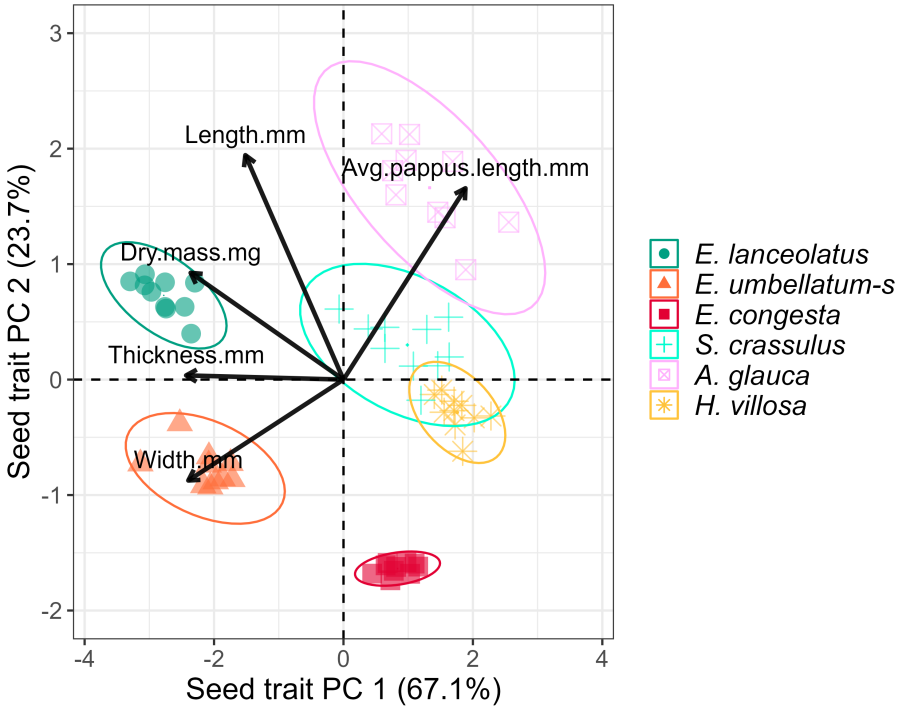

Figure 3.6: Principal component analysis biplot for six seed functional traits important for dispersal (length (mm), width (mm), thickness (mm), pappus length (mm), and dry mass (mg)) for six alpine plant species (*Elymus lanceolatus*, *Eriogonum umbellatum*, *Eremogone congesta*, *Senecio crassulus*, *Agoseris glauca*, and *Heterotheca villosa*) with 95% confidence ellipses. Seed taxa are listed in ascending order of mean PC 1.

In the seed retention model with seed traits as predictors, the fixed effects alone explained 32.2% of the variation (marginal R2, conditional R2 = 45.4%). Dispersal probability was influenced by interval duration (df1 = 1, df2 = 6196, F = 6.753, p = 0.0094), seed trait PC 1 (df1 = 1, df2 = 6196, F = 67.051, p < 0.0001), microsite (df1 = 6, df2 = 6196, F = 45.647, p < 0.0001), the interaction between seed trait PC 1 and microsite (df1 = 6, df2 = 6196, F = 3.327, p = 0.0028), and the interaction between seed trait PC 2 and microsite (df1 = 6, df2 = 6196, F = 6.829, p < 0.0001). We did not find a significant effect of seed trait PC 2 on seed retention. In comparisons of the re-leveled retention model with different microsites as part of the intercept, greater values of seed trait PC 1 (i.e., longer pappus, thinner and less-heavy seeds) increased dispersal in non-vegetated microsites, *Elymus lanceolatus*, *Eriogonum umbellatum*, *Heterotheca villosa*, *Lupinus argenteus*, and *Senecio crassulus*. Higher values of PC 2 (i.e., longer length) increased dispersal in non-vegetated microsites and plants with low basal vegetation, *Lupinus argenteus* and *Senecio crassulus* (Fig 3.9).

Dispersal probability was higher in non-vegetated microsites compared to *Elymus lance-*

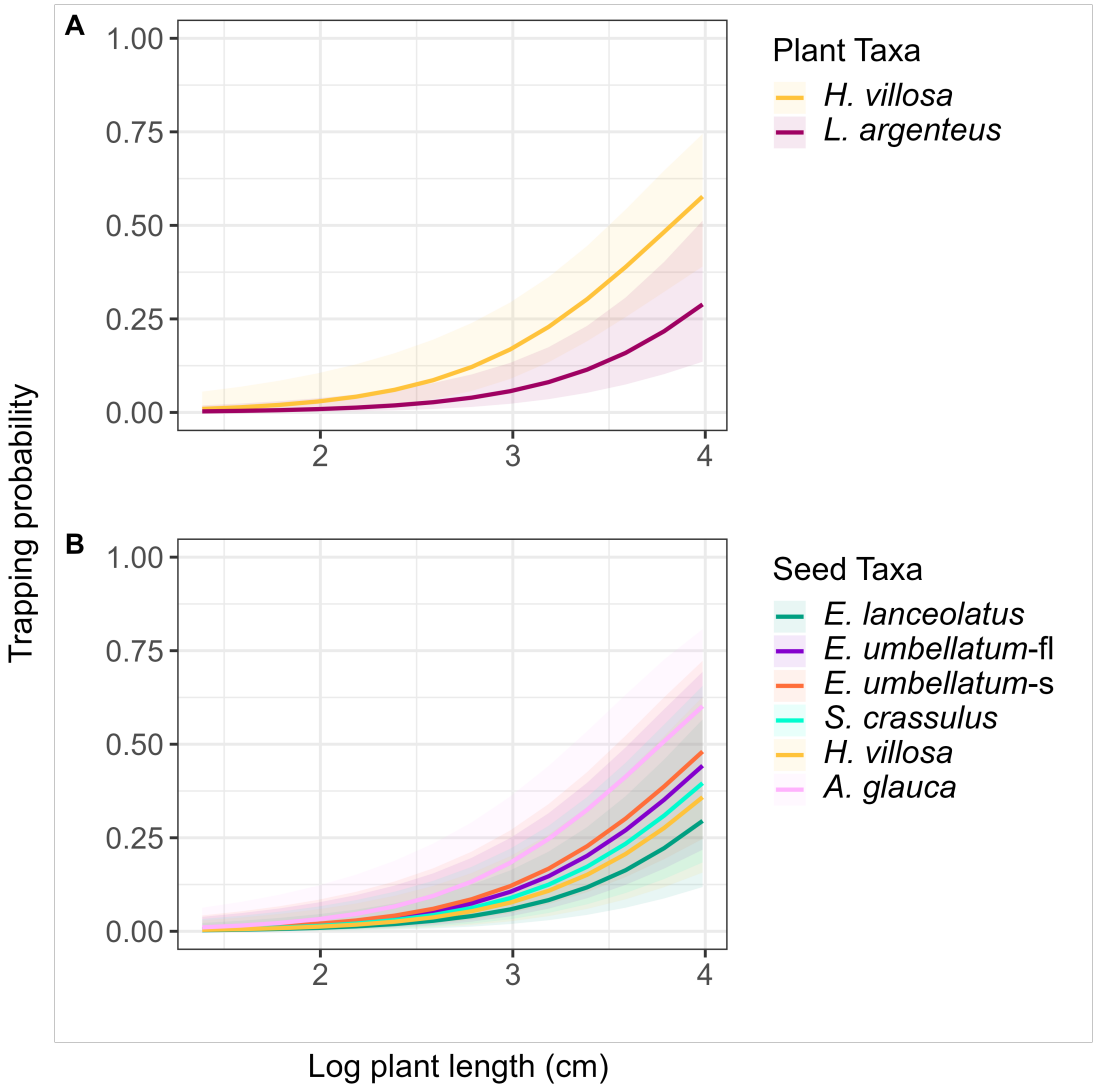

Figure 3.7: Predicted trapping probability by plant length (log, cm) with 95% confidence bands for A) *Heterotheca villosa* (yellow line) and *Lupinus argenteus* (purple line), and B) across seed taxa. Trapping probabilities are averaged across seed taxa in panel A and across plant taxa in Panel B. Seed taxa are in ascending order of mean PC 1. Colors representing taxa are consistent across host plants and seed taxa. The 'fl' and 's' indicate that *Eriogonum umbellatum* was tested in flower and in seed, respectively.

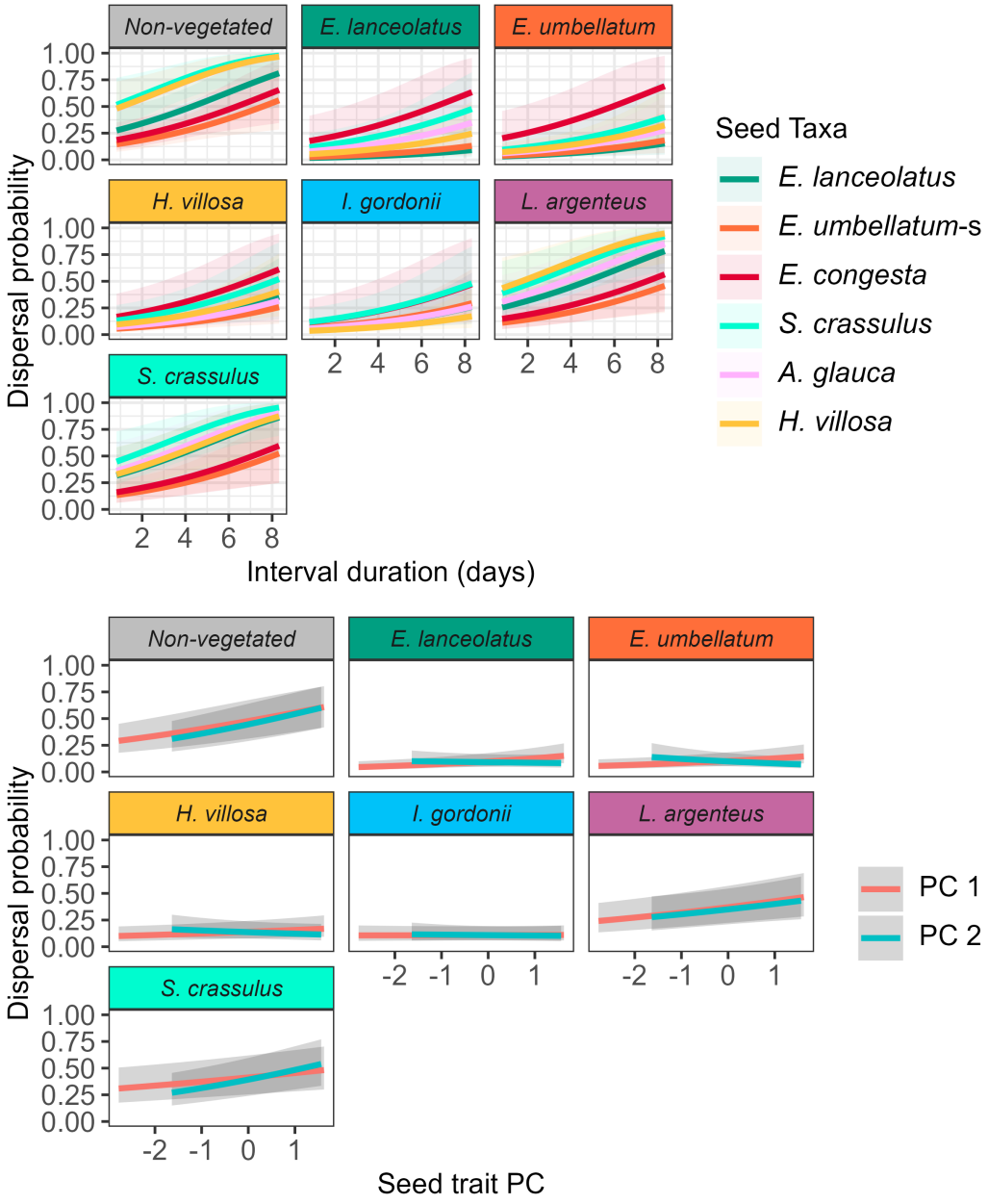

Figure 3.8: Estimated dispersal probabilities for (Top) seed taxa and (Bottom) seed trait principal components (colored lines) by microsite at different interval durations (days) and with 95% confidence bands. Seed taxa are listed in ascending order of mean PC 1. Colors representing taxa are consistent across seeds and microsites (facets). The 's' indicates that *Eriogonum umbellatum* was tested in seed rather than in flower.

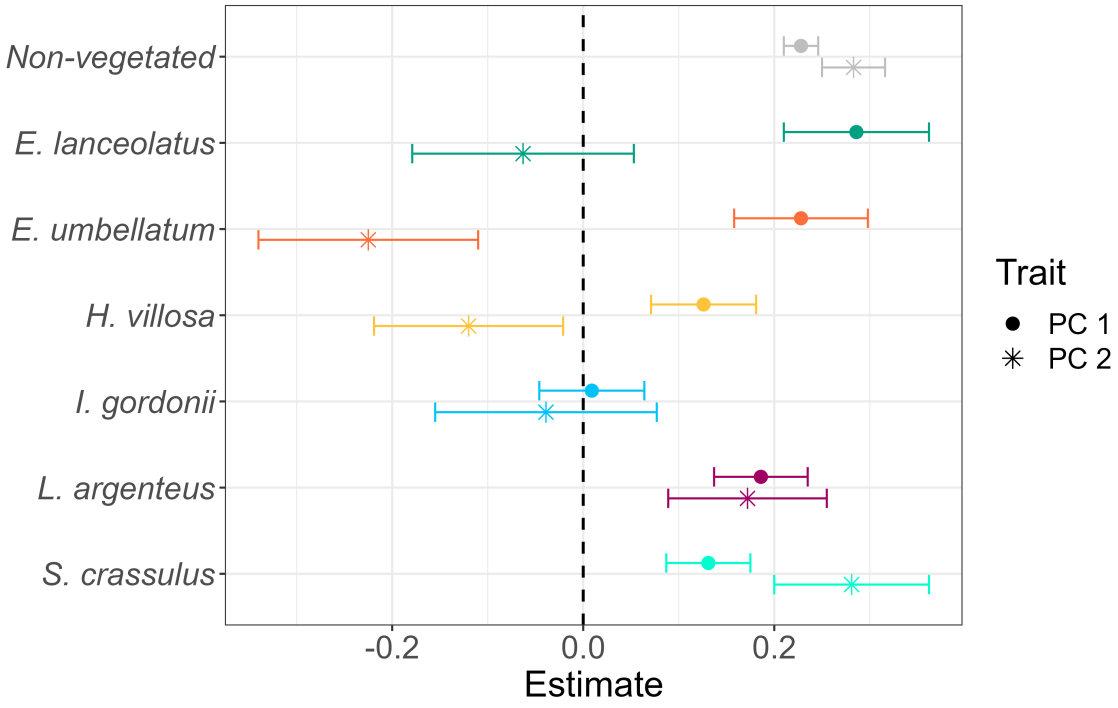

Figure 3.9: Coefficient estimates for seed traits, PC 1 (circles) and PC 2 (stars), on dispersal probability depending on the microsite term (colors) in the model intercept. Error bars represent +/- 1 standard error.

olatus (est = 0.364, SE= 0.071, $p < 0.0001$), *Eriogonum umbellatum* (est = 0.358, SE = 0.070, $p < 0.0001$), *Heterotheca villosa* (est = 0.320, SE = 0.063, $p < 0.0001$), *Ivesia gordonii* (est = 0.347, SE = 0.067, $p < 0.0001$), and (unlike the first model) *Lupinus argenteus* (est = 0.100, SE = 0.047, p = 0.032). Dispersal probabilities were lower in several vegetated microsites than in *Lupinus argenteus* and *Senecio crassulus*, which have sparse basal vegetation (Table 3.5). Compared to *Lupinus argenteus*, we observed lower dispersal in *Elymus lanceolatus*, *Eriogonum umbellatum*, *Heterotheca villosa*, and *Ivesia gordonii*. Compared to *Senecio crassulus*, we observed lower dispersal in *Elymus lanceolatus*, *Eriogonum umbellatum*, *Heterotheca villosa*, and *Ivesia gordonii*.

3.4 Discussion

Main findings

Our study demonstrates that seed trapping and retention are contingent on the functional characteristics of the interacting partners. Host plants differed in their ability to trap seeds by size and taxa, while seed retention varied by host plant taxa, seed taxa, and interactions

between plant and seed taxa. Our results support earlier studies showing that the physical structure of a community, including topography and distribution of other organisms, influences dispersal outcomes [2, 67, 77]. This work adds to a growing body of literature indicating that abiotic dispersal agents such as wind and water can generate non-random seed dispersal outcomes, similar to animal dispersal. Thus, there may be selection on seed and plant traits to either promote or reduce these interactions.

We observed little seed trait overlap among species in the PCA (Q1), with most of the variation explained by pappus length and seed thickness (PC 1) and seed length (PC 2). Despite this trait variation, we did not observe differences among seeds in trapping (Q2) but did observe differences in retention (Q3). Pappused seeds dispersed more than non-pappused seeds. Thus, secondary dispersal (i.e., any seed mobility following initial dispersal from the parent plant) for pappused seeds may occur over longer durations, with potentially more plant-plant interactions compared to non-pappused seeds.

The physical attributes of host plant taxa also influenced trapping and retention outcomes. In our trapping experiment (Q2), we demonstrated that larger plants are better at trapping seeds than smaller plants, likely due to having more biomass that intercepts seeds and prevents them from passing through. Bushier canopies, such as those found in *Heterotheca villosa* compared to *Lupinus argenteus*, might also contribute to greater trapping ability, as we observed higher trapping probabilities in *Heterotheca villosa*. By design, only seed launches where the seed was in physical contact with the plant were considered valid in our study; however, this criterion precludes consideration of the role of vegetation in modifying wind profiles. In plants, growth form, size, woodiness, and leaf density could affect how plants modify local wind and water flow profiles and, thus, the likelihood of a seed encountering a plant. Even within species, local wind profiles near plants could vary with plant age and shape (e.g., [24]). Thus, greater variation in trapping and retention due to plant morphology may exist in field conditions.

In our retention experiment Q3, we found that dispersal depended on microsite and seed taxa, with significant interactions between microsite and seed taxa. Dispersal from bushy plants (*Elymus lanceolatus*, *Eriogonum umbellatum*, *Heterotheca villosa*, *Ivesia gordonii*) was lower than *Lupinus argenteus* and *Senecio crassulus*; *Elymus lanceolatus* and *Lupinus argenteus* had dispersal probabilities comparable to non-vegetated microsites. These results suggest that dispersal promotes spatial co-occurrence of some seeds and host plants, which could generate downstream effects on demographic outcomes, which we will explore in future studies.

Implications for community assembly

Dispersal can strongly affect population and community dynamics [21]. Our seed trapping and retention study does not yet link these interaction mechanisms and their population or community consequences. As trapping and retention depend on the host and seed taxa, some interaction pairs may affect community structure more strongly than others. In this community, the host with the highest retention rates (*Elymus lanceolatus*, *Eriogonum umbellatum*,

Heterotheca villosa, *Ivesia gordonii*) vary in their ability to buffer temperatures and locally increase soil moisture [96]. Thus, seed trapping and retention could contribute to the spatial patterning of seed rain in this community and differential success during recruitment and later life stages. However, although seed trapping and retention may be frequent or likely in a community, it does not indicate that the microenvironment is suitable for germination or that seed-plant interactions are facilitative [107].

Dispersal and seed-plant interactions may act in tandem in some plant communities with large effects on community dynamics. Through these interactions, abiotic dispersal may generate non-random species distributions and co-occurrence patterns, acting as an initial step before other environmental and biotic community assembly mechanisms. Prior studies of species interactions in alpine settings have predominantly focused on facilitative effects by one or a small number of species in a community (frequently cushion plants), e.g., [47]. However, for some alpine plant taxa, such as *Silene ciliata*, a dominant cushion plant in the Mediterranean alpine, non-random seed dispersal is promoted by short dispersal distances from the parent plant rather than trapping or retention [62].

Understanding the role of seed dispersal in community assembly and population dynamics is challenging because it is often a complex multi-step process [120, 119]. Seed trapping and retention can occur during the initial transportation of the seed from the parent plant (primary dispersal) or subsequent seed movement (secondary dispersal). Further stages of seed dispersal may still be possible, as well. For example, in this community, *Ivesia gordonii*, *Eriogonum umbellatum*, and *Phacelia hastata* frequently host ant nests (*Formica* sp., *neogagates* species group). These ants are omnivorous [35] and may transport seeds into or out of plants (potentially trapping or freeing them). Snow dispersal is also likely important because regolith is reworked and transported by snow-related processes annually. Vertical seed dispersal (e.g., into the soil) also affects seed fates, with its likelihood varying across dispersal mechanisms and as a function of seed size and substrate grain size. For example, heavy rainfall may push some seeds beneath the surface. We observed this occurring most in the smallest focal seed taxon, *Eremogone congesta*.

Prevalence across biomes

Abiotic dispersal is a common feature in environmentally stringent ecosystems (e.g., deserts, alpine, tundra) [21] and is often treated as a stochastic process in plant communities [120]. Here, we show larger plants have a greater capacity for trapping seeds, with evidence that seed trapping is greater in plant taxa with higher bushiness. We also demonstrate that seed retention by plants depends on plant and seed taxa identity, with greater retention in plants with higher bushiness and for seeds that lack a pappus. Seed trapping and retention thus non-randomly contribute to post-dispersal processes, such as germination success and establishment. Our results suggest that wind-driven seed-plant interactions may be common in open and high-wind communities. We speculate that plant-plant dispersal interactions are frequent in communities with sparse or clustered vegetation and high winds/heavy precipitation events, allowing for unimpeded seed movement from plant to plant.

Table 3.1: Estimated marginal means contrasts for plant taxa in the trapping model.

	estimate	SE	df	t.ratio	p.value
H. villosa - *L. argenteus*	0.098	0.045	48	2.164	0.035

Table 3.2: Estimated marginal means contrasts for seed taxa in the trapping model.

	estimate	SE	df	t.ratio	p.value
E. lanceolatus - *E. umbellatum*-fl	-0.041	0.044	48	-0.936	0.35
E. lanceolatus - *E. umbellatum*-s	-0.054	0.047	48	-1.161	0.25
E. lanceolatus - *S. crassulus*	-0.026	0.040	48	-0.663	0.51
E. lanceolatus - *A. glauca*	-0.11	0.061	48	-1.800	0.078
E. lanceolatus - *H. villosa*	-0.016	0.037	48	-0.423	0.67
E. umbellatum-fl - *E. umbellatum*-s	-0.013	0.053	48	-0.253	0.80
E. umbellatum-fl - *S. crassulus*	0.015	0.048	48	0.308	0.76
E. umbellatum-fl - *A. glauca*	-0.069	0.065	48	-1.066	0.29
E. umbellatum-fl - *H. villosa*	0.025	0.046	48	0.545	0.59
E. umbellatum-s - *S. crassulus*	0.028	0.050	48	0.559	0.58
E. umbellatum-s - *A. glauca*	-0.055	0.066	48	-0.838	0.41
E. umbellatum-s - *H. villosa*	0.039	0.049	48	0.788	0.43
S. crassulus - *A. glauca*	-0.083	0.063	48	-1.329	0.19
S. crassulus - *H. villosa*	0.011	0.043	48	0.247	0.81
A. glauca - *H. villosa*	0.094	0.062	48	1.512	0.14

Conclusions

Seed trapping and retention are seed-plant interactions shaped by the physical attributes of the interacting pairs. As many plant communities where seed-plant interactions are expected to be prevalent are also undergoing large shifts in community structure due to invasive species, shrubification, and range shifts, dispersal outcomes may also shift. Plant size may also change as climate and land use pressures change (e.g., due to intensified grazing). Incorporating seed retention and trapping interactions is thus vital for modeling dynamics in communities with high prevalence of abiotic dispersal.

Table 3.3: Estimated marginal means contrasts for microsites in the seed taxa retention model.

	estimate	SE	df	t.ratio	p.value
Non-vegetated - *E. lanceolatus*	0.371	0.070	6175	5.327	1.0e-07
Non-vegetated - *E. umbellatum*	0.356	0.067	6175	5.327	1.0e-07
Non-vegetated - *H. villosa*	0.317	0.061	6175	5.238	1.7e-07
Non-vegetated - *I. gordonii*	0.356	0.067	6175	5.333	1.0e-07
Non-vegetated - *L. argenteus*	0.091	0.052	6175	1.750	0.080
Non-vegetated - *S. crassulus*	0.062	0.050	6175	1.236	0.22
E. lanceolatus - *E. umbellatum*	-0.014	0.025	6175	-0.575	0.57
E. lanceolatus - *H. villosa*	-0.053	0.031	6175	-1.735	0.083
E. lanceolatus - *I. gordonii*	-0.014	0.025	6175	-0.566	0.57
E. lanceolatus - *L. argenteus*	-0.28	0.072	6175	-3.861	0.00011
E. lanceolatus - *S. crassulus*	-0.308	0.075	6175	-4.126	3.7e-05
E. umbellatum - *H. villosa*	-0.039	0.030	6175	-1.288	0.20
E. umbellatum - *I. gordonii*	0	0.025	6175	0.010	0.99
E. umbellatum - *L. argenteus*	-0.265	0.070	6175	-3.773	0.00016
E. umbellatum - *S. crassulus*	-0.294	0.073	6175	-4.054	5.1e-05
H. villosa - *I. gordonii*	0.039	0.030	6175	1.300	0.19
H. villosa - *L. argenteus*	-0.226	0.066	6175	-3.438	0.00059
H. villosa - *S. crassulus*	-0.255	0.068	6175	-3.769	0.00017
I. gordonii - *L. argenteus*	-0.266	0.070	6175	-3.776	0.00016
I. gordonii - *S. crassulus*	-0.294	0.073	6175	-4.058	5.0e-05
L. argenteus - *S. crassulus*	-0.029	0.065	6175	-0.444	0.66

Table 3.4: Estimated marginal means contrasts for seed taxa in the seed taxa retention model.

	estimate	SE	df	t.ratio	p.value
E. lanceolatus - E. umbellatum	0.040	0.021	6175	1.931	0.054
E. lanceolatus - E. congesta	-0.100	0.039	6175	-2.55	0.011
E. lanceolatus - S. crassulus	-0.173	0.041	6175	-4.173	3.1e-05
E. lanceolatus - A. glauca	-0.075	0.027	6175	-2.78	0.0055
E. lanceolatus - H. villosa	-0.073	0.027	6175	-2.686	0.0073
E. umbellatum - E. congesta	-0.140	0.043	6175	-3.254	0.0011
E. umbellatum - S. crassulus	-0.213	0.048	6175	-4.473	7.9e-06
E. umbellatum - A. glauca	-0.115	0.031	6175	-3.742	0.00018
E. umbellatum - H. villosa	-0.112	0.031	6175	-3.68	0.00024
E. congesta - S. crassulus	-0.073	0.038	6175	-1.91	0.056
E. congesta - A. glauca	0.025	0.034	6175	0.747	0.46
E. congesta - H. villosa	0.028	0.034	6175	0.811	0.42
S. crassulus - A. glauca	0.098	0.030	6175	3.271	0.0011
S. crassulus - H. villosa	0.100	0.030	6175	3.308	0.00095
A. glauca - H. villosa	0.003	0.022	6175	0.118	0.91

Table 3.5: Estimated marginal means contrasts for microsite in the seed trait retention model.

	estimate	SE	df	t.ratio	p.value
Non-vegetated - *E. lanceolatus*	0.364	0.071	6196	5.129	3.0e-07
Non-vegetated - *E. umbellatum*	0.358	0.070	6196	5.135	2.9e-07
Non-vegetated - *H. villosa*	0.320	0.063	6196	5.115	3.2e-07
Non-vegetated - *I. gordonii*	0.347	0.067	6196	5.157	2.6e-07
Non-vegetated - *L. argenteus*	0.100	0.047	6196	2.148	0.032
Non-vegetated - *S. crassulus*	0.054	0.046	6196	1.164	0.24
E. lanceolatus - *E. umbellatum*	-0.006	0.022	6196	-0.283	0.78
E. lanceolatus - *H. villosa*	-0.044	0.027	6196	-1.625	0.10
E. lanceolatus - *I. gordonii*	-0.018	0.023	6196	-0.772	0.44
E. lanceolatus - *L. argenteus*	-0.264	0.069	6196	-3.853	0.00012
E. lanceolatus - *S. crassulus*	-0.310	0.075	6196	-4.151	3.4e-05
E. umbellatum - *H. villosa*	-0.038	0.027	6196	-1.418	0.16
E. umbellatum - *I. gordonii*	-0.011	0.023	6196	-0.502	0.62
E. umbellatum - *L. argenteus*	-0.258	0.068	6196	-3.823	0.00013
E. umbellatum - *S. crassulus*	-0.304	0.074	6196	-4.129	3.7e-05
H. villosa - *I. gordonii*	0.027	0.026	6196	1.010	0.31
H. villosa - *L. argenteus*	-0.220	0.062	6196	-3.547	0.00039
H. villosa - *S. crassulus*	-0.266	0.068	6196	-3.926	8.7e-05
I. gordonii - *L. argenteus*	-0.247	0.065	6196	-3.766	0.00017
I. gordonii - *S. crassulus*	-0.293	0.072	6196	-4.091	4.3e-05
L. argenteus - *S. crassulus*	-0.046	0.058	6196	-0.788	0.43

Chapter 4

Demographic buffering is stage-dependent in response to environmental stochasticity

4.1 Background

Environmental stochasticity shapes communities [109] through its effects on demography [27] and coexistence [66]. Understanding how populations respond to environmental stochasticity is timely due to predicted increases in environmental variation due to climate change [8]. In response to environmental stochasticity, natural selection has led to several strategies to maximize a population's stochastic growth rate, λ_s, by modulating vital rates (e.g., survival, growth, fertility). One of these strategies is demographic buffering, the coordination of vital rates to minimize variation in annual population growth rates, λ_t, in response to perturbations in vital rate mean or variance from environmental stochasticity [93, 43, 104]. These λ_t are averaged over time to generate λ_s.

Demographic buffering is a conservative demographic strategy that reduces changes in λ_s due to perturbations in vital rates from environmental stochasticity [75, 43]. Other demographic strategies, such as demographic lability, have fluctuating stochastic growth rates that track environmental conditions, leading to proportionately higher gains in λ_t in 'good years' and proportionately lower losses in 'bad years.' Organisms with demographic buffering strategies are often theorized to have higher λ_s compared to those with labile strategies [117], but it is increasingly recognized that demographic lability is sometimes also adaptive (especially when juvenile and adult survival are low) [58].

A population's, species', or developmental stage's propensity to demographic buffering can be estimated with the summation of stochasticities of variance, which measures the effect of increased vital rate variance on λ_s to generate a 'buffering value.' By understanding the ranges and drivers of different buffering values across species, we can better understand how natural populations respond to environmental stochasticity. For example, demographic

buffering covaries with life expectancy. As seen across 36 plant and animal species in [80], vital rates in species with longer generation times are more buffered against environmental stochasticity than in species with shorter generation times. This demographic buffering and life expectancy relationship is adaptive as long-lived species in stochastic environments can experience many high- and low-quality years. If λ_t fluctuates across the lifespan of a long-lived organism, the cumulative effect of both high and low λ_t values could result in a lower λ_s compared to λ_t values with low variation across time. Similarly, whether a species buffers λ_s is often thought to depend on the riskiness of the strategy relative to the organism's position on the fast-slow continuum with more buffering of λ_s in slower species [75, 63]. Thus, demographic buffering has been characterized as a life history strategy— representing a population's evolutionary response to environmental stochasticity.

While buffering values can vary among species, the contribution of different life-cycle stages within a population to buffering of λ_s may also vary. For example, differences in vital rate sensitivity to environmental drivers between age classes, as seen in yellow-bellied marmots [26], could lead to different buffering values. Compared to adults, juveniles might also have a lower ability to buffer λ_s under environmentally stressful conditions, such as drought and high temperatures, due to trait differences that result in lower capacity to access and conserve resources (e.g., [36]). Differences in juvenile and adult buffering of specific vital rates have been demonstrated in mammals, including higher buffering of adult survival compared to juvenile survival [37]. However, there have been no comprehensive comparisons within a plant community that would allow for comparisons of demographic buffering of λ_s between species and developmental stages sharing common environmental conditions.

Community-level comparisons of demographic strategies are invaluable partly because environmental conditions can have contrasting effects on vital rates within and across species (e.g., [61]). Communities with high seasonality and environmental stochasticity are ideal settings for comparing demographic buffering between co-occurring species and developmental stages due to high variation in environmental conditions within and across years.

For example, in many alpine and subalpine plant communities, the start of the growing season is determined by the amount of prior winter precipitation and snowmelt date. Low winter snowfall can cause phenological advances that reduce reproduction through frost mortality of flower buds [50]. However, low winter snowfall can also extend the growing season, potentially allowing for increased acquisition of photosynthates that could benefit other vital rates. For example, in a subalpine plant community, [48] observed reduced plant survival in years with low snowpack and increased investment in reproduction in the subsequent year.

Resource acquisition, growth, and reproduction are temporally constrained in seasonal environments. Due to these temporal constraints, individual size can drastically increase during a growing season, potentially increasing an organism's ability to access resources. In accordance, organisms might be more able to buffer λ_s in response to adverse environmental conditions late in the growing season compared to adverse conditions early in the growing season. However, it has not been explored whether buffering values differ in their sensitivity

to environmental conditions at different intervals within the growing season.

Here, we compared buffering values using long-term demographic data for two co-occurring species in an alpine plant community. In this community, we identified two orthogonal axes of environmental variation corresponding to winter precipitation and growing season temperature (*E-PC1*) and growing season precipitation (*E-PC2*) (see methods). We used eight years of vital rate data (survival, growth, reproduction) for *Ivesia gordonii* and *Senecio crassulus* (**Figure 4.1**). We selected these species due to their high abundance in this community, their distinct growth forms that might contribute to ecological differences, and because the species differed in population trends across years. From 2014 to 2021, the total abundance of *Ivesia gordonii* decreased from 186 to 114 individuals (% change = -38.71), nearly twice the decrease observed in *Senecio crassulus* (18 to 15 individuals, % change = -16.67) (**Figure 4.1**).

Understanding the potentially contrasting effects of environmental drivers on λ_s and their differential effects on different age classes/developmental stages requires structured population models, such as integral projection models (IPMs), that are environmentally explicit. Using IPMs and proportionally perturbing vital rate variances, we estimated the contribution of vital rate variance to λ_s as a metric of demographic buffering for pre-reproductive and reproductive individuals (hereafter, juveniles and adults, respectively). We predicted (**H1**) that adults would buffer λ_s more than juveniles due to their often greater ability to access and conserve resources. Across species, we predicted (**H2**) that *Senecio crassulus* would buffer more than *Ivesia gordonii* because its abundance changed the least during the study period. We also predicted (**H3.a**) that due to increased freezing risk and other potential adverse effects of advanced phenology, adults and juveniles for both species would buffer λ_s more in environments with warmer growing season conditions and low snowpack (lower *E-PC1*) to maintain λ_s when risks of population declines are highest. Similarly, we predicted (**H3.b**) that in response to drier conditions later in the growing season (higher *E-PC2*), juveniles and adults for both focal species would buffer λ_s more than in wetter conditions (lower *E-PC2*).

4.2 Methods

Study site

To test our hypotheses, we collected demographic information from two species over eight years at an alpine plant community in southwest Colorado in the Gunnison National Forest (38.978725°N, 107.042104°W, ∼3540 m above sea level). The vegetation at this site has low (∼5%) cover over a substrate that is dominantly Mancos shale scree (∼5 cm depth) over bedrock. Between 18-20 species of woody and herbaceous perennial plants occur in our census plots, with ∼40-50 species in the surrounding community. The site is typically covered by snow from October through May, with June through September forming the growing season. Water availability varies seasonally in this system, with early-season water dominantly from

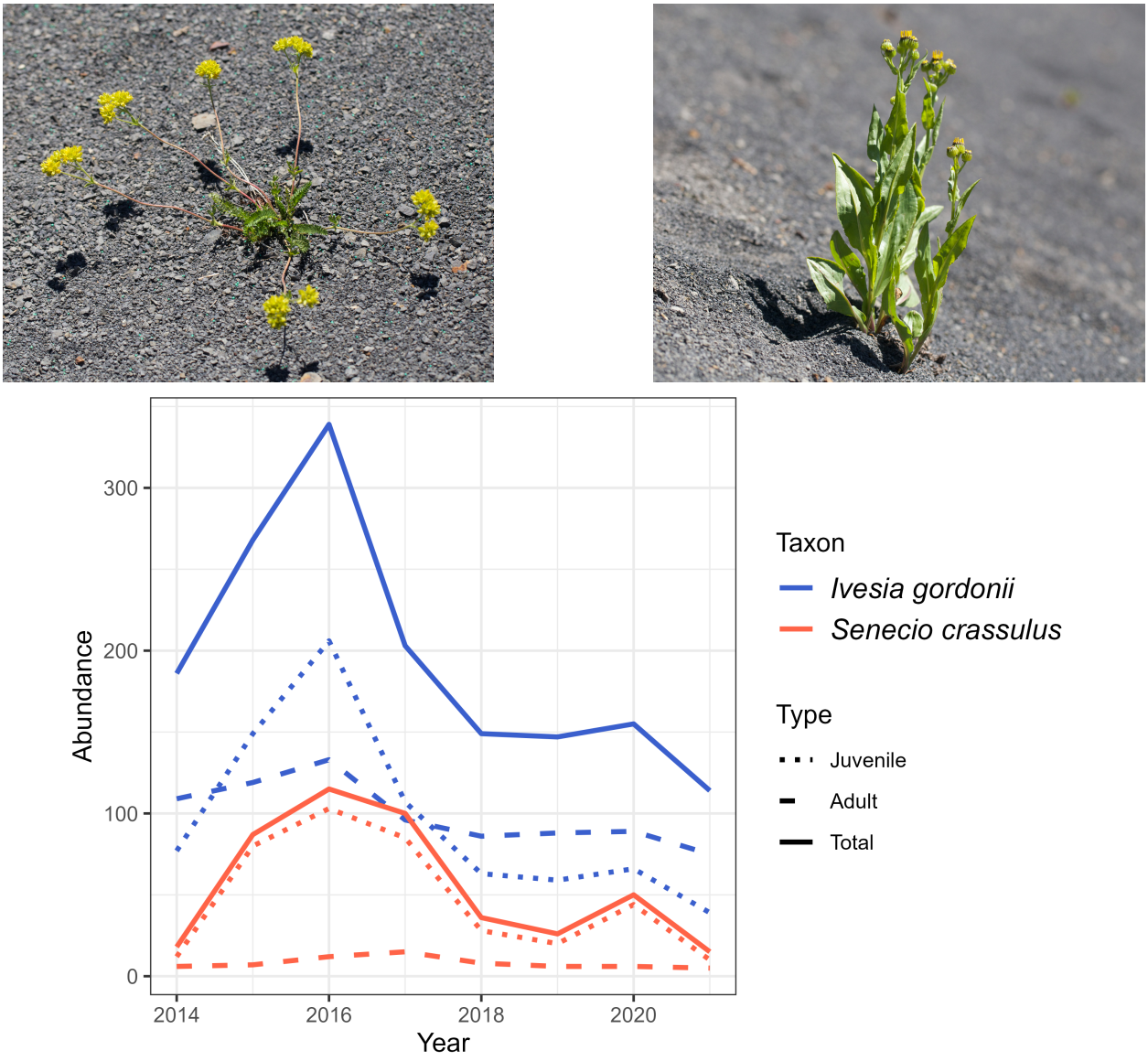

Figure 4.1: Representative images of the two species analyzed in this study: Top left) *Ivesia gordonii* and Top right) *Senecio crassulus*. Bottom) Abundance of focal species by abundance type (i.e., Juvenile, Adult, Total). The total abundance of *Ivesia gordonii* decreased by 38.71%, including a 49.35% decrease in juveniles and a 31.19% decrease in adults. The total abundance of *Senecio crassulus* decreased by 16.67%, including a 16.67% decrease in juveniles and a 16.67% decrease in adults.

snow melt and late-season (July-August) water from monsoonal rains.

Focal species

We compared demographic buffering in two species, *Ivesia gordonii* (Gordon's mousetail, Rosaceae) and *Senecio crassulus* (thickleaf ragwort, Asteraceae). We selected these species due to their relatively high abundance at the research site and due to their differing population trends during the study period. These species also differ in growth form, which may affect their response to environmental stochasticity (sensu [121, 17]. *Ivesia gordonii* is a rosette dicotyledon plant that typically develops a dense basal rosette with age, and *Senecio crassulus* is an erect dicotyledon with typically a sparse basal rosette (**Figure 4.1**).

Demographic census

From 2014-2021, we estimated survival, size (the horizontal length of the longest axis in both species), and reproductive output (number of flowers/capitulescences) for all individuals in fifty 2 x 2 m^2 plots. The measurements occurred annually during peak growing season (generally over ∼two weeks from late July to August). To track individuals across years, we tagged each plant with a uniquely numbered tag and mapped the location of each plant using x-y Cartesian coordinates relative to the bottom left plot corner. As vegetative die-back is common in this community, we considered an individual to have survived if it produced aboveground vegetation with no hiatuses greater than one year. After two consecutive years without aboveground vegetation, we retroactively recorded the individual as dead, starting in the first year of two without vegetative growth. For a complete description of the field site and census protocol, see [12].

Environmental conditions

We used local weather station data (Schofield Pass SNOTEL) to assess if buffering values vary in response to environmental conditions (**H3**). This SNOTEL site is at 3,261 m above sea level, ∼4.3 km from and ∼300 m lower than the census site. We downloaded all available years with air temperature, precipitation, and snow depth data to compare climate patterns during the study period with trends over recent decades (n=22, 1998-2021, n.b.: 2004 was not available, downloaded on February 24, 2022, USDA-NRCS, https://wcc.sc.egov.usda.gov). We then summarized these climate data into the following metrics: growing season precipitation (cm), winter precipitation (cm), the average number of consecutive days during the growing season without precipitation, growing degree days (GDD, °C) accumulated during the growing season, and the number of days during the growing season above 20°C. We defined the growing season as the first snow-free day in spring to the first day with a minimum temperature below -3.89°C (25°F) following conventions in [51] and [97]. We selected these climate variables as they capture metrics of water availability during different periods of the growing season as well as thermal conditions. We used a principal component analysis to reduce the dimensionality of our climate dataset using the *prcomp* function in R. To do so, we used the Kaiser criterion [55], whereby we retained all principal components with associated eigenvalues greater than 1. To emphasize that these principal components represent

environmental conditions, we refer to them as *'E'* in all subsequent sections (e.g., *E-PC1*).

The eight years coinciding with the demographic census were highly variable, including a range of *E-PC1* and *E-PC2* values that were comparable to the distribution of climate conditions from 1998 to 2021 (**Figure 4.3**). The first principal component explained 41.8% of the variance, and the second principal component explained 38.3% of the variance. Higher values of *E-PC1* corresponded to wetter early growing season conditions and cooler growing season temperatures with higher prior winter precipitation, fewer growing season days above 20°C, and fewer growing degree days. Higher values of *E-PC2* corresponded to drier conditions later in the growing season, with more consecutive days without precipitation and less total precipitation during the growing season.

Statistical analysis overview

To test our hypotheses, we identified the developmental stage of individuals in each year as juvenile or adult, and fit generalized linear (mixed) models (GL(M)Ms) to vital rates for each developmental stage. Using coefficients from the GL(M)Ms, we parameterized a two-stage sized-based environmentally stochastic IPM [31].

An IPM is a population model structured by a continuous variable. In its simplest iteration, an IPM is used to project a single continuous state variable, x (e.g., size), to another state, y, across a single time step, t to t+1 [33]. Model coefficients for vital rates, as functions of the state variable, parameterize IPMs. An IPM typically results in two sub-kernels, the survival and growth kernel, P, and the fecundity kernel, F. Collectively, P and F represent the K kernel, which describes the full life cycle. To separate contributions to λ_s from juveniles and adults to test (**H1**), we separated our data into two continuous states, juvenile size and adult size, for the IPM. Thus, our two-state IPM generated four sub-kernels: **1**) $P_{Juv,Juv}$(x,y) for juveniles in t that remain juveniles t+1; **2**) $P_{Adu,Juv}$(x,y) for juveniles in t that transition to adulthood in t+1, **3**) $P_{Adu,Adu}$(x,y) for adults; and **4**) $F_{Juv,Adu}$(x,y) for reproduction. Collectively, these four sub-kernels form a mega-kernel. Due to our inclusion of discrete environmental variables in the IPM (i.e., random effects of year in some vital rate models), the IPM generated four sub-kernels for each of the n=8 census years.

Next, we discretized the mega-matrices for each year. To estimate the effect of increased vital rate variance on λ_s as a metric of demographic buffering, we one-by-one perturbed matrix elements in a given year and then calculated the perturbed λ_s (i.e., λ_s^*). We compared λ_s^* to λ_s to estimate the matrix element elasticity. Then, after iterating the perturbation individually through each matrix element and year, we generated mega-matrices of matrix element elasticities for each year.

Finally, we calculated the summation of stochastic elasticities of variance for each side of the elasticity mega-matrices with the left side, $P_{Juv,Juv}$(x,y) and $P_{Adu,Juv}$(x,y), corresponding to juvenile buffering values, and the right side, $P_{Adu,Adu}$(x,y) and $F_{Juv,Adu}$(x,y), corresponding to adult buffering values. Through this summation, we generated developmental stage- and species-specific buffering values for each year to test (**H1**) and (**H2**).

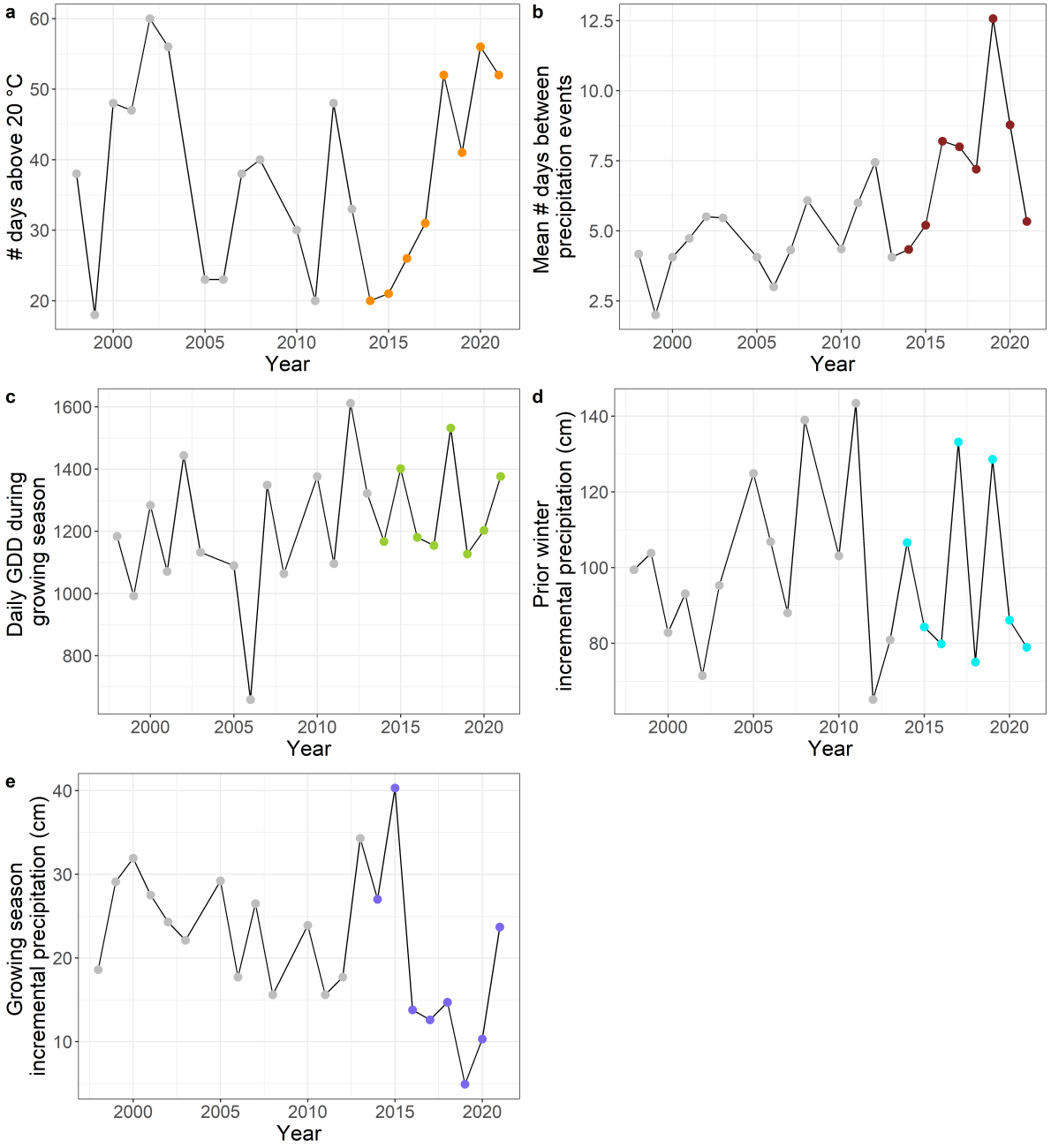

Figure 4.2: Annual trends in the five climate parameters used to calculate the environmental principal components: (a) the number of days during the growing season above 20 °C, (b) the mean number of consecutive days during the growing season without precipitation, (c) growing degree days (GDD, °C) accumulated during the growing season, (d) prior winter incremental precipitation (cm), and (e) growing season incremental precipitation (cm). The eight right-most colored points correspond to census years. Due to data unavailability, 2004 is not included.

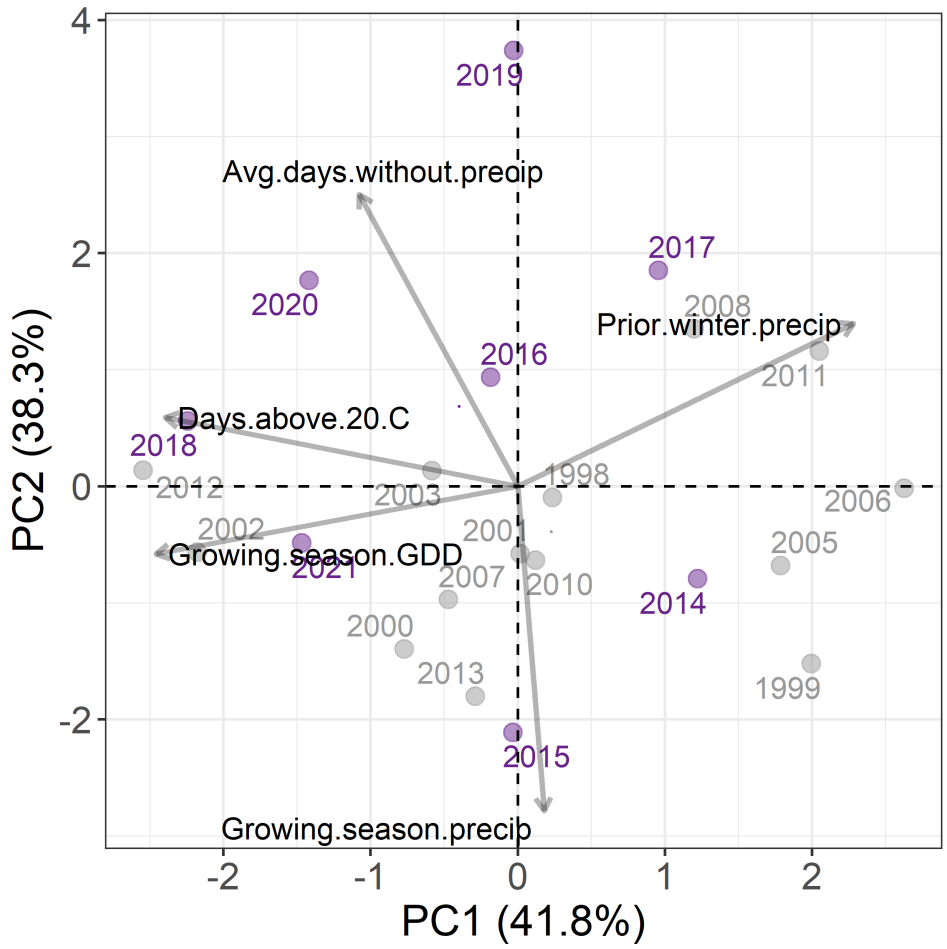

Figure 4.3: Principal component analysis biplot for five annual climate parameters (the number of days during the growing season above 20 °C, the mean number of consecutive days during the growing season without precipitation, growing degree days (GDD, °C) accumulated during the growing season, prior winter incremental precipitation (cm), and growing season incremental precipitation (cm)). The circles represent the climate for each year, with purple and gray circles for years that overlap and do not overlap, respectively, with the demography census data. Higher values of *E-PC1* correspond to cooler summers and greater prior winter precipitation. Higher values of *E-PC2* correspond to drier conditions during the mid-late growing season.

Step 1: Developmental stages

We analyzed vital rates for two developmental stages: 'juveniles'—individuals that at time t or before have never reproduced, and 'adults'—individuals that reproduced at or before time t. To parameterize the transition kernel for juveniles to adults, $P_{Adu,Juv}$(x,y), we separately analyzed growth for juveniles that are first reproductive at time t+1. For each year in our data, we identified the developmental stage of each individual based on its reproduction in that year, as well as prior and subsequent years. The adult-to-juvenile transition for individuals is assumed to not occur in this system. As some adult plants might not have reproduced in the first census year, we corrected for missing assignments through a size-based approach. To do this, we calculated a size-based determinant of adulthood for each species by calculating the inflection point of a logistic curve fit to data for whether the plant reproduced in that year versus size. For the first census year only, individuals larger than the threshold size were considered to be adults, even if they were non-reproductive that year.

Step 2: Model selection and vital rate analyses

We considered the following drivers for survival and growth models: *log (size$_{t+1}$)*, *E-PC1*, and *E-PC2*. Due to the presence of size 0 individuals in the data, '1' was added to each size prior to the natural log transformation. For simplicity, hereafter, *log (size$_{t+1}$)* is referred to as *size$_t$*. For each age class and vital rate, we fit 16 GL(M)Ms with different drivers and levels of complexity, including two-way interactions (**Table 1-10**). Eight of the models were GLMs. One model included only *size$_t$* as a fixed effect. Three models were purely additive, with either *size$_t$* and *E-PC1*, *size$_t$* and *E-PC2*, or all three parameters (*size$_t$*, *E-PC1*, *E-PC2*) as fixed effects. The remaining four GLMs included interactions between the parameters *size$_t$*, *E-PC1*, and *E-PC2*, including (in *lme4* notation):

Response$\sim$*size$_t$*+*E.PC1*+*size$_t$***E.PC1*;

Response$\sim$*size$_t$*+*E.PC2*+*size$_t$***E.PC2*;

Response$\sim$*size$_t$*+*E.PC1*+*E.PC2*+*size$_t$***E.PC1*+*size$_t$***E.PC2*;

Response$\sim$*size$_t$*+*E.PC1*+*E.PC2*+*size$_t$***E.PC1*+*size$_t$***E.PC2*+*E.PC1***E.PC2*.

The other eight models were GLMMs with identical model structures to the previous eight, except for including year as a random effect. We selected the vital rate model with the lowest Akaike information criterion (AIC). In cases where models had comparable AIC values (<2 difference), we selected the model with the fewest coefficients and interaction terms.

We fit Gaussian-family models for size in year t+1 (growth) using an identity link function for all developmental stages. We fit binomial-family models (logit link) for the probability of survival in year t+1. To increase model power, we fit models for survival for all individuals, regardless of age class. To parameterize growth in the juvenile to adult transition sub-kernel $P_{Adu,Juv}$(x,y), we used the same 16 model structures as above. We estimated the probability of remaining a juvenile (i.e., of not reproducing) in year t+1 with binomial families and logit link functions.

Due to low levels of recruitment across years and, thus, low statistical power to test for links between environmental stochasticity and reproduction, we did not follow the model

selection criteria above. Instead, we used a simpler recruitment model to parameterize the $F_{Juv,Adu}$(x,y) sub-kernel:

Number of recruits t+1 $\sim$ Number of adults in year t.

For a complete description of the model selection, including model structure and AIC scores, see **Tables 1-10**.

Step 3: Integral projection models

For each species and year (2014-2021), we built a discrete two-stage environmentally-stochastic IPM [31]. For each P kernel that included parameters from vital rate models with a random effect of year, we estimated transition probabilities using year-specific coefficients, thus generating a sequence of P kernels per year [76]. To simulate the stochastic environment for each IPM iteration, for *E-PC1* and *E-PC2*, we randomly sampled values from a normal distribution defined by the mean and standard deviation of these parameters' values observed during the study period, *E-PC1* (μ = -0.3994, sd = 1.2172) and *E-PC2* (μ = 0.6837, sd = 1.8239). We iterated the stochastic run of our IPMs 1,000 times, each sampling randomly generated *E-PC1* and *E-PC2* values and each producing a sequence of kernels for each year-specific kernel type. We removed the first 15% of iterations to allow "burn in" of the model. We then calculated the stochastic population growth rate, λ_s, from our simulation as the exponentiated expected geometric mean of λ_t across a time series:

$$\lambda_s = exp\left(E\left[ln\left(\frac{N_{t+1}}{N_t}\right)\right]\right)$$

Equation 1: Formula for λ_s where N_t indicates the number of individuals at time t and N_{t+1} is the number of individuals at time t+1 [20].

Step 4: Perturbation analysis

Vital rate elasticities show the proportional contribution of a vital rate to the population growth rate, λ [60]. The summation of stochastic elasticities of variance (Equation 2) represents the impact of proportional increases in vital rate variance on λ_s. We used a numeric approach to calculate the summation of stochastic elasticities of variance, as in [38]. In Step 3, we iterated each IPM for 1,000 time steps for each year, with each iteration generating a kernel. Now, for each matrix element in a given year (e.g., matrix element a_{ij} in kernels parameterized based on vital rate coefficients from 2014), we increased the matrix element variance by a small proportional amount (+0.000001) and calculated the perturbed stochastic growth rate, λ_s^*, across all time steps. We perturbed all matrix elements individually to calculate the effect of increased matrix element variance on λ_s.

Step 5: Buffering analyses

By one-by-one perturbing matrix elements, we estimated the stochastic elasticity for each matrix element. We used the summation of all matrix element stochastic elasticities from the kernels, $P_{Juv,Juv}$(x,y) and $P_{Adu,Juv}$(x,y), to calculate juvenile buffering values. Similarly,

the summation of all matrix element stochastic elasticities from the kernels $P_{Adu,Adu}$(x,y) and $F_{Juv,Adu}$(x,y) were used to calculate adult buffering values. Buffering values are negative, with values closer to 0 indicating more buffering of λ_s.

$$\Sigma E^{\sigma^2}_{a_{ij}} = \Sigma_{a_{ij}} \left[\frac{var\left(a_{ij}\right)}{\lambda_s} * \frac{\lambda_s^{*aj} - \lambda_s}{0.00001 * var\left(a_{ij}\right)} \right]$$

Equation 2: Summation of the stochastic elasticities of variance of vital rates with respect to λ_s (sensu "Equation 5" in [38])

Step 6: Testing hypotheses

To test for differences in buffering values between developmental stages (**H1**) and between species with different changes in total abundance during the study period (**H2**), we first fit an ordinary least squares (OLS) regression with buffering value as the response variable and species and developmental stage as fixed effects. Both predictors were factors. We used Tukey contrasts (α=0.05) in post-hoc analyses to compare buffering values within factor levels. We tested for differences in buffering values between juveniles and adults within species (**H1**) by fitting an OLS regression to buffering values for *Ivesia gordonii* and *Senecio crassulus* separately. In these models, the only predictor was developmental stage as a factor. To address (**H3**), we fit separate OLS regressions for each species and developmental stage with buffering value as the response variable and *E-PC1* and *E-PC2* as fixed effects.

We conducted all analyses in R, version 4.2.2. Linear models were fitted using the *lme4* package [6]. We constructed IPMs using the package, *ipmr* [65]. We used the package [**multcomp**] [46] for Tukey contrasts.

4.3 Results

Both focal species populations are decreasing (**Figure 4.1**) under the current ranges of environmental stochasticity (**Figure 4.2**). Based on the mean mega-kernel with averaged transition probabilities across years (**Figure 4.4**), the stochastic growth rates (λ_s) for *Ivesia gordonii* and *Senecio crassulus* were 0.695 and 0.902, respectively. This inference is consistent with the observation of decreases in total abundance for *Ivesia gordonii* (38.71%) and *Senecio crassulus* (16.67%) (**Figure 4.1**).

The summation of stochastic elasticities of variance. Buffering values closer to 0 indicate more buffering of of λ_s compared to more negative values. Across year-specific kernels (i.e., parameterized with year-specific intercept terms), we observed (**H1**) less buffering of λ_s in *Ivesia gordonii* juveniles (range: -0.0355 to -0.0264, mean = -0.0302, sd = 0.0032) compared to adults (range: -0.0279 to -0.0119, mean = -0.0196, sd = 0.00526). In contrast, we observed similar buffering values in juvenile *Senecio crassulus* (range: -0.0107 to -0.0048, mean = -0.0074, sd = 0.0019) compared to adults (range: -0.0122 to -0.0046, mean = -0.0080, sd = 0.0029) (**Figure 4.5**).

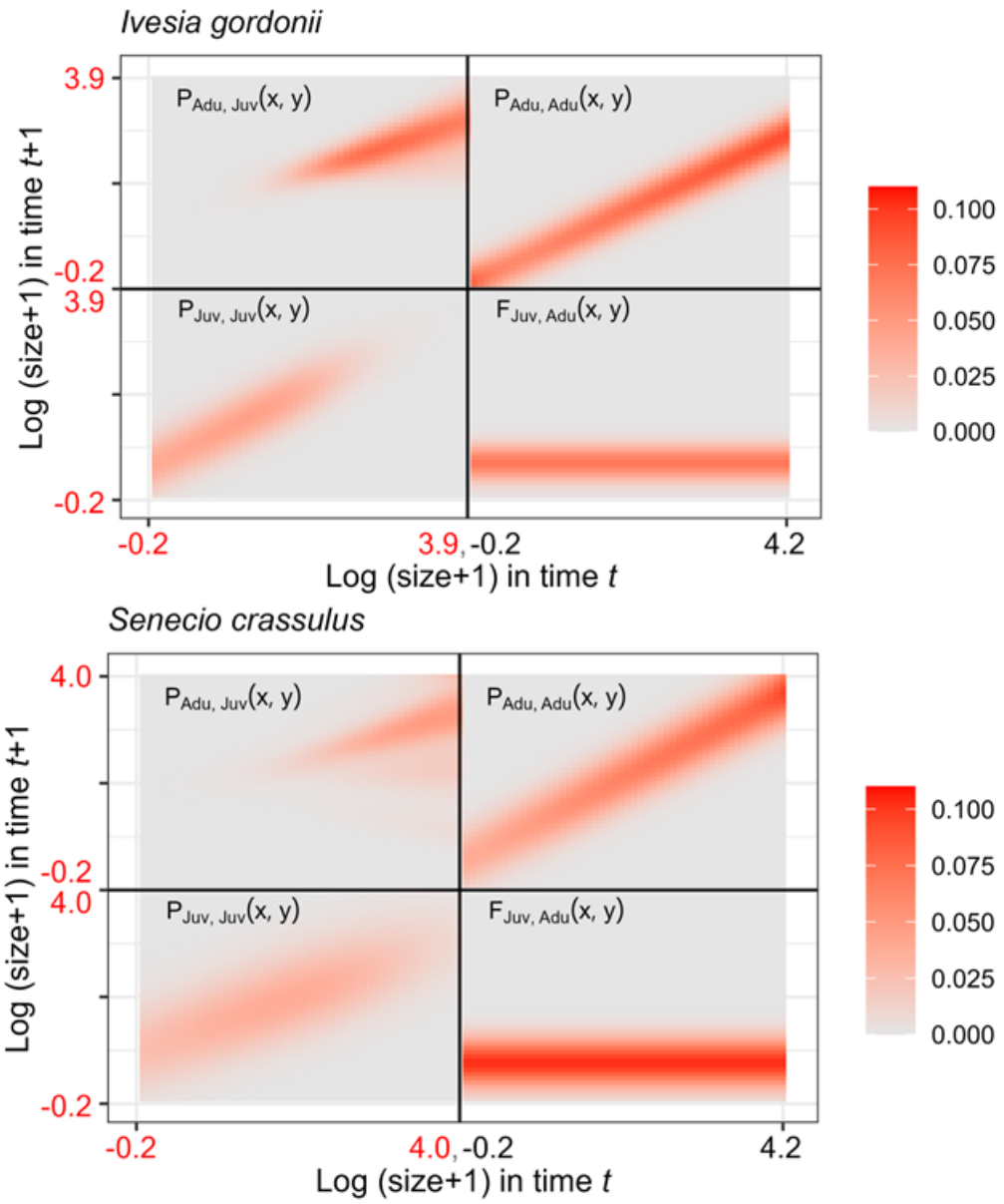

Figure 4.4: Discretized mega-kernels for Top) *Ivesia gordonii* and Bottom) *Senecio crassulus*. In each mega-kernel, the four sub-kernels represent the average transition probabilities across years (2014-2021) from *log (size+1)* in time t to *log (size+1)* in time t+1. We added 1 to all sizes before using a natural log transformation due to the presence of living plants that were size 0 in the data. Log sizes on the axes are color-coded for juveniles (red) and adults (black). The bottom left sub-kernel is $P_{Juv,Juv}$(x,y) for juveniles in time t that remain juveniles in time t+1. The top left sub-kernel is $P_{Adu,Juv}$(x,y) for juveniles in t that transition to adulthood in t+1. The top right sub-kernel is $P_{Adu,Adu}$(x,y) for adults. The bottom right sub-kernel represents the per capita contribution to new recruits, $F_{Juv,Adu}$(x,y).

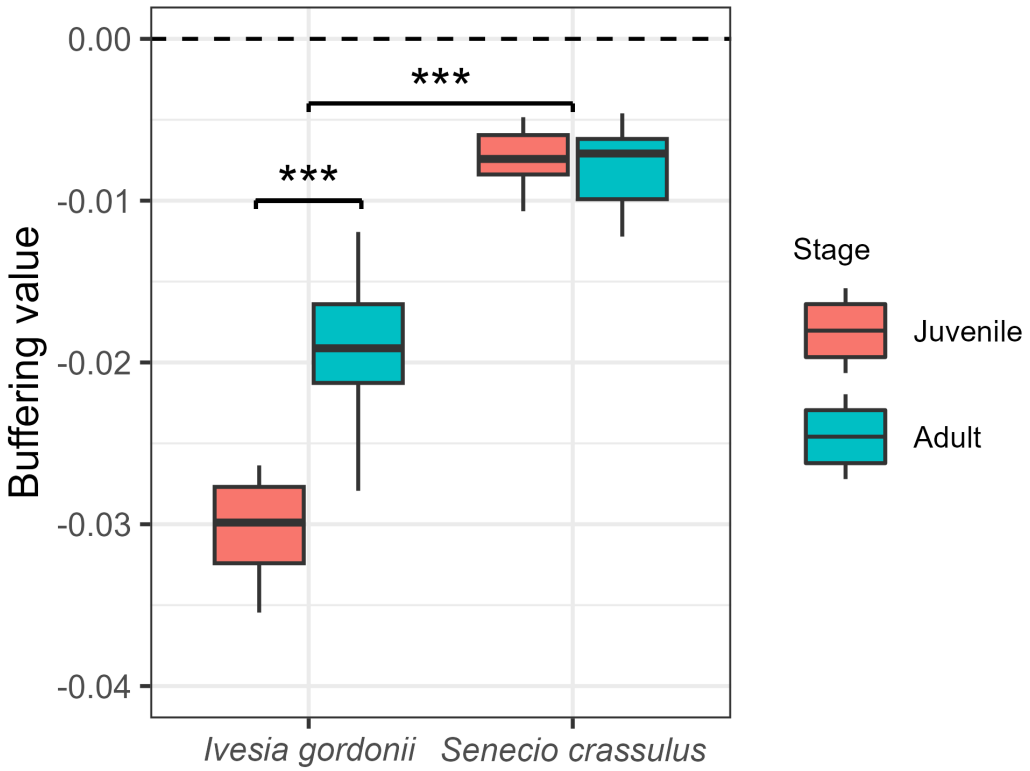

Figure 4.5: Boxplot of buffering values for juvenile (red) and adult (teal) *Ivesia gordonii* and *Senecio crassulus*. The dashed line at y=0 delineates complete buffering. Buffering decreases with increasingly negative buffering values. Asterisks indicate significance values of comparisons (***, $p < 0.01$).

In a post-hoc analysis across both species, we found similar trends. Compared to a reference intercept of *Ivesia gordonii* and juvenile plants for mean *E-PC1* and *E-PC2*, (**H1**) adults had higher buffering values (estimate = 0.005027, p = 0.00182). For (**H2**), the species with the lowest population declines during the study period (*Senecio crassulus*) had higher buffering values than the species with the highest declines (*Ivesia gordonii*, estimate = 0.017214, $p < 0.001$).

Within species, (**H2**) buffering was higher in adults than juveniles for *Ivesia gordonii* (estimate = 0.010664, p = 0.000237), but not *Senecio crassulus*. We did not find any support for greater buffering of λ_s in warmer growing seasons with low snowpack (**H3.a**). However, we found evidence that adult *Senecio crassulus* buffered λ_s (**H3.b**) in response to drier conditions (estimate = 0.0011220, p = 0.0495) later in the growing season, but not juvenile *Senecio crassulus* or *Ivesia gordonii* in either developmental stage.

4.4 Discussion

We found (**H1**) overall higher buffering of λ_s in adults than juveniles, but within species, we only observed ontogenetic differences in demographic buffering of *Ivesia gordonii*, not *Senecio crassulus*. The focal species with the least change in abundance, *Senecio crassulus*, buffered λ_s more than the focal species with large declines in abundance, *Ivesia gordonii* (**H2**). We also found evidence that (**H3**) buffering of λ_s responds to late-growing season water availability (*E-PC2*) in adult *Senecio crassulus* (**Figure 4.6**). Thus, as environmental stochasticity increases with climate change, our results suggest buffering λ_s can contribute to persistence.

As demographic buffering indicates a population's ability to maintain λ_s during periods of environmental stochasticity, differences in buffering values between juveniles and adults might originate from multiple factors. Higher buffering values in adults might reflect that sensitive vital rates are already high (e.g., probability of survival is at or near 1), so small increases do not have a large effect on λ_s. High adult buffering of λ_s may thus reflect an ability to adopt a lower-risk response to environmental stochasticity, potentially due to greater access to resources (e.g., through more extensive root networks).

Despite co-occurring in the same community and experiencing the same climatic conditions, we observed higher buffering in *Senecio crassulus* compared to *Ivesia gordonii* (**H2**). This difference might reflect contrasting positions on the fast-slow continuum [63] and differences in lifespans [58, 75]. Also, while both species also have declining populations ($\lambda_s < 1$), *Ivesia gordonii* is declining faster than *Senecio crassulus*. As juvenile *Ivesia gordonii* buffer λ_s less than adults (**Figure 4.5**), *Ivesia gordonii* may be less able to tolerate environmental stochasticity compared to other species (e.g., *Senecio crassulus*).

Although winter and growing season precipitation are highly variable in this community (**Figure 4.2**), increased buffering of λ_s in response to drier climatic conditions (higher *E-PC2*) might be especially advantageous. The amount of water available at the start of the growing season for juveniles and adults is likely comparable due to a common snowmelt source. Later in the growing season, when water availability fluctuates with the timing of monsoon rains, adult plants may have traits that allow them to better access and conserve water compared to juveniles (e.g., [36]). Higher buffering of λ_s in adults, but not juveniles, in climates with drier late-growing season conditions (higher *E-PC2*) suggests that adults are more drought tolerant than juveniles in this system.

Our results suggest that demographic buffering benefits population persistence. However, projecting future populations under increased environmental stochasticity is challenged by multiple factors. For example, buffering may not be sufficient to prevent population declines if adverse conditions are frequent in long-lived species, such as many alpine plants [100]. Adverse conditions that are rare, but extreme, can also play an important role in shaping plant demography, including changing the relative magnitude of vital rates [68]. Changes in vital rate correlation due to increased environmental stochasticity (e.g., [49]) might also influence buffering values. Finally, demographic lability, which was not tested here, may also influence population persistence. As alpine forbs near this study site (including *Ivesia*

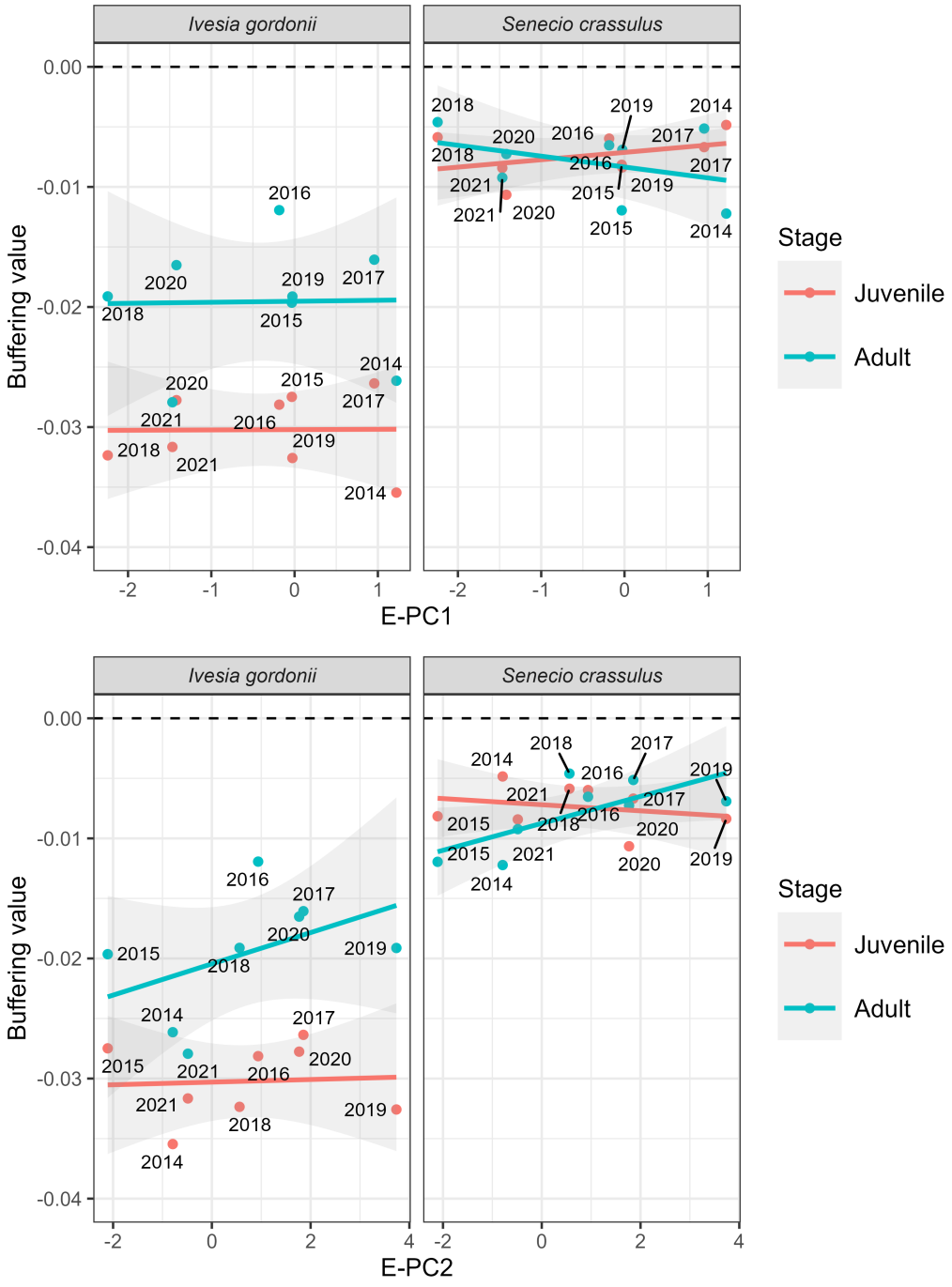

Figure 4.6: Visualization of Buffering values (points) by year, species, and age class versus Top) *E-PC1* and Bottom) *E-PC2*. Standard errors are shaded in gray. Buffering values closer to zero (dashed line) indicate more buffering compared to more negative values.

gordonii and *Senecio* congeners) have declined in recent decades [127], future studies might find increased evidence that demographic buffering promotes population persistence in alpine species with stable or increasing populations.

There are limitations to the current study and models. For example, biological interactions reduce variation in local microclimates and shape vital rates in this community [97]. Because our stochastic climate parameters (*E-P1*) and (*E-PC2*) were based on macroclimate conditions, not microclimate conditions, our estimates of environmental stochasticity in this community might not align with what many plants directly experienced. Similarly, some effects ascribed to climate (e.g., demographic buffering response to *E-PC2* in adult *Senecio crassulus*) might be correlational shadows of species interactions.

Another important limitation of this study is that the $F_{Juv,Adu}$(x,y) sub-kernel is currently modeled as environmentally independent. Reproduction responds to environmental stochasticity in plant communities neighboring the study site (e.g., [50, 48]). Increased understanding of the relationship between recruitment, the seed bank, and environmental stochasticity in this system in future studies will provide a fuller picture of species and ontogenetic differences in demographic buffering.

Conclusions

Organismal response to climate change is shaped by increased environmental stochasticity. Here, we demonstrate evidence for ontogenetic and species-level differences in co-occurring plants. As both species are among the most abundant in this community, this study supports that multiple demographic strategies could contribute to commonness in a community. However, both species are also in decline, with the species with the lowest buffering values and the largest difference between adult and juvenile buffering values declining the most.

This study is the first to the authors' knowledge to show ontogenetic differences in demographic buffering in plants, suggesting that different developmental stages can differ in their response to environmental stochasticity. Future studies will explore whether this pattern is consistent across multiple species and more growth forms in this community.

Table 4.1: Formulae, degrees of freedom (DF), and AICs for model selection for *Ivesia gordonii* survival for all individuals (All $Survival_{t+1}$). 'Checked' models in the 'Lowest' column had either the lowest AIC score or an AIC score within 2 of the lowest. We selected the least complex model from the models with the lowest AIC scores to parameterize the IPM.

Model type	Model	Model	DF	AIC	Lowest	Selected
Ivesia gordonii All $Survival_{t+1}$	1	$\sim \log size_t$	2	1542.88		
	2	$\sim \log size_t + PC1$	3	1544.88		
	3	$\sim \log size_t + PC2$	3	1497.88		
	4	$\sim \log size_t + PC1 + PC2$	4	1499.85		
	5	$\sim \log size_t + PC1 + \log size_t * PC1$	4	1545.95		
	6	$\sim \log size_t + PC2 + \log size_t * PC2$	4	1497.04		
	7	$\sim \log size_t + PC1 + PC2 + \log size_t * PC1 + \log size_t * PC2$	6	1500.11		
	8	$\sim \log size_t + PC1 + PC2 + \log size_t * PC1 + \log size_t * PC2 + PC1 * PC2$	7	1498.80		
	9	$\sim \log size_t + (1\|Year)$	3	1358.28	✓	✓
	10	$\sim \log size_t + PC1 + (1\|Year)$	4	1360.07	✓	
	11	$\sim \log size_t + PC2 + (1\|Year)$	4	1358.61	✓	
	12	$\sim \log size_t + PC1 + PC2 + (1\|Year)$	5	1360.33		
	13	$\sim \log size_t + PC1 + \log size_t * PC1 + (1\|Year)$	5	1360.48		
	14	$\sim \log size_t + PC2 + \log size_t * PC2 + (1\|Year)$	5	1360.27	✓	
	15	$\sim \log size_t + PC1 + PC2 + \log size_t * PC1 + \log size_t * PC2 + (1\|Year)$	7	1362.49		
	16	$\sim \log size_t + PC1 + PC2 + \log size_t * PC1 + \log size_t * PC2 + PC1 * PC2 + (1\|Year)$	8	1363.20		

Table 4.2: Formulae, degrees of freedom (DF), and AICs for model selection for *Ivesia gordonii* juvenile growth (JJ growth). 'Checked' models in the 'Lowest' column had either the lowest AIC score or an AIC score within 2 of the lowest. We selected the least complex model from the models with the lowest AIC scores to parameterize the IPM.

Model type	Model	Model	DF	AIC	Lowest	Selected
Ivesia gordonii JJ growth	1	$\sim \log size_t$	2	410.63		
	2	$\sim \log size_t + PC1$	3	406.11	✓	✓
	3	$\sim \log size_t + PC2$	3	412.50		
	4	$\sim \log size_t + PC1 + PC2$	4	408.07	✓	
	5	$\sim \log size_t + PC1 + \log size_t * PC1$	4	407.72	✓	
	6	$\sim \log size_t + PC2 + \log size_t * PC2$	4	414.00		
	7	$\sim \log size_t + PC1 + PC2 + \log size_t * PC1 + \log size_t * PC2$	6	411.40		
	8	$\sim \log size_t + PC1 + PC2 + \log size_t * PC1 + \log size_t * PC2 + PC1 * PC2$	7	413.10		
	9	$\sim \log size_t + (1\|Year)$	3	421.79		
	10	$\sim \log size_t + PC1 + (1\|Year)$	4	424.87		
	11	$\sim \log size_t + PC2 + (1\|Year)$	4	429.97		
	12	$\sim \log size_t + PC1 + PC2 + (1\|Year)$	5	433.64		
	13	$\sim \log size_t + PC1 + \log size_t * PC1 + (1\|Year)$	5	431.21		
	14	$\sim \log size_t + PC2 + \log size_t * PC2 + (1\|Year)$	5	437.62		
	15	$\sim \log size_t + PC1 + PC2 + \log size_t * PC1 + \log size_t * PC2 + (1\|Year)$	7	447.82		
	16	$\sim \log size_t + PC1 + PC2 + \log size_t * PC1 + \log size_t * PC2 + PC1 * PC2 + (1\|Year)$	8	454.78		

Table 4.3: Formulae, degrees of freedom (DF), and AICs for model selection for *Ivesia gordonii* probability of remaining a juvenile (J remain). 'Checked' models in the 'Lowest' column had either the lowest AIC score or an AIC score within 2 of the lowest. We selected the least complex model from the models with the lowest AIC scores to parameterize the IPM.

Model type	Model	Model	DF	AIC	Lowest	Selected
Ivesia gordonii J remain	1	$\sim \log size_t$	2	352.60		
	2	$\sim \log size_t + PC1$	3	353.44		
	3	$\sim \log size_t + PC2$	3	346.77	✓	✓
	4	$\sim \log size_t + PC1 + PC2$	4	348.36		
	5	$\sim \log size_t + PC1 + \log size_t * PC1$	4	354.62		
	6	$\sim \log size_t + PC2 + \log size_t * PC2$	4	345.26	✓	
	7	$\sim \log size_t + PC1 + PC2 + \log size_t * PC1 + \log size_t * PC2$	6	348.56		
	8	$\sim \log size_t + PC1 + PC2 + \log size_t * PC1 + \log size_t * PC2 + PC1 * PC2$	7	349.25		
	9	$\sim \log size_t + (1\|Year)$	3	352.75		
	10	$\sim \log size_t + PC1 + (1\|Year)$	4	354.16		
	11	$\sim \log size_t + PC2 + (1\|Year)$		Singular fit		
	12	$\sim \log size_t + PC1 + PC2 + (1\|Year)$		Singular fit		
	13	$\sim \log size_t + PC1 + \log size_t * PC1 + (1\|Year)$	5	355.19		
	14	$\sim \log size_t + PC2 + \log size_t * PC2 + (1\|Year)$		Singular fit		
	15	$\sim \log size_t + PC1 + PC2 + \log size_t * PC1 + \log size_t * PC2 + (1\|Year)$		Singular fit		
	16	$\sim \log size_t + PC1 + PC2 + \log size_t * PC1 + \log size_t * PC2 + PC1 * PC2 + (1\|Year)$		Singular fit		

Table 4.4: Formulae, degrees of freedom (DF), and AICs for model selection for *Ivesia gordonii* juveniles that transition to adulthood in $year_{t+1}$ (AJ Growth). 'Checked' models in the 'Lowest' column had either the lowest AIC score or an AIC score within 2 of the lowest. We selected the least complex model from the models with the lowest AIC scores to parameterize the IPM.

Model type	Model	Model	DF	AIC	Lowest	Selected
Ivesia gordonii AJ Growth	1	$\sim \log size_t$	3	12.66		
	2	$\sim \log size_t + PC1$	4	13.78		
	3	$\sim \log size_t + PC2$	4	13.74		
	4	$\sim \log size_t + PC1 + PC2$	5	14.50		
	5	$\sim \log size_t + PC1 + \log size_t * PC1$	5	-1.71	✓	✓
	6	$\sim \log size_t + PC2 + \log size_t * PC2$	5	15.39		
	7	$\sim \log size_t + PC1 + PC2 + \log size_t * PC1 + \log size_t * PC2$	7	-2.26	✓	
	8	$\sim \log size_t + PC1 + PC2 + \log size_t * PC1 + \log size_t * PC2 + PC1 * PC2$	8	-0.83	✓	
	9	$\sim \log size_t + (1\|Year)$	4	23.30		
	10	$\sim \log size_t + PC1 + (1\|Year)$	5	30.03		
	11	$\sim \log size_t + PC2 + (1\|Year)$	5	31.04		
	12	$\sim \log size_t + PC1 + PC2 + (1\|Year)$	6	37.59		
	13	$\sim \log size_t + PC1 + \log size_t * PC1 + (1\|Year)$	6	17.22		
	14	$\sim \log size_t + PC2 + \log size_t * PC2 + (1\|Year)$	6	37.46		
	15	$\sim \log size_t + PC1 + PC2 + \log size_t * PC1 + \log size_t * PC2 + (1\|Year)$	8	30.97		
	16	$\sim \log size_t + PC1 + PC2 + \log size_t * PC1 + \log size_t * PC2 + PC1 * PC2 + (1\|Year)$	9	29.64		

Table 4.5: Formulae, degrees of freedom (DF), and AICs for model selection for *Ivesia gordonii* adult growth (AA Growth). 'Checked' models in the 'Lowest' column had either the lowest AIC score or an AIC score within 2 of the lowest. We selected the least complex model from the models with the lowest AIC scores to parameterize the IPM.

Model type	Model	Model	DF	AIC	Lowest	Selected
Ivesia gordonii AA Growth	1	$\sim \log size_t$	3	294.04		
	2	$\sim \log size_t + PC1$	4	281.73		
	3	$\sim \log size_t + PC2$	4	291.10		
	4	$\sim \log size_t + PC1 + PC2$	5	275.31		
	5	$\sim \log size_t + PC1 + \log size_t * PC1$	5	283.17		
	6	$\sim \log size_t + PC2 + \log size_t * PC2$	5	288.76		
	7	$\sim \log size_t + PC1 + PC2 + \log size_t * PC1 + \log size_t * PC2$	7	274.49		
	8	$\sim \log size_t + PC1 + PC2 + \log size_t * PC1 + \log size_t * PC2 + PC1 * PC2$	8	272.05	✓	
	9	$\sim \log size_t + (1\|Year)$	4	272.73	✓	✓
	10	$\sim \log size_t + PC1 + (1\|Year)$	5	277.54		
	11	$\sim \log size_t + PC2 + (1\|Year)$	5	280.06		
	12	$\sim \log size_t + PC1 + PC2 + (1\|Year)$	6	284.64		
	13	$\sim \log size_t + PC1 + \log size_t * PC1 + (1\|Year)$	6	284.43		
	14	$\sim \log size_t + PC2 + \log size_t * PC2 + (1\|Year)$	6	282.72		
	15	$\sim \log size_t + PC1 + PC2 + \log size_t * PC1 + \log size_t * PC2 + (1\|Year)$	8	294.42		
	16	$\sim \log size_t + PC1 + PC2 + \log size_t * PC1 + \log size_t * PC2 + PC1 * PC2 + (1\|Year)$	9	300.61		

Table 4.6: Formulae, degrees of freedom (DF), and AICs for model selection for *Senecio crassulus* survival for all individuals (All $Survival_{t+1}$). 'Checked' models in the 'Lowest' column had either the lowest AIC score or an AIC score within 2 of the lowest. We selected the least complex model from the models with the lowest AIC scores to parameterize the IPM.

Model type	Model	Model	DF	AIC	Lowest	Selected
Senecio crassulus All $Survival_{t+1}$	1	$\sim \log size_t$	2	593.35		
	2	$\sim \log size_t + PC1$	3	593.79		
	3	$\sim \log size_t + PC2$	3	550.83		
	4	$\sim \log size_t + PC1 + PC2$	4	551.74		
	5	$\sim \log size_t + PC1 + \log size_t * PC1$	4	584.75		
	6	$\sim \log size_t + PC2 + \log size_t * PC2$	4	552.78		
	7	$\sim \log size_t + PC1 + PC2 + \log size_t * PC1 + \log size_t * PC2$	6	550.05		
	8	$\sim \log size_t + PC1 + PC2 + \log size_t * PC1 + \log size_t * PC2 + PC1 * PC2$	7	547.90		
	9	$\sim \log size_t + (1\|Year)$	3	518.09	✓	✓
	10	$\sim \log size_t + PC1 + (1\|Year)$	4	519.93		
	11	$\sim \log size_t + PC2 + (1\|Year)$	4	517.12	✓	
	12	$\sim \log size_t + PC1 + PC2 + (1\|Year)$	5	518.92	✓	
	13	$\sim \log size_t + PC1 + \log size_t * PC1 + (1\|Year)$	5	519.75		
	14	$\sim \log size_t + PC2 + \log size_t * PC2 + (1\|Year)$	5	519.11	✓	
	15	$\sim \log size_t + PC1 + PC2 + \log size_t * PC1 + \log size_t * PC2 + (1\|Year)$	7	520.81		
	16	$\sim \log size_t + PC1 + PC2 + \log size_t * PC1 + \log size_t * PC2 + PC1 * PC2 + (1\|Year)$	8	522.78		

Table 4.7: Formulae, degrees of freedom (DF), and AICs for model selection for *Senecio crassulus* juvenile growth (JJ growth). 'Checked' models in the 'Lowest' column had either the lowest AIC score or an AIC score within 2 of the lowest. We selected the least complex model from the models with the lowest AIC scores to parameterize the IPM.

Model type	Model	Model	DF	AIC	Lowest	Selected
Senecio crassulus JJ growth	1	$\sim \log size_t$	2	283.82		
	2	$\sim \log size_t + PC1$	3	276.19		
	3	$\sim \log size_t + PC2$	3	275.6		
	4	$\sim \log size_t + PC1 + PC2$	4	267.45		
	5	$\sim \log size_t + PC1 + \log size_t * PC1$	4	277.82		
	6	$\sim \log size_t + PC2 + \log size_t * PC2$	4	277.08		
	7	$\sim \log size_t + PC1 + PC2 + \log size_t * PC1 + \log size_t * PC2$	6	270.29		
	8	$\sim \log size_t + PC1 + PC2 + \log size_t * PC1 + \log size_t * PC2 + PC1 * PC2$	7	263.27	✓	✓
	9	$\sim \log size_t + (1\|Year)$	3	270.07		
	10	$\sim \log size_t + PC1 + (1\|Year)$	4	274.05		
	11	$\sim \log size_t + PC2 + (1\|Year)$	4	274.63		
	12	$\sim \log size_t + PC1 + PC2 + (1\|Year)$	5	278.61		
	13	$\sim \log size_t + PC1 + \log size_t * PC1 + (1\|Year)$	5	279.28		
	14	$\sim \log size_t + PC2 + \log size_t * PC2 + (1\|Year)$	5	281.36		
	15	$\sim \log size_t + PC1 + PC2 + \log size_t * PC1 + \log size_t * PC2 + (1\|Year)$	7	290.52		
	16	$\sim \log size_t + PC1 + PC2 + \log size_t * PC1 + \log size_t * PC2 + PC1 * PC2 + (1\|Year)$	8	293.19		

Table 4.8: Formulae, degrees of freedom (DF), and AICs for model selection for *Senecio crassulus* probability of remaining a juvenile (J remain). 'Checked' models in the 'Lowest' column had either the lowest AIC score or an AIC score within 2 of the lowest. We selected the least complex model from the models with the lowest AIC scores to parameterize the IPM.

Model type	Model	Model	DF	AIC	Lowest	Selected
Senecio crassulus J remain	1	$\sim \log size_t$	2	115.08	✓	✓
	2	$\sim \log size_t + PC1$	3	117.07		
	3	$\sim \log size_t + PC2$	3	113.34	✓	
	4	$\sim \log size_t + PC1 + PC2$	4	115.30	✓	
	5	$\sim \log size_t + PC1 + \log size_t * PC1$	4	118.74		
	6	$\sim \log size_t + PC2 + \log size_t * PC2$	4	113.96	✓	
	7	$\sim \log size_t + PC1 + PC2 + \log size_t * PC1 + \log size_t * PC2$	6	117.60		
	8	$\sim \log size_t + PC1 + PC2 + \log size_t * PC1 + \log size_t * PC2 + PC1 * PC2$	7	118.61		
	9	$\sim \log size_t + (1\|Year)$	3	117.08		
	10	$\sim \log size_t + PC1 + (1\|Year)$	4	119.07		
	11	$\sim \log size_t + PC2 + (1\|Year)$	4	115.34	✓	
	12	$\sim \log size_t + PC1 + PC2 + (1\|Year)$	5	117.30		
	13	$\sim \log size_t + PC1 + \log size_t * PC1 + (1\|Year)$	5	120.74		
	14	$\sim \log size_t + PC2 + \log size_t * PC2 + (1\|Year)$	5	115.96		
	15	$\sim \log size_t + PC1 + PC2 + \log size_t * PC1 + \log size_t * PC2 + (1\|Year)$	7	119.60		
	16	$\sim \log size_t + PC1 + PC2 + \log size_t * PC1 + \log size_t * PC2 + PC1 * PC2 + (1\|Year)$	8	120.61		

Table 4.9: Formulae, degrees of freedom (DF), and AICs for model selection for *Senecio crassulus* juveniles that transition to adulthood in $year_{t+1}$ (AJ Growth). 'Checked' models in the 'Lowest' column had either the lowest AIC score or an AIC score within 2 of the lowest. We selected the least complex model from the models with the lowest AIC scores to parameterize the IPM.

Model type	Model	Model	DF	AIC	Lowest	Selected
Senecio crassulus AJ Growth	1	$\sim \log size_t$	3	22.76		
	2	$\sim \log size_t + PC1$	4	16.23		
	3	$\sim \log size_t + PC2$	4	21.01		
	4	$\sim \log size_t + PC1 + PC2$	5	13.86		
	5	$\sim \log size_t + PC1 + \log size_t * PC1$	5	17.74		
	6	$\sim \log size_t + PC2 + \log size_t * PC2$	5	22.39		
	7	$\sim \log size_t + PC1 + PC2 + \log size_t * PC1 + \log size_t * PC2$	7	15.50		
	8	$\sim \log size_t + PC1 + PC2 + \log size_t * PC1 + \log size_t * PC2 + PC1 * PC2$	8	6.13	✓	✓
	9	$\sim \log size_t + (1\|Year)$	4	25.34		
	10	$\sim \log size_t + PC1 + (1\|Year)$	5	26.07		
	11	$\sim \log size_t + PC2 + (1\|Year)$	5	29.64		
	12	$\sim \log size_t + PC1 + PC2 + (1\|Year)$	6	30.00		
	13	$\sim \log size_t + PC1 + \log size_t * PC1 + (1\|Year)$	6	27.69		
	14	$\sim \log size_t + PC2 + \log size_t * PC2 + (1\|Year)$	6	33.10		
	15	$\sim \log size_t + PC1 + PC2 + \log size_t * PC1 + \log size_t * PC2 + (1\|Year)$	8	34.68		
	16	$\sim \log size_t + PC1 + PC2 + \log size_t * PC1 + \log size_t * PC2 + PC1 * PC2 + (1\|Year)$	9	36.39		

Table 4.10: Formulae, degrees of freedom (DF), and AICs for model selection for *Senecio crassulus* adult growth (AA Growth). 'Checked' models in the 'Lowest' column had either the lowest AIC score or an AIC score within 2 of the lowest. We selected the least complex model from the models with the lowest AIC scores to parameterize the IPM.

Model type	Model	Model	DF	AIC	Lowest	Selected
Senecio crassulus AA Growth	1	$\sim \log size_t$	3	58.93		
	2	$\sim \log size_t + PC1$	4	60.93		
	3	$\sim \log size_t + PC2$	4	55.51	✓	✓
	4	$\sim \log size_t + PC1 + PC2$	5	57.50		
	5	$\sim \log size_t + PC1 + \log size_t * PC1$	5	61.17		
	6	$\sim \log size_t + PC2 + \log size_t * PC2$	5	54.14	✓	
	7	$\sim \log size_t + PC1 + PC2 + \log size_t * PC1 + \log size_t * PC2$	7	55.23	✓	
	8	$\sim \log size_t + PC1 + PC2 + \log size_t * PC1 + \log size_t * PC2 + PC1 * PC2$	8	56.00	✓	
	9	$\sim \log size_t + (1\|Year)$	4	65.89		
	10	$\sim \log size_t + PC1 + (1\|Year)$	5	71.10		
	11	$\sim \log size_t + PC2 + (1\|Year)$	5	68.53		
	12	$\sim \log size_t + PC1 + PC2 + (1\|Year)$	6	74.07		
	13	$\sim \log size_t + PC1 + \log size_t * PC1 + (1\|Year)$	6	73.84		
	14	$\sim \log size_t + PC2 + \log size_t * PC2 + (1\|Year)$	6	71.29		
	15	$\sim \log size_t + PC1 + PC2 + \log size_t * PC1 + \log size_t * PC2 + (1\|Year)$	8	79.40		
	16	$\sim \log size_t + PC1 + PC2 + \log size_t * PC1 + \log size_t * PC2 + PC1 * PC2 + (1\|Year)$	9	84.17		

Chapter 5

Conclusion

My dissertation seeks to understand how community assembly processes determine species compositions and how variation in climate affects these processes. Collectively, these three research chapters demonstrate the value of long-term datasets and place-based studies to generate novel insights into community assembly mechanisms.

My chapters are linked through their insights into species interactions and response to environmental conditions. In my first research chapter, I found that microenvironment modification and spatial overlapping of individuals were key drivers of demography, including promoting spatial heterogeneity of vital rates that may promote spatial clustering. In my next chapter, I found that seed trapping and retention depend on seed and host plant identity. Finally, in my last research chapter, I found that although co-occurring species and developmental stages experience similar environmental conditions, they can differ in the extent that the stochastic population growth rate is buffered to environmental stochasticity.

Collectively these chapters suggest novel interactions between assembly mechanisms. For example, if a species' seeds frequently germinate next to other plants due to seed trapping and retention, they likely experience less variable climate conditions and may have lower demographic buffering values compared to a species that typically does not have neighbors. Also, as we found evidence that juvenile plants in this system are more sensitive to environmental stochasticity. Thus, seeds and seedlings may especially benefit from seed trapping, seed retention, and microclimate modification.

Species abundances have decreased at the Mt. Baldy study site since the initial census in 2014. Declines in alpine forbs are also occurring in nearby plant communities [127], which echo the recent shifts in composition and plant traits seen globally in tundra ecosystems [11]. Through my role as an ecologist and demographer, I have documented community change at the study site over the last six years. By extending demographic data collection at the Mt. Baldy study site into its second decade in the coming years, we will be able to better link intervals of change and stasis to mechanisms.

Bibliography

[1] Peter B Adler et al. "Functional traits explain variation in plant life history strategies." In: *Proc. Natl. Acad. Sci. U.S.A.* 111.2 (2014), pp. 740–5. ISSN: 0027-8424. DOI: 10.1073/pnas.1315179111.

[2] MR R Aguiar and Osvaldo E Sala. "Seed distribution constrains the dynamics of the Patagonian steppe". In: *Ecology* 78.1 (1997), pp. 93–100.

[3] Fabien Anthelme, Lohengrin A. Cavieres, and Olivier Dangles. "Facilitation among plants in alpine environments in the face of climate change". In: *Frontiers in Plant Science* 5 (2014), pp. 1–15. ISSN: 1664-462X. URL: https://www.frontiersin.org/article/10.3389/fpls.2014.00387.

[4] Lisette M. Bakker, Liesje Mommer, and Jasper van Ruijven. "Can root trait diversity explain complementarity effects in a grassland biodiversity experiment?" en. In: *Journal of Plant Ecology* 11.1 (Jan. 2018), pp. 73–84. ISSN: 1752-9921. DOI: 10.1093/jpe/rtw111. URL: https://academic.oup.com/jpe/article/11/1/73/2729969.

[5] Christophe Baltzinger, Sorour Karimi, and Ushma Shukla. "Plants on the Move: Hitch-Hiking With Ungulates Distributes Diaspores Across Landscapes". In: *Frontiers in Ecology and Evolution* 7 (2019). ISSN: 2296-701X. URL: https://www.frontiersin.org/articles/10.3389/fevo.2019.00038.

[6] Douglas Bates et al. *lme4: Linear Mixed-Effects Models using 'Eigen' and S4*. July 2023. URL: https://cran.r-project.org/web/packages/lme4/index.html.

[7] Douglas Bates et al. *lme4: linear mixed-effects models using 'Eigen' and S4*. June 2021. URL: https://CRAN.R-project.org/package=lme4.

[8] Sebastian Bathiany et al. "Climate models predict increasing temperature variability in poor countries". In: *Science Advances* 4.5 (May 2018), eaar5809. DOI: 10.1126/sciadv.aar5809. URL: https://www.science.org/doi/10.1126/sciadv.aar5809.

[9] Mark D Bertness and Ragan Callaway. "Positive interactions in communities". In: *Trends in ecology & evolution* 9.5 (1994), pp. 191–193. ISSN: 0169-5347. DOI: 10.1016/0169-5347(94)90088-4.

[10] Roger Bivand et al. *rgeos: interface to Geometry Engine - Open Source ('GEOS')*. Dec. 2021. URL: https://CRAN.R-project.org/package=rgeos.

[11] Anne D Bjorkman et al. "Plant functional trait change across a warming tundra biome". In: *Nature* 562.7725 (2018), pp. 57–62. ISSN: 0028-0836. DOI: 10.1038/s41586-018-0563-7.

[12] Benjamin Blonder et al. "Microenvironment and functional-trait context dependence predict alpine plant community dynamics". In: *Journal of Ecology* 106.4 (2018), pp. 1323–1337. ISSN: 0022-0477. DOI: 10.1111/1365-2745.12973.

[13] Teun van den Brand. *ggh4x: Hacks for 'ggplot2'*. Nov. 2022. URL: https://CRAN.R-project.org/package=ggh4x.

[14] DD Breshears et al. "Effects of woody plants on microclimate in a semiarid woodland: soil temperature and evaporation in canopy and intercanopy patches". In: *International Journal of Plant Sciences* 159.6 (1998), pp. 1010–1017. ISSN: 1058-5893. DOI: 10.1086/297622.

[15] Mollie E. Brooks et al. "glmmTMB Balances Speed and Flexibility Among Packages for Zero-inflated Generalized Linear Mixed Modeling". en. In: *The R Journal* 9.2 (2017), pp. 378–400. ISSN: 2073-4859. URL: https://journal.r-project.org/archive/2017/RJ-2017-066/index.html.

[16] James M. Bullock and Ibby L. Moy. "Plants as seed traps: inter-specific interference with dispersal". en. In: *Acta Oecologica* 25.1-2 (Mar. 2004), pp. 35–41. ISSN: 1146609X. DOI: 10.1016/j.actao.2003.10.005. URL: https://linkinghub.elsevier.com/retrieve/pii/S1146609X03001152.

[17] TV Callaghan et al. "Arctic tundra and polar desert ecosystems". In: Cambridge University Press, 2005, pp. 243–352.

[18] Ragan M Callaway and Lawrence R Walker. "Competition and facilitation: a synthetic approach to interactions in plant communities". In: *Ecology* 78.7 (1997), p. 1958. ISSN: 0012-9658. DOI: 10.2307/2265936.

[19] Ragan M Callaway et al. "Positive interactions among alpine plants increase with stress". In: *Nature* 417.6891 (2002), nature00812. ISSN: 1476-4687. DOI: 10.1038/nature00812.

[20] Hal Caswell. *Matrix population models*. 2nd ed. Vol. 1. Sinauer Sunderland, MA, 2000.

[21] Jeanne C. Chambers and James A. MacMahon. "A Day in the Life of a Seed: Movements and Fates of Seeds and Their Implications for Natural and Managed Systems". In: *Annual Review of Ecology and Systematics* 25 (1994). Publisher: Annual Reviews, pp. 263–292. ISSN: 0066-4162. URL: http://www.jstor.org/stable/2097313.

[22] Jeanne C. Chambers, James A. MacMahon, and James H. Haefner. "Seed Entrapment in Alpine Ecosystems: Effects of Soil Particle Size and Diaspore Morphology". In: *Ecology* 72.5 (1991). Publisher: Ecological Society of America, pp. 1668–1677. ISSN: 0012-9658. DOI: 10.2307/1940966. URL: http://www.jstor.org/stable/1940966.

[23] Philippe Choler, Richard Michalet, and Ragan M Callaway. "Facilitation and competition on gradients in alpine plant communities". In: *Ecology* 82.12 (2001), pp. 3295–3308. ISSN: 1939-9170. DOI: 10.1890/0012-9658(2001)082[3295:FACOGI]2.0.CO;2.

[24] Madeleine L Combrinck. "Wind and seed: a conceptual model of shape-formation in the cushion plant Azorella Selago". en. In: *Plant Soil* (2020), p. 28.

[25] Benjamin I. Cook, Toby R. Ault, and Jason E. Smerdon. "Unprecedented 21st century drought risk in the American Southwest and Central Plains". en. In: *Science Advances* 1.1 (Feb. 2015). Publisher: American Association for the Advancement of Science Section: Research Article, e1400082. ISSN: 2375-2548. DOI: 10.1126/sciadv.1400082. URL: https://advances.sciencemag.org/content/1/1/e1400082.

[26] Line S. Cordes et al. "Contrasting effects of climate change on seasonal survival of a hibernating mammal". In: *Proceedings of the National Academy of Sciences* 117.30 (July 2020), pp. 18119–18126. DOI: 10.1073/pnas.1918584117. URL: https://www.pnas.org/doi/full/10.1073/pnas.1918584117 (visited on 08/24/2023).

[27] Elizabeth E. Crone. "Contrasting effects of spatial heterogeneity and environmental stochasticity on population dynamics of a perennial wildflower". en. In: *Journal of Ecology* 104.2 (2016), pp. 281–291. ISSN: 1365-2745. DOI: 10.1111/1365-2745.12500. URL: https://onlinelibrary.wiley.com/doi/abs/10.1111/1365-2745.12500.

[28] Jared M Diamond. "Assembly of species in communities". In: Harvard University Press, 1975, pp. 342–444.

[29] T.D. Drezner. "Plant facilitation in extreme environments: The non-random distribution of saguaro cacti (*Carnegiea gigantea*) under their nurse associates and the relationship to nurse architecture". In: *Journal of Arid Environments* 65.1 (2006), pp. 46–61. ISSN: 0140-1963. DOI: 10.1016/j.jaridenv.2005.06.027.

[30] Stefan Dullinger et al. "Extinction debt of high-mountain plants under twenty-first-century climate change". In: *Nat Clim Change* 2.8 (2012), pp. 619–622. ISSN: 1758-6798. DOI: 10.1038/nclimate1514.

[31] Michael R. Easterling, Stephen P. Ellner, and Philip M. Dixon. "Size-Specific Sensitivity: Applying a New Structured Population Model". en. In: *Ecology* 81.3 (2000), pp. 694–708. ISSN: 1939-9170. DOI: 10.1890/0012-9658(2000)081[0694:SSSAAN]2.0.CO;2. URL: https://onlinelibrary.wiley.com/doi/abs/10.1890/0012-9658%282000%29081%5B0694%3ASSSAAN%5D2.0.CO%3B2.

[32] Johan Ehrlén and William F Morris. "Predicting changes in the distribution and abundance of species under environmental change". In: *Ecology Letters* 18.3 (2015), pp. 303–314.

[33] Stephen P. Ellner, Dylan Z. Childs, and Mark Rees. *Data-driven Modelling of Structured Populations: A Practical Guide to the Integral Projection Model*. en. Lecture Notes on Mathematical Modelling in the Life Sciences. Cham: Springer International Publishing, 2016. ISBN: 978-3-319-28891-8 978-3-319-28893-2. URL: http://link.springer.com/10.1007/978-3-319-28893-2.

[34] Sarah C Elmendorf et al. "Plot-scale evidence of tundra vegetation change and links to recent summer warming". In: *Nat Clim Change* 2.6 (2012), pp. 453–457. ISSN: 1758-6798. DOI: 10.1038/nclimate1465.

[35] Brian L. Fisher and Stefan P. Cover. *Ants of North America: A guide to the genera*. University of California Press, 2007.

[36] Jennifer L Funk, Julie E Larson, and Gregory Vose. "Leaf traits and performance vary with plant age and water availability in Artemisia californica". In: *Annals of Botany* 127.4 (Apr. 2021), pp. 495–503. ISSN: 0305-7364. DOI: 10.1093/aob/mcaa106. URL: https://doi.org/10.1093/aob/mcaa106.

[37] Jean-Michel Gaillard and Nigel Gilles Yoccoz. "Temporal Variation in Survival of Mammals: A Case of Environmental Canalization?" en. In: *Ecology* 84.12 (2003), pp. 3294–3306. ISSN: 1939-9170. DOI: https://doi.org/10.1890/02-0409.

[38] Samuel J. L. Gascoigne et al. *Structured demographic buffering: A framework to explore the environment drivers and demographic mechanisms underlying demographic buffering*. en. July 2023. DOI: 10.1101/2023.07.20.549848. URL: https://www.biorxiv.org/content/10.1101/2023.07.20.549848v1.

[39] Michael Gottfried et al. "Continent-wide response of mountain vegetation to climate change". In: *Nat Clim Change* 2.2 (2012), pp. 111–115. ISSN: 1758-6798. DOI: 10.1038/nclimate1329.

[40] Charne A. Gouws, Natalie S. Haussmann, and Peter C. le Roux. "Seed trapping or a nurse effect? Disentangling the drivers of fine-scale plant species association patterns in a windy environment". en. In: *Polar Biology* 44.8 (Aug. 2021), pp. 1619–1628. ISSN: 0722-4060, 1432-2056. DOI: 10.1007/s00300-021-02898-1. URL: https://link.springer.com/10.1007/s00300-021-02898-1.

[41] Brandon Greenwell M. "pdp: an R package for constructing partial dependence plots". en. In: *The R Journal* 9.1 (2017), p. 421. ISSN: 2073-4859. DOI: 10.32614/RJ-2017-016. URL: https://journal.r-project.org/archive/2017/RJ-2017-016/index.html.

[42] Florian Hartig and Lukas Lohse. *DHARMa: Residual Diagnostics for Hierarchical (Multi-Level / Mixed) Regression Models*. Sept. 2022. URL: https://CRAN.R-project.org/package=DHARMa.

[43] Christoffer H. Hilde et al. "The Demographic Buffering Hypothesis: Evidence and Challenges". en. In: *Trends in Ecology & Evolution* 35.6 (June 2020), pp. 523–538. ISSN: 0169-5347. DOI: 10.1016/j.tree.2020.02.004.

[44] J. HilleRisLambers et al. "Rethinking community assembly through the lens of coexistence theory". In: *Annual Review of Ecology, Evolution, and Systematics* 43.1 (2012), pp. 227–248. DOI: 10.1146/annurev-ecolsys-110411-160411. URL: https://doi.org/10.1146/annurev-ecolsys-110411-160411.

[45] C Holzapfel and BE Mahall. "Bidirectional facilitation and interference between shrubs and annuals in the Mojave Desert". In: *Ecology* 80.5 (1999), p. 1747. ISSN: 0012-9658. DOI: 10.2307/176564.

[46] Torsten Hothorn et al. *multcomp: simultaneous inference in general parametric models*. Jan. 2022. URL: https://CRAN.R-project.org/package=multcomp.

[47] Nicole Hupp et al. "Alpine cushion plants have species–specific effects on microhabitat and community structure in the tropical Andes". en. In: *Journal of Vegetation Science* 28.5 (2017), pp. 928–938. ISSN: 1654-1103. DOI: 10.1111/jvs.12553. URL: http://onlinelibrary.wiley.com/doi/abs/10.1111/jvs.12553.

[48] Amy M. Iler et al. "Reproductive losses due to climate change-induced earlier flowering are not the primary threat to plant population viability in a perennial herb". en. In: *Journal of Ecology* 107.4 (2019), pp. 1931–1943. ISSN: 1365-2745. DOI: 10.1111/1365-2745.13146. URL: https://onlinelibrary.wiley.com/doi/abs/10.1111/1365-2745.13146.

[49] David T. Iles, Robert F. Rockwell, and David N. Koons. "Shifting Vital Rate Correlations Alter Predicted Population Responses to Increasingly Variable Environments". eng. In: *The American Naturalist* 193.3 (Mar. 2019), E57–E64. ISSN: 1537-5323. DOI: 10.1086/701043.

[50] David W. Inouye. "Effects of Climate Change on Phenology, Frost Damage, and Floral Abundance of Montane Wildflowers". en. In: *Ecology* 89.2 (2008), pp. 353–362. ISSN: 1939-9170. DOI: 10.1890/06-2128.1. URL: https://onlinelibrary.wiley.com/doi/abs/10.1890/06-2128.1.

[51] DW Inouye et al. "Climate change is affecting altitudinal migrants and hibernating species". In: *Proceedings of the National Academy of Sciences* 97.4 (2000), pp. 1630–1633. ISSN: 0027-8424. DOI: 10.1073/pnas.97.4.1630.

[52] Daniel H. Janzen. "Herbivores and the Number of Tree Species in Tropical Forests". In: *The American Naturalist* 104.940 (Nov. 1970), pp. 501–528. ISSN: 0003-0147. DOI: 10.1086/282687. URL: https://www.journals.uchicago.edu/doi/10.1086/282687.

[53] Eelke Jongejans and Hans De Kroon. "Space versus time variation in the population dynamics of three co-occurring perennial herbs". en. In: *Journal of Ecology* 93.4 (2005), pp. 681–692. ISSN: 1365-2745. DOI: 10.1111/j.1365-2745.2005.01003.x. URL: https://besjournals.onlinelibrary.wiley.com/doi/abs/10.1111/j.1365-2745.2005.01003.x.

[54] Eelke Jongejans et al. "Plant populations track rather than buffer climate fluctuations". en. In: *Ecology Letters* 13.6 (2010), pp. 736–743. ISSN: 1461-0248. DOI: 10.1111/j.1461-0248.2010.01470.x. URL: https://onlinelibrary.wiley.com/doi/abs/10.1111/j.1461-0248.2010.01470.x (visited on 10/17/2020).

[55] Henry F. Kaiser. "The application of electronic computers to factor analysis". In: *Educational and psychological measurement* 20.1 (1960), pp. 141–151.

[56] Mark Kirkpatrick. "Demographic models based on size, not age, for organisms with indeterminate growth". In: *Ecology* 65.6 (1984), pp. 1874–1884. ISSN: 0012-9658. DOI: 10.2307/1937785. URL: http://www.jstor.org/stable/1937785.

[57] Kari Klanderud. "Climate change effects on species interactions in an alpine plant community". en. In: *Journal of Ecology* 93.1 (2005), pp. 127–137. ISSN: 1365-2745. DOI: 10.1111/j.1365-2745.2004.00944.x. URL: https://onlinelibrary.wiley.com/doi/abs/10.1111/j.1365-2745.2004.00944.x.

[58] David N. Koons et al. "Is life-history buffering or lability adaptive in stochastic environments?" en. In: *Oikos* 118.7 (2009), pp. 972–980. ISSN: 1600-0706. DOI: 10.1111/j.1600-0706.2009.16399.x. URL: http://onlinelibrary.wiley.com/doi/abs/10.1111/j.1600-0706.2009.16399.x.

[59] Christian Körner. *Alpine plant life: functional plant ecology of high mountain ecosystems*. 2nd. Springer, 2003. ISBN: 3-540-00347-9. DOI: 10.1007/978-3-642-18970-8_8.

[60] Hans de Kroon et al. "Elasticity: The Relative Contribution of Demographic Parameters to Population Growth Rate". In: *Ecology* 67 (Oct. 1986), p. 1427. DOI: 10.2307/1938700.

[61] Alexander V. Kumar et al. "Contrasting seasonal effects of climate change influence density in a cold-adapted species". en. In: *Global Change Biology* 28.21 (2022), pp. 6228–6238. ISSN: 1365-2486. DOI: 10.1111/gcb.16352.

[62] Carlos Lara-Romero et al. "What causes conspecific plant aggregation? Disentangling the role of dispersal, habitat heterogeneity and plant–plant interactions". en. In: *Oikos* 125.9 (2016), pp. 1304–1313. ISSN: 1600-0706. DOI: 10.1111/oik.03099. URL: http://onlinelibrary.wiley.com/doi/abs/10.1111/oik.03099.

[63] Christie Le Coeur et al. "Life history adaptations to fluctuating environments: Combined effects of demographic buffering and lability". en. In: *Ecology Letters* 25.10 (2022), pp. 2107–2119. ISSN: 1461-0248. DOI: 10.1111/ele.14071. URL: https://onlinelibrary.wiley.com/doi/abs/10.1111/ele.14071.

[64] Russell V. Lenth et al. *emmeans: estimated marginal means, aka least-squares means*. Jan. 2022. URL: https://CRAN.R-project.org/package=emmeans.

[65] Sam Levin et al. *ipmr: Integral Projection Models*. Feb. 2023. URL: https://cran.r-project.org/web/packages/ipmr/index.html.

[66] Jonathan M. Levine and Mark Rees. "Effects of Temporal Variability on Rare Plant Persistence in Annual Systems." In: *The American Naturalist* 164.3 (Sept. 2004), pp. 350–363. ISSN: 0003-0147. DOI: 10.1086/422859. URL: https://www.journals.uchicago.edu/doi/abs/10.1086/422859.

[67] María Lucrecia Lipoma et al. "Not gone with the wind: Vegetation complexity increases seed retention during windy periods in the Argentine Semiarid Chaco". en. In: *Journal of Vegetation Science* 30.3 (2019), pp. 542–552. ISSN: 1654-1103. DOI: 10.1111/jvs.12747. URL: http://onlinelibrary.wiley.com/doi/abs/10.1111/jvs.12747.

[68] Francisco Lloret et al. "Extreme climatic events and vegetation: the role of stabilizing processes". en. In: *Global Change Biology* 18.3 (2012), pp. 797–805. ISSN: 1365-2486. DOI: 10.1111/j.1365-2486.2011.02624.x. URL: https://onlinelibrary.wiley.com/doi/abs/10.1111/j.1365-2486.2011.02624.x (visited on 09/11/2023).

[69] Richard N Mack and John L Harper. "Interference in dune annuals: spatial pattern and neighbourhood effects". In: *Journal of Ecology* 65.2 (1977), p. 345. ISSN: 0022-0477. DOI: 10.2307/2259487.

[70] Ilya M. D. Maclean et al. "On the measurement of microclimate". en. In: *Methods in Ecology and Evolution* 12.8 (2021), pp. 1397–1410. ISSN: 2041-210X. DOI: 10.1111/2041-210X.13627. URL: http://onlinelibrary.wiley.com/doi/abs/10.1111/2041-210X.13627.

[71] Fernando T Maestre et al. "Refining the stress-gradient hypothesis for competition and facilitation in plant communities". In: *Journal of Ecology* 97.2 (2009), pp. 199–205. ISSN: 1365-2745. DOI: 10.1111/j.1365-2745.2008.01476.x.

[72] Fernando T. Maestre et al. "Potential for using facilitation by grasses to establish shrubs on a semiarid degraded steppe". In: *Ecological Applications* 11.6 (2001). Publisher: Ecological Society of America, pp. 1641–1655. ISSN: 1051-0761. DOI: 10.2307/3061085. URL: http://www.jstor.org/stable/3061085.

[73] Max Mallen-Cooper, Bente J Graae, and Will K Cornwell. "Lichens buffer tundra microclimate more than the expanding shrub *Betula nana*". en. In: *Annals of Botany* 128.4 (Sept. 2021), pp. 407–418. ISSN: 0305-7364, 1095-8290. DOI: 10.1093/aob/mcab041. URL: https://academic.oup.com/aob/article/128/4/407/6170697.

[74] Luis Matías et al. "An experimental extreme drought reduces the likelihood of species to coexist despite increasing intransitivity in competitive networks". In: *Journal of Ecology* 106.3 (2018), pp. 826–837. ISSN: 0022-0477. DOI: 10.1111/1365-2745.12962.

[75] Jenni L McDonald et al. "Divergent demographic strategies of plants in variable environments". In: *Nat Ecol Evol* 1.2 (2017), p. 29. ISSN: 2397-334X. DOI: 10.1038/s41559-016-0029.

[76] C. Jessica E. Metcalf et al. "Statistical modelling of annual variation for inference on stochastic population dynamics using Integral Projection Models". en. In: *Methods in Ecology and Evolution* 6.9 (2015), pp. 1007–1017. ISSN: 2041-210X. DOI: 10.1111/2041-210X.12405. URL: https://onlinelibrary.wiley.com/doi/abs/10.1111/2041-210X.12405.

[77] Lukas Meysick, Eduardo Infantes, and Christoffer Boström. "The influence of hydrodynamics and ecosystem engineers on eelgrass seed trapping". en. In: *PLOS ONE* 14.9 (Sept. 2019). Publisher: Public Library of Science, e0222020. ISSN: 1932-6203. DOI: 10.1371/journal.pone.0222020. URL: https://journals.plos.org/plosone/article?id=10.1371/journal.pone.0222020.

[78] Maria N. Miriti. "Ontogenetic shift from facilitation to competition in a desert shrub". en. In: *Journal of Ecology* 94.5 (2006), pp. 973–979. ISSN: 1365-2745. DOI: 10.1111/j.1365-2745.2006.01138.x. URL: http://onlinelibrary.wiley.com/doi/abs/10.1111/j.1365-2745.2006.01138.x.

[79] C. Mix et al. "Regional gene flow and population structure of the wind-dispersed plant species Hypochaeris radicata (Asteraceae) in an agricultural landscape". en. In: *Molecular Ecology* 15.7 (2006), pp. 1749–1758. ISSN: 1365-294X. DOI: 10.1111/j.1365-294X.2006.02887.x. URL: http://onlinelibrary.wiley.com/doi/abs/10.1111/j.1365-294X.2006.02887.x.

[80] William F. Morris et al. "Longevity Can Buffer Plant and Animal Populations Against Changing Climatic Variability". en. In: *Ecology* 89.1 (2008), pp. 19–25. ISSN: 1939-9170. DOI: 10.1890/07-0774.1. URL: https://onlinelibrary.wiley.com/doi/abs/10.1890/07-0774.1 (visited on 08/12/2023).

[81] Cecilia I. Nuñez, Marcelo A. Aizen, and Cecilia Ezcurra. "Species associations and nurse plant effects in patches of high-Andean vegetation". In: *Journal of Vegetation Science* 10.3 (1999). Publisher: Wiley, pp. 357–364. ISSN: 1100-9233. DOI: 10.2307/3237064. URL: http://www.jstor.org/stable/3237064.

[82] M. Nyakatya and M. McGeoch. "Temperature variation across Marion Island associated with a keystone plant species (*Azorella selago* Hook. (Apiaceae))". In: *Polar Biology* 31.2 (Feb. 2008), pp. 139–151. ISSN: 07224060. DOI: 10.1007/s00300-007-0341-8. URL: https://search.ebscohost.com/login.aspx?direct=true&db=eih&AN=27605612&site=ehost-live.

[83] Kristin O. Nystuen et al. "Lichens facilitate seedling recruitment in alpine heath". In: *Journal of Vegetation Science* 30.5 (2019), pp. 868–880. ISSN: 1654-1103. DOI: 10.1111/jvs.12773. URL: http://onlinelibrary.wiley.com/doi/abs/10.1111/jvs.12773.

[84] Lisa-Maria Ohler, Martin Lechleitner, and Robert R. Junker. "Microclimatic effects on alpine plant communities and flower-visitor interactions". en. In: *Scientific Reports* 10.1 (Jan. 2020). Number: 1 Publisher: Nature Publishing Group, p. 1366. ISSN: 2045-2322. DOI: 10.1038/s41598-020-58388-7. URL: https://www.nature.com/articles/s41598-020-58388-7.

[85] MF Oldfather and DD Ackerly. "Microclimate and demography interact to shape stable population dynamics across the range of an alpine plant". In: *New Phytologist* 222.1 (2019), pp. 193–205. ISSN: 0028-646X. DOI: 10.1111/nph.15565.

[86] Øystein H. Opedal, W. Scott Armbruster, and Bente J. Graae. "Linking small-scale topography with microclimate, plant species diversity and intra-specific trait variation in an alpine landscape". en. In: *Plant Ecology & Diversity* 8.3 (May 2015), pp. 305–315. ISSN: 1755-0874, 1755-1668. DOI: 10.1080/17550874.2014.987330. URL: http://www.tandfonline.com/doi/full/10.1080/17550874.2014.987330.

[87] Øystein H. Opedal et al. "Refining predictions of metacommunity dynamics by modeling species non-independence". en. In: *Ecology* 101.8 (2020), e03067. ISSN: 1939-9170. DOI: https://doi.org/10.1002/ecy.3067. URL: https://esajournals.onlinelibrary.wiley.com/doi/abs/10.1002/ecy.3067.

[88] Gianluigi Ottaviani et al. "The neglected belowground dimension of plant dominance". en. In: *Trends in Ecology & Evolution* 35.9 (Sept. 2020), pp. 763–766. ISSN: 0169-5347. DOI: 10.1016/j.tree.2020.06.006. URL: http://www.sciencedirect.com/science/article/pii/S0169534720301683.

[89] Edzer Pebesma et al. *sf: simple features for R*. Dec. 2021. URL: https://CRAN.R-project.org/package=sf.

[90] Edzer Pebesma et al. *sp: classes and methods for spatial data*. Nov. 2021. URL: https://CRAN.R-project.org/package=sp.

[91] N Pérez-Harguindeguy et al. "New handbook for standardised measurement of plant functional traits worldwide". In: *Australian Journal of Botany* 61.3 (2013), p. 167. ISSN: 0067-1924. DOI: 10.1071/bt12225.

[92] Brian G. Peterson et al. *PerformanceAnalytics: econometric tools for performance and risk analysis*. Feb. 2020. URL: https://CRAN.R-project.org/package=PerformanceAnalytics.

[93] CA Pfister. "Patterns of variance in stage-structured populations: Evolutionary predictions and ecological implications". In: *Proc National Acad Sci* 95.1 (1998), pp. 213–218. ISSN: 0027-8424. DOI: 10.1073/pnas.95.1.213.

[94] Francisco I. Pugnaire, Peter Haase, and Juan Puigdefabregas. "Facilitation between higher plant species in a semiarid environment". en. In: *Ecology* 77.5 (1996), pp. 1420–1426. ISSN: 1939-9170. DOI: https://doi.org/10.2307/2265539. URL: https://esajournals.onlinelibrary.wiley.com/doi/abs/10.2307/2265539.

[95] D. A. Rae et al. "Influence of microclimate and species interactions on the composition of plant and invertebrate communities in alpine northern Norway". en. In: *Acta Oecologica* 29.3 (May 2006), pp. 266–282. ISSN: 1146-609X. DOI: 10.1016/j.actao.2005.11.007. URL: http://www.sciencedirect.com/science/article/pii/S1146609X05001232.

[96] Courtenay A. Ray et al. "Linking microenvironment modification to species interactions and demography in an alpine plant community". en. In: *BioRxiv* (June 2022). DOI: 10.1101/2022.06.21.497097. URL: http://biorxiv.org/lookup/doi/10.1101/2022.06.21.497097.

[97] Courtenay A. Ray et al. "Linking microenvironment modification to species interactions and demography in an alpine plant community". en. In: *Oikos* 2023.3 (2023), e09235. ISSN: 1600-0706. DOI: 10.1111/oik.09235. URL: https://onlinelibrary.wiley.com/doi/abs/10.1111/oik.09235.

[98] Mark Rees, Peter J Grubb, and Dave Kelly. "Quantifying the impact of competition and spatial heterogeneity on the structure and dynamics of a four-species guild of winter annuals". In: *American Naturalist* 147.1 (1996), pp. 1–32. ISSN: 0003-0147. DOI: 10.1086/285837.

[99] David Reznick. "The structure of guppy life histories: the tradeoff between growth and reproduction". en. In: *Ecology* 64.4 (1983), pp. 862–873. ISSN: 1939-9170. DOI: 10.2307/1937209. URL: https://esajournals.onlinelibrary.wiley.com/doi/abs/10.2307/1937209.

[100] Roberto C. Rodríguez-Caro et al. "The limits of demographic buffering in coping with environmental variation". en. In: *Oikos* 130.8 (2021), pp. 1346–1358. ISSN: 1600-0706. DOI: 10.1111/oik.08343. URL: https://onlinelibrary.wiley.com/doi/abs/10.1111/oik.08343.

[101] Susana Rodríguez-Echeverría et al. "A role for below-ground biota in plant–plant facilitation". en. In: *Journal of Ecology* 101.6 (2013), pp. 1420–1428. ISSN: 1365-2745. DOI: 10.1111/1365-2745.12159. URL: https://onlinelibrary.wiley.com/doi/abs/10.1111/1365-2745.12159.

[102] Tobias Roth, Matthias Plattner, and Valentin Amrhein. "Plants, birds and butterflies: short-term responses of species communities to climate warming vary by taxon and with altitude". In: *PLOS One* 9.1 (2014), e82490. DOI: 10.1371/journal.pone.0082490.

[103] Serguei Saavedra et al. "A structural approach for understanding multispecies coexistence". In: *Ecological Monographs* 87.3 (2017), pp. 470–486. ISSN: 1557-7015. DOI: 10.1002/ecm.1263.

[104] Gabriel Silva Santos et al. *A unified framework to identify demographic buffering in natural populations*. en. July 2023. DOI: 10.1101/2023.07.03.547528. URL: https://www.biorxiv.org/content/10.1101/2023.07.03.547528v1.

[105] Daniel Scherrer and Christian Körner. "Topographically controlled thermal-habitat differentiation buffers alpine plant diversity against climate warming". In: *Journal of Biogeography* 38.2 (2011), pp. 406–416. ISSN: 1365-2699. DOI: 10.1111/j.1365-2699.2010.02407.x.

[106] Barret Schloerke et al. *GGally: extension to 'ggplot2'*. June 2021. URL: https://CRAN.R-project.org/package=GGally.

[107] Eugene W. Schupp. "Seed-Seedling Conflicts, Habitat Choice, and Patterns of Plant Recruitment". In: *American Journal of Botany* 82.3 (1995), pp. 399–409. ISSN: 0002-9122. DOI: 10.2307/2445586. URL: https://www.jstor.org/stable/2445586.

[108] Frank M. Schurr et al. "A mechanistic model for secondary seed dispersal by wind and its experimental validation". en. In: *Journal of Ecology* 93.5 (2005), pp. 1017–1028. ISSN: 1365-2745. DOI: 10.1111/j.1365-2745.2005.01018.x. URL: https://onlinelibrary.wiley.com/doi/abs/10.1111/j.1365-2745.2005.01018.x.

[109] Lauren G. Shoemaker et al. "Integrating the underlying structure of stochasticity into community ecology". en. In: *Ecology* 101.2 (2020), e02922. ISSN: 1939-9170. DOI: 10.1002/ecy.2922. URL: https://onlinelibrary.wiley.com/doi/abs/10.1002/ecy.2922.

[110] Forrest Shreve. "Physical Conditions in Sun and Shade". In: *Ecology* 12.1 (1931). Publisher: Ecological Society of America, pp. 96–104. ISSN: 0012-9658. DOI: 10.2307/1932935. URL: http://www.jstor.org/stable/1932935.

[111] Santiago Soliveres et al. "Intransitive competition is widespread in plant communities and maintains their species richness". In: *Ecology Letters* 18.8 (2015), pp. 790–798. ISSN: 1461-023X. DOI: 10.1111/ele.12456.

[112] Jordan Stark et al. "Does environmental heterogeneity drive functional trait variation? A test in montane and alpine meadows". In: *Oikos* 126.11 (2017), pp. 1650–1659. ISSN: 1600-0706. DOI: 10.1111/oik.04311.

[113] S. C. Stearns. "Trade-offs in life-history evolution". In: *Functional Ecology* 3.3 (1989). Publisher: [British Ecological Society, Wiley], pp. 259–268. ISSN: 0269-8463. DOI: 10.2307/2389364. URL: https://www.jstor.org/stable/2389364.

[114] Matthew Sturm et al. "Winter biological processes could help convert arctic tundra to shrubland". en. In: *BioScience* 55.1 (2005), p. 17. ISSN: 0006-3568. DOI: 10.1641/0006-3568(2005)055[0017:WBPCHC]2.0.CO;2. URL: https://academic.oup.com/bioscience/article/55/1/17-26/248282.

[115] R Core Team. *R: A language and environment for statistical computing*. Vienna, Austria, 2021. URL: https://www.R-project.org/.

[116] A Traveset. "Effect of seed passage through vertebrate frugivores' guts on germination: a review". en. In: *Perspectives in Plant Ecology, Evolution and Systematics* 1.2 (1998), pp. 151–190. ISSN: 14338319. DOI: 10.1078/1433-8319-00057. URL: https://linkinghub.elsevier.com/retrieve/pii/S1433831904700104.

[117] Shripad D. Tuljapurkar. "Population dynamics in variable environments. III. Evolutionary dynamics of r-selection". In: *Theoretical Population Biology* 21.1 (Feb. 1982), pp. 141–165. ISSN: 0040-5809. DOI: 10.1016/0040-5809(82)90010-7. URL: https://www.sciencedirect.com/science/article/pii/0040580982900107.

[118] Werner Ulrich et al. "Species interactions and random dispersal rather than habitat filtering drive community assembly during early plant succession". In: *Oikos* 125.5 (2016), pp. 698–707. ISSN: 1600-0706. DOI: 10.1111/oik.02658.

[119] Stephen B. Vander Wall, Kellie M. Kuhn, and Maurie J. Beck. "Seed Removal, Seed Predation, and Secondary Dispersal". In: *Ecology* 86.3 (2005). Publisher: Ecological Society of America, pp. 801–806. ISSN: 0012-9658. URL: http://www.jstor.org/stable/3450673.

[120] Stephen B. Vander Wall and William S. Longland. "Diplochory: are two seed dispersers better than one?" en. In: *Trends in Ecology & Evolution* 19.3 (Mar. 2004), pp. 155–161. ISSN: 01695347. DOI: 10.1016/j.tree.2003.12.004. URL: https://linkinghub.elsevier.com/retrieve/pii/S0169534703003781.

[121] PJ Webber et al. "The vegetation: pattern and succession". In: *An Arctic ecosystem : The coastal tundra at Barrow, Alaska*. Ed. by J Brown et al. Dowden, Hutchinson, and Ross, Inc., 1980, pp. 186–218.

[122] Claus O. Wilke and Brenton M. Wiernik. *ggtext: Improved Text Rendering Support for 'ggplot2'*. Sept. 2022. URL: https://CRAN.R-project.org/package=ggtext.

[123] A. Park Williams et al. "Large contribution from anthropogenic warming to an emerging North American megadrought". en. In: *Science* 368.6488 (Apr. 2020). Publisher: American Association for the Advancement of Science Section: Report, pp. 314–318. ISSN: 0036-8075, 1095-9203. DOI: 10.1126/science.aaz9600. URL: https://science.sciencemag.org/content/368/6488/314 (visited on 11/23/2020).

[124] Mary Wisz et al. "The role of biotic interactions in shaping distributions and realised assemblages of species: implications for species distribution modelling." In: *Biological reviews* 88.1 (2012), pp. 15–30. ISSN: 1464-7931. DOI: 10.1111/j.1469-185x.2012.00235.x.

[125] A.J. Wright et al. "Stress gradients and biodiversity: monoculture vulnerability drives stronger biodiversity effects during drought years". en. In: *Ecology* 102.1 (Jan. 2021). ISSN: 0012-9658, 1939-9170. DOI: 10.1002/ecy.3193. URL: https://onlinelibrary.wiley.com/doi/10.1002/ecy.3193.

[126] Alexandra Wright, Stefan A Schnitzer, and Peter B Reich. "Daily environmental conditions determine the competition-facilitation balance for plant water status". In: *Journal of Ecology* 103.3 (2015), pp. 648–656. ISSN: 0022-0477. DOI: 10.1111/1365-2745.12397.

[127] Stephanie D. Zorio, Charles F. Williams, and Ken A. Aho. "Sixty-Five Years of Change in Montane Plant Communities in Western Colorado, U.S.A." In: *Arctic, Antarctic, and Alpine Research* 48.4 (Nov. 2016), pp. 703–722. ISSN: 1523-0430. DOI: 10.1657/AAAR0016-011. URL: https://doi.org/10.1657/AAAR0016-011 (visited on 08/30/2023).

[128] CB Zou et al. "Soil moisture redistribution as a mechanism of facilitation in savanna tree–shrub clusters". In: *Oecologia* 145.1 (2005), pp. 32–40. ISSN: 0029-8549. DOI: 10.1007/s00442-005-0110-8.